2016

Extraction and Biochemical Characterization of Alligator mississippiensis glycosaminoglycans and an Ex-vivo Murine Pilot Study to Test their Potential Effect on a Selected Panel of Genes Associated with Cystic Fibrosis

Jose Daniel Estrada Andino
Louisiana State University and Agricultural and Mechanical College

EXTRACTION AND BIOCHEMICAL CHARACTERIZATION OF *ALLIGATOR MISSISSIPPIENSIS* GLYCOSAMINOGLYCANS AND AN *EX-VIVO* MURINE PILOT STUDY TO TEST THEIR POTENTIAL EFFECT ON A SELECTED PANEL OF GENES ASSOCIATED WITH CYSTIC FIBROSIS

A Dissertation

Submitted to the Graduate Faculty of the
Louisiana State University and
Agricultural and Mechanical College
in partial fulfillment of the
requirements for the degree of
Doctor of Philosophy

in

The School of Nutrition and Food Science

by
Jose Daniel Estrada Andino
B.S., Escuela Agrícola Panamericana Zamorano, 2007
M.S., Louisiana State University, 2011
August 2016

This work is dedicated to my amazing wife Monika and all of my family in Honduras, Germany and Poland.

ACKNOWLEDGEMENTS

I want to express my deepest gratitude to everyone who played a role in the completion of this work. First of all I thank God for the daily assurance of purpose in my life and for all the people whom he used for my academic, professional, personal and academic growth during the past few years.

To Dr. Jack Losso, thank you so much for being an admirable person, great friend, and an inspiring and always supportive mentor. Thank you for trusting in me to conduct such a relevant project for the Louisiana alligator industry and for simultaneously allowing me to have a well-rounded experience through my involvement in national new product development competitions, IFT competitions and an amazing food industry internship. Under your mentorship I have become a better person and professional.

To my committee members, Dr. Joan King, Dr. Roger Laine, Dr. Grover Waldrop, Dr. Yogesh Saini, Mr. Mark Shirley and Dr. Erin Casey, thank you for your valuable time and guidance. Special thanks to Mr. Mark Shirley and Dr. Yogesh Saini for their hands-on support and training in the field and laboratory, respectively.

To all my collaborators in the experiments carried out for this dissertation, Mr. Cristian Macoto, Dr. Marvin Moncada, Dr. Luis Espinoza and Ms. Jeimy Menjivar in the processing of alligator by-products, Dr. Richard Cooper for allowing me to use his molecular biology laboratory

and equipment, Dr. George Stanley for his FT-IR training and Dr. Kenneth Smith at Thermo Fisher Scientific for his kind support with FT-IR data collection.

I would also like to thank all my labmates and friends at the School of Nutrition and Food Science and around the LSU campus for all their support and encouragement expressed in many different ways. Especially, Srikanth, Namrata, Kennet, Ryan, Reynaldo, Alejandro and Damir. To my Baton Rouge parents Mark and Alicia, your friendship and care have made this town feel like home. To my SBRPC family, thank you for supporting me in prayer and also in many practical ways even before I arrived here.

Finally, to my wife Monika and my family in Honduras, Poland and Germany. Thank you for supporting my goals and always believing in my potential. I would not have made it so far without all of you. Monika, your willingness to move from Germany to Baton Rouge gave me the gift of an outstanding PhD student experience next to you.

TABLE OF CONTENTS

LIST OF TABLES

LIST OF FIGURES

ABBREVIATIONS INDEX

ABS	alligator backstraps
ACS	alligator carcasses
AEB	alligator eyeballs
AFT	alligator feet
ALI	air-liquid-interface
AMP	adenosine mono-phosphate
AMPK	AMP-activated kinase
ANOVA	analysis of variance
ASL	airway surface liquid
ATP	adenosine triphosphate
BAL	bronchoalveolar lavage
BCA	bicinchoninic acid
BSA	bovine serum albumin
cAMP-PKA	cyclic adenosine monophosphate-dependent protein kinase A
CCL27	cutaneous T cell-attracting chemokine
CF	cystic fibrosis
CFTR	cystic fibrosis transmembrane conductance regulator
ChrAses	chondroitinases
COPD	chronic obstructive pulmonary disease
CPC	cetylpyridinium chloride
CRBD	completely randomized block design
CS	chondroitin sulfate
C_T	threshold cycle
DMB	dimethylmethylene blue
DMEM	Dulbecco's Modified Eagle Medium

DNase	deoxyribonuclease
DS	dermatan sulfate
ECM	extracellular matrix
EDTA	ethylenediaminetetraacetic acid
ENaC	epithelial sodium channel
FBS	fetal bovine serum
FEV_1	forced expiratory volume in 1 second
FT-IR	fourier transform infrared spectroscopy
FVC	forced vital capacity
GAGs	glycosaminoglycans
GalNAc	n-acetylgalactosamine
GDC	genomic DNA control
GlcA	glucuronic acid
GlcNAc	n-acetylglucosamine
HA	hyaluronic acid
HAases	hyaluronidases
HARE	hyaluronan receptor for endocytosis
HAS1-3	hyaluronic acid synthases 1-3
HCl	hydrochloric acid
HIV-1	human immunodeficiency virus type 1
HP	heparin
HS	heparan sulfate
HSP	heat shock protein
HSV-1	herpes simplex virus type 1
HMW	high molecular weight
HTS	hypertonic saline
ICP-AES	inductively coupled plasma atomic emission spectrometry

IdA	iduronic acid
IL-1β	interleukin 1 beta
IL-6	interleukin 6
IL-8	interleukin 8
IL-10	interleukin 10
IRAK	interleukin 1 associated kinase-M
KS	keratan sulfate
LMW	low molecular weight
LYVE1	lymphatic vessel endothelial hyaluronan receptor 1
MCC	mucociliary clearance
MIP-2	macrophage inflammatory protein 2
MMP	matrix metalloproteinase
MMW	medium molecular weight
MSD1-2	membrane spanning domains 1 and 2
MTEC	mouse tracheal epithelial cells
MTEC+Y27632	MTEC media containing Y27632 ROCK inhibitor (10 μM)
MTEC+NuSerum	MTEC media containing NuSerum (2%)
MWCO	molecular weight cut-off
NBD1-2	nucleotide binding domains
NE	neutrophil elastase
NF- κβ	nuclear factor kappa beta
oHA	hyaluronic acid oligosaccharides
PBS	phosphate buffered saline
PBST	phosphate buffered saline-Tween
PCR	polymerase chain reaction
PPARγ	peroxisome proliferator-activated receptor-gamma
PPC	positive PCR control

R^2	correlation coefficient
RD	regulatory domain
RHAMM	receptor for hyaluronan mediated motility
ROS	reactive oxygen species
RTC	reverse-transcription control
SD	standard deviation
STAT3	signal transducer and activator of transcription 3
TBE	tris borate-EDTA
TCA	trichloroacetic acid
TGAse	tissue transglutaminase
TLRs	toll-like receptors
TNF-α	tumor necrosis factor
TSG-6	tumor necrosis factor-alpha stimulated gene-6

ABSTRACT

Cystic fibrosis (CF) is a genetic disorder with a median survival age of 40.7 years. Chronic airway inflammation and dehydration are critical features of CF. The size and structure-dependent hydration and anti-inflammatory properties of glycosaminoglycans (GAGs) such as hyaluronic acid (HA) may help ameliorate these symptoms. The GAGs contained in farmed *Alligator mississippiensis* by-products offer a potential to improve waste management practices and increase revenue in the alligator industry, through their development for use in biomedical applications. This study aimed to efficiently extract and characterize GAGs from alligator carcasses (ACS), backstraps (ABS), feet (AFT) and eyeballs (AEB), to evaluate their effects on CF-like airways *ex-vivo*. Samples were collected from local alligator processing facilities and extractions were conducted according to a randomized complete block design. The contents of sulfated and non-sulfated GAGs were determined using dimethylmethylene blue and HA ELISA assays, respectively. Total GAG content was confirmed by the carbazole reaction assay. Protein content, mineral content and molecular weight (MW) were determined by the bicinchoninic acid assay, inductively coupled plasma and 0.75% agarose electrophoresis, respectively. FTIR spectroscopy was conducted to fingerprint the structures of the extracted GAGs. Multi-step processes for the extraction of GAGs from alligator by-products were developed and ABS had the highest ($p \leq 0.05$) total GAG content (15.53±0.27 mg/g), followed by AFT (4.72±0.05 mg/g), AEB (0.79±0.01 mg/g) and ACS (0.60±0.00 mg/g). These results are equivalent to ~2.13 g GAGs per harvest-size farmed alligator or an estimated GAG production of ~0.73 tons/year in Louisiana. The GAGs in all samples were predominantly (>97%) HA with a poly-disperse MW of up to 1600 kDa. FTIR revealed spectra showing characteristic GAG features such as -OH, -NH, -CH and amide signals

from residual protein, comparable to previous studies on animal-sourced GAGs. *Ex-vivo* gene expression analysis of *Scnn1b*-Tg mice tracheal epithelial cells indicated that AEB GAGs (0.5 mg/12 mm insert) have the potential to regulate the expression of genes which may aid in restoring the protease/anti-protease balance, reducing inflammation, and regulating ASL osmotic homeostasis. Alligator GAGs may also aid in the treatment of other inflammatory conditions such as wound healing and arthritis in humans and animals.

CHAPTER 1
INTRODUCTION

The state of Louisiana has the largest alligator (*Alligator mississippiensis*) industry in the United States. A total of over 350,000 farm-raised and wild alligators are harvested yearly through a world-renowned sustainable system managed by the Louisiana Department of Wildlife and Fisheries. This model generates a significant revenue, as well as protection of the wetland habitats [1]. In the processing of slaughtered alligators for their skin and meat, the industry generates waste which is currently being disposed in landfills or marketed at very low prices. These by-products contain valuable anti-inflammatory glycosaminoglycans (GAGs) that can be extracted in a promising effort to improve current waste management practices and further increase the industry's value.

Hyaluronic acid (HA) is a linear, negatively charged, highly hydrophilic and non-sulfated GAG found mainly in the extracellular matrix (ECM) in the form of sodium salt [2,3]. This high molecular weight (HMW) GAG, which is degraded by hyaluronidases (HAases), chondroitinases (ChrAses) and reactive oxygen species (ROS), possesses multiple size-dependent signaling properties. There is consensus that larger HA chains have anti-inflammatory properties and smaller ones have pro-inflammatory activity, however there is no clear categorization about the molecular weight of HA [4–6]. HA fragments (6-12 disaccharides) have been reported to significantly increase the expression of inflammatory cytokines and tissue degrading enzymes such as matrix metalloproteinases (MMP) [7]. In the airways, HA interacts with a variety of cell surface receptors and HA-binding proteins to activate intracellular events through various pathways [8,9]. Inflammation in mice cystic fibrosis (CF) airways has been effectively mitigated by nebulized HA

as measured by the reduction of TNF-α, myeloperoxidase activity, ROS and tissue transglutaminase (TGAse) activity [10]. Moreover, Scuri and Abraham reported dose dependent inhibition of human NE induced airway responses in sheep pretreated with 150 or 300 kDa HA [11]. It has also been proposed that the water binding properties of HA may increase the elasticity of lung elastic fibers, thus improving pulmonary mechanics [12] or purulent mucus clearance. The abundance of carboxyl groups in HA may also result in an interaction with Ca^{2+} [13,14], therefore limiting TGAse inflammatory activity in the airways of CF patients.

CF is a severely life shortening genetic disorder that globally affects around 70,000 individuals primarily of Caucasian descent. Mutations in both copies of the CF transmembrane conductance regulator (CFTR) gene disrupt normal production of the CFTR protein which is a chloride channel expressed in the epithelium of multiple organs including the lungs [15]. The defective CFTR results in abnormal transport of chloride and sodium across the cell membrane which leads to a high morbidity due to obstructive lung disease [10,15,16]. CF is also characterized by an early and dysregulated inflammatory scenario in the airways which has been associated with increased levels of pro-inflammatory cytokines and enzymes [17–21]. The extent of inflammatory response in these patients is disproportionately increased compared to patients without CF both in presence or absence of bacterial infection [22]. Upregulation of nuclear factor kappa beta (NF-κβ) increases the production of interleukin-8 (IL-8) and tumor necrosis factor alpha (TNF-α), which mediate neutrophil activity and the secretion of neutrophil elastase (NE), a serine protease designed for bacterial phagocytosis but that can also degrade airway tissues and cause lung damage [18,23,24]. Currently, anti-inflammatory treatments with corticosteroids and high-dose ibuprofen have shown benefits, however side-effects limit their continuous use [25,26]. Furthermore, TGAse

is an enzyme that catalyzes cross-links or deamidation of target proteins in the presence or absence of Ca^{2+} [27,28] and it has been shown that innate increased oxidative stress in CF airway epithelia induces TGAse up-regulation. For this reason TGAse has been recognized as a potential target enzyme for healing of lung inflammation and injuries [29,30].

HA is a natural component of the respiratory system that has been safely used in European CF Centers to improve the tolerability of hypertonic saline and to test its efficacy in the treatment of bacterial rhinosinusitis in combination with tobramycin [24,31,32]. Globally, the HA market is estimated over US$1 billion in the biomedical (knee osteoarthritis, ophthalmic procedures and dermal fillers), cosmetic and food industries [33,34]. This compound alone or in the presence of other GAGs may aid in the down-regulation of the chronic and uncontrolled pro-inflammatory responses in CF by reducing the expression of potent cytokines and TGAse. In aggregate the currently available information on CF, GAGs, and the abundance of waste products containing GAGs in the Louisiana alligator industry, support the relevance of extracting *A. mississippiensis* by-product GAGs to evaluate their potential to ameliorate inflammation, mediate osmotic homeostasis, and recover the protease/anti-protease balance in CF airways, as well as potentially generate economic development through increased revenue and creation of new labor and high technology jobs.

The main objective of this research was to determine the yield and biochemical characteristics of *A. mississippiensis* by-product GAGs and explore their potential regulatory role on a selected panel of genes associated with CF in mice CF-like airways *ex-vivo*. The specific aims that derive from this objective are:

1. To develop a method for the extraction of GAGs from alligator carcasses (ACS), feet (AFT) and backstraps (ABS).

2. To develop a method for the extraction of GAGs from alligator eyeballs (AEB).

3. To quantify and characterize the GAGs extracted from ACS, AFT, ABS and AEB.

4. To evaluate the effects of *A. mississippiensis* AEB GAGs on the *ex-vivo* expression of selected genes in *Scnn1b*-Tg mice tracheal epithelial cells (MTEC).

CHAPTER 2
LITERATURE REVIEW

2.1. Louisiana Alligator Farming

American alligators (*Alligator mississippiensis)* have been used commercially for their valuable leather since the 1800s and their harvest was generally unregulated through the 1900s. This resulted in severely reduced harvests in the 1950s and a hunting ban from 1962 to 1972 [35]. Since 1972, Louisiana alligators have been managed as a commercial, renewable natural resource by the Louisiana Department of Wildlife and Fisheries through a successful and world renowned sustained use program. The program regulates harvest, assures long term benefits to the survival of the species and provides significant economic benefits and incentives to private landowners to protect alligator wetland habitats [36]. After rebuilding the population through research, management and law enforcement in the 1960's, the wild harvest from 1972 through 2014 produced over 975,000 wild skins. Currently, most of the A. *mississippiensis* farming activity occurs in the southeastern United States and it is led by Louisiana [37] which supplies ca. 20% of the global commercial crocodilian skins [38]. In January 2014, there were 34 licensed farms with stock mainly in the Livingston, Terrebonne, Lafourche, St. Tammany and Vermilion parishes [36]. In calendar year 2014 alone, Louisiana sold 341,887 farm raised skins and 35,945 from wild harvest. Including all skins, meat and egg collection the industry generated over $100,000,000 in economic benefit to the state of Louisiana [39]. Singapore, Japan, Germany, France and Italy are the main high-end markets for skins at an average $8.50/cm (width) in 2013, while the meat (~3 lb./alligator) is commercialized within the United States at an average of $7.00/lb. (2011-13) [36].

Since 1986, alligator eggs have been collected from the wild between the months of June and August to be incubated in private hatcheries. Eggs are incubated at ~30 to 34°C from 1.5 to 3 months [40]. Most of the hatchlings are raised for their hide and meat, however to maintain the wild population stable, ~14% of the hatchlings are returned to the same location where they were collected [41]. The remaining ~86% of the hatchlings are placed in different types of indoor buildings (large round sheds, small rectangular sheds, etc.) under controlled air and water temperature (80°F), animal density (1 ft^2/ alligator of less than 24 inches long and 3 ft^2/ alligator of 25-48 inches long) and feeding conditions (diet with 45-55% protein) during 10 to 18 months. After slaughtering alligators at market length (≥ 4 ft.) using approved methods, hide and meat processors generate approximately 500 tons of by-products per year including ACS, AFT, ABS and AEB that are currently disposed in landfill or sold at very low prices (1¢ per lb) for pet foods. However, with increased regulations regarding pet feed, few animal feed processors are buying these by-products. Efforts have been made to better understand and increase the profitability of alligator carcasses and by-products [42], however little has been reported to date regarding feasible opportunities. Teeth, heads and skulls are also used as tourist curios. To the best of our knowledge, there are currently no processes or businesses established to utilize alligator by-products in a profitable and sustainable manner.

2.2. Medicinal Properties of Crocodilians

Since ancient times, zootherapy has been an alternative in the treatment of different illnesses. "*Medicine men*" in different tribes around the world have used animal-based traditional medicine for centuries. The folk medicinal use of crocodilians has been documented in populations in Mexico, India, and Nigeria [43–45] which leads to investigation of the existence of therapeutic

and bioactive compounds in these organisms. This becomes significant considering that these reptiles have a low incidence of diseases in the highly contaminated conditions of marshes and swamps and most of their wounds heal properly and completely [46]. Recently, studies conducted in South Africa and the United States investigated the antimicrobial, amoebicidal, anti-inflammatory and antiviral properties of crocodilian body parts [47–49]. These properties may partially explain the evolutionary success of crocodilians while living in wild and farm aquatic environments teeming with bacteria and/or agricultural residues [46,50,51].

Crocodile-based treatments play a role in the indigenous medicine of Nigerian communities. Nile crocodile (*Crocodylus niloticus*) has been reported to be used in the treatment of rheumatism (whole tail bones), snake poisoning (scales or tip of tail) and male impotency (whole male animal) [44], although scientific proof is lacking and the placebo effect not tested. In a review of traditional medicine in the state of Kerala, India, Padmanabhan and Sujana [43] reported the use of *Crocodile palustris* eggs by tribal medicine men for asthma treatment. Even though the GAG composition of crocodilian eggs has not been reported in detail, the presence of GAGs is known [52]. Abundance of GAGs, including HA, has been reported in all components of the chicken egg [53]. In China, crocodile bile is another folk medicine alternative remedy for asthma and allergies [54]. The Chinese also believe that crocodile meat can help asthma sufferers, a person getting a cold, and even improve the strength of the lungs [55], although such claims lack scientific basis. Farmed crocodile tail oil has been evaluated for the treatment of microbial infections and inflammatory conditions [47]. Buthelezi and others, showed that *Staphylococcus aureus*, *Klebsiella pneumoniae* and *Candida albicans* are susceptible to 6-15% (w/v) oil preparations. Furthermore, in an induced auricular edema mice model they showed that oral administration and

topical application of crocodile oil resulted in optimal anti-inflammatory effects after 3 h and 12 h, respectively. Many functional properties have been attributed to collagen and gelatin from different animal sources [56] and it could be that other non-proteinaceous components of the ECM, such as HA extracted along with the collagen may account for the claimed bioactivities.

It has been observed that American alligators (*A. mississippiensis*) often sustain serious injuries and damage due to territorial disputes with other alligators. However, these reptiles exhibit a remarkable ability to heal rapidly and without infection. In a cell based assay, serum collected from wild alligators demonstrated antiviral activity against human immunodeficiency virus type 1 (HIV-1), West Nile virus and Herpes simplex virus type 1 (HSV-1). These and other reports by Merchant and others suggest that alligators have evolved a complex innate immune system, however other mechanisms such as the serum complement system are also active [48,49,57]. Antimicrobial peptides extracted from *A. mississippiensis* leukocytes have displayed antibacterial activity against Gram negative and positive bacteria, antifungal activity against six pathogenic *Candida* yeast spp. species and antiviral properties against HIV-1 and HSV-1 [58]. Four novel antimicrobial peptides (leucrocins I-IV) were recently extracted and purified from Siamese crocodile (*Crocodylus siamensis*) white blood cells [59]. Multivariate analyses of the serum from all twenty-three known living members of the Crocodylia were tested for antibacterial activity against eight bacterial species and it was revealed that the innate immune activities of the Alligatoroidea were remarkable and statistically higher than those of the Crocodyloidea and Gavialoidea [60]. This brief review demonstrates that there is evidence in favor of some potential alligator-based medicine treatments, however more information must be generated to support these

practices, determine the bioactive compounds responsible for the claimed effects and elucidate action mechanisms.

2.3. Hyaluronic Acid and Sulfated Glycosaminoglycans

2.3.1. Classification and Structures

GAGs are large heteropolysaccharides that are composed of repeating disaccharide units. All GAGs are made of an amino sugar, typically n-acetylglucosamine (GlcNAc) or n-acetylgalactosamine (GalNAc), and a uronic acid, typically glucuronic acid (GlcA). However, there are two main types of GAGs. Sulfated GAGs include heparan sulfate (HS), of which heparin (HP) is a highly sulfated member, which are based on *D*-GlcNAc and *D*-GlcA or iduronic acid (IdA), respectively. Chondroitin sulfate (CS) is based on *D*-GalNAc and *D*-GlcA, while dermatan sulfate (DS) is composed of *D*-GalNAc and *L*-IdA. Keratan sulfate (KS) is the most heterogeneous GAG and is based on *D*-GalNAc and *D*-galactose. The non-sulfated GAGs include hyaluronan, also called sodium hyaluronate or HA, and it is composed of *D*-GlcNAc and *D*-GlcA bound together through β1,4 and β1,3 glycosidic bonds, respectively (Figure 2.1) [61–64]. Since HA is the major non-proteinaceous component of the ECM [5] and consequently the most abundant GAG found in alligator by-products, this literature review will focus mainly on HA's features including biosynthesis, degradation, biological properties, sources and applications.

2.3.2. Biosynthesis

HA is ubiquitously expressed in the ECM of the animal kingdom. It was first identified in the vitreous humor of cattle eyes by Meyer and Palmer in 1934 [65]. In contrast to sulfated GAGs that are produced in the Golgi apparatus, HA is synthesized at the inner face of the plasma membrane as a free linear polymer not anchored to any proteins by three transmembrane glycosyl-

Hyaluronic Acid

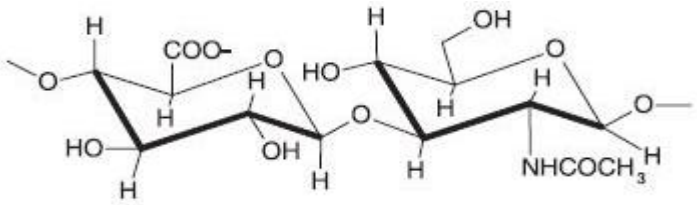

Chondroitin Sulfate

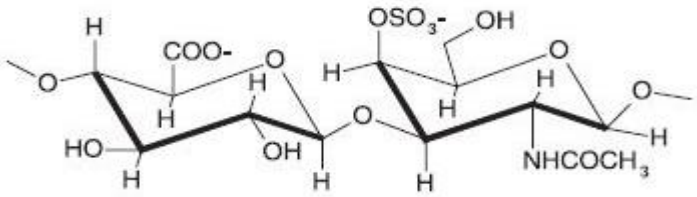

Dermatan Sulfate

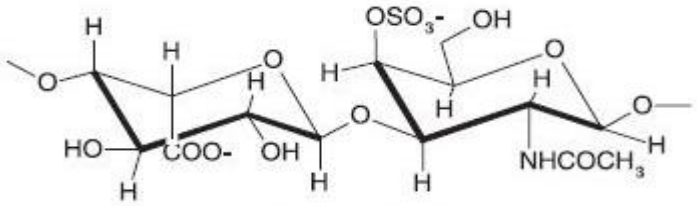

Keratan Sulfate

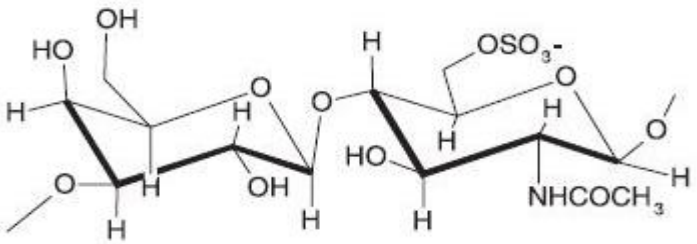

Heparan Sulfate*

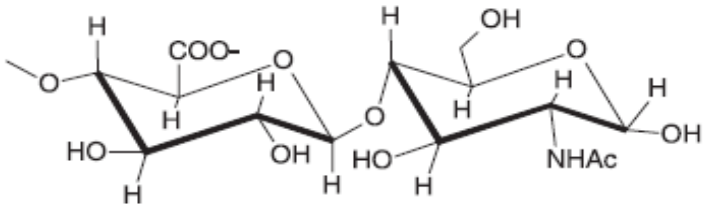

Heparin

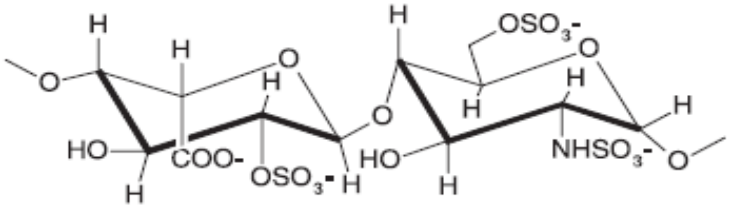

Figure 2.1. Repeating disaccharide units of the GAGs [Adapted from 10]. *HS shows a lower degree of sulfation (0.6-1.5 sulfates/disaccharide) than HP (2.3-2.8 sulfates/disaccharide) [66].

transferases or HA synthases (HAS1, HAS2, and HAS3) (Figure 2.2) [67]. Although these isozymes synthesize an identical HA molecule, they have been shown to have distinct stability, elongation rate of HA and K_m values, which potentially regulate the biological function of HA [68]. HAS2 is the main HA synthetic enzyme in adult cells and it generates HA with an extremely large and broad molecular weight distribution (>2000 kDa or a degree of polymerization around 5,000 disaccharides), whereas HAS1 (200-2000 kDa) and HAS3 (100-1000 kDa) produce shorter dipeptide chains [61,68]. HASs are regulated by a number of mechanisms from temporal expression patterns during development [69], to a wide range of cytokines and receptors [70] and/or availability of substrates for HA synthesis [61].

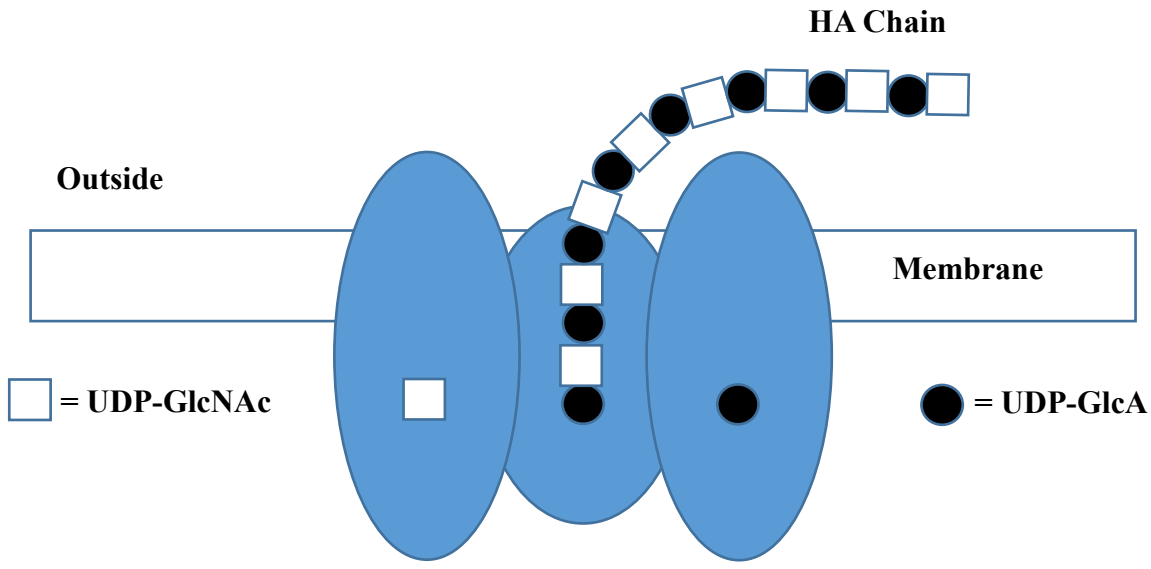

Figure 2.2. Addition of GlcNAc and GlcA by the HA transmembrane synthases

Over decades, there has been no consensus or clear nomenclature in regards to the molecular weight categorization of HA. Cyphert and colleagues recently proposed the following

designations: HMW-HA for >1000 kDa, low molecular weight HA (LMW-HA) for <1,000 kDa to >20 monosaccharides, and HA oligosaccharides (oHA) for <20 monosaccharides in length [6]. Monslow and others (2015) categorized HA sizes more distinctly as HMW-HA (>1000 kDa), medium molecular weight HA (MMW-HA) (250-1000 kDa), LMW-HA (10-250 kDa) and oHA (<10 kDa) [5]. Monslow's classification will be followed in this study. HA is usually found in synovial fluid, vitreous humor and connective tissue. Sulfated GAGs are smaller than HA and their size ranges from 4-70 kDa. CS has a molecular weight of 5-50 kDa and is found in cartilage, tendon, ligaments and arteries. DS (15-40 kDa) is found in skin, blood vessels and heart valves and KS (4-19 kDa) is found in the cornea and in cartilage aggregated with CS. HP (10-12 kDa) is a naturally occurring anticoagulant stored in mast cell vesicles especially in the liver, lungs and skin. HS (10-70 kDa) is ubiquitously expressed in animal cell surfaces [63,64,66].

2.3.3. Signaling and Biological Functions of Hyaluronan

Despite their simple chemical composition, GAGs fulfill several distinct molecular functions. For many years HA was considered an inert filler in the ECM, however it is now known that it possesses a plethora of often opposing size-dependent biological functions [71]. HA contributes not only to the structural and physiological characteristics of tissues, but also mediates cell behavior during morphogenesis, tissue remodeling, inflammation and diseases. As a signaling molecule, HA interacts with a variety of cell surface receptors to activate intracellular events to mediate cell functions [8]. HA is the main ligand to CD44, a receptor expressed on the surface of almost all human cells involved in many cell-cell interactions and in a wide variety of cellular functions [61,72]. A study by Teder and others suggests that CD44 plays a critical role in HA clearance and homeostasis following lung injury which influences the recovery from pulmonary inflammation. Moreover, they showed that mice accumulate LMW-HA following bleomycin

induced lung injury, however after inflammation is resolved, HMW-HA synthesis is predominant [73]. LMW-HA levels in the bronchoalveolar lavage (BAL) of CD44-negative mice have been reported to be 2-fold higher than wild type [74]. Jiang and others showed that HA fragments induce pro-inflammatory macrophage inflammatory protein-2 (MIP-2), the murine equivalent to human IL-8, and lung epithelial cell-specific overexpression of HMW-HA was protective against lung injury [75]. Similarly, mice and macrophages exposed to HMW-HA prior to LPS injection had greatly decreased interleukin-6 (IL-6) and TNF-α levels in serum and mRNA expression, respectively. This effect was not observed in CD44-negative mice or macrophages [76]. HA can also modulate key cancer cell functions through interaction with its CD44 and receptor for hyaluronan mediated motility (RHAMM) receptors [77].

The interaction of HA with the RHAMM can also trigger several signaling cascades including the NF-κβ pathway [61]. RHAMM is normally localized intracellularly and is only released by some poorly defined stimuli. Extracellularly, RHAMM associates with CD44 and upon binding with HA, it activates intracellular signaling pathways [8]. The interaction of RHAMM with a oHA (6-mer) was shown to play an important role in the inflammatory and fibrotic processes resulting from acute lung injury by bleomycin in mice [78]. A study using primary tracheal epithelial cell cultures treated with HA (200 kDa) at 50 ug/mL proposed a model in which HA serves a key role in mucosal host defense. HA, through its interaction with RHAMM, stimulated ciliary beating and hence the clearance of foreign material from mucosal surfaces while still regulating enzyme (lactoperoxidase and tissue kallikrein) homeostasis [79].

Toll like receptors (TLRs) are able to rapidly initiate the innate immune response, which represents the first defense against pathogens. The negative and positive effects of TLRs interaction with LMW-HA and HMW-HA, respectively, have been previously reviewed [61]. In a murine lung injury model, the knockout of TLR2 and TLR4 abolished completely the activation of chemokines in macrophages. Moreover, oHA induced the nuclear translocation of NF-κβ and production of TNF-α [75]. The expression of MMP-2 and IL-8 is also stimulated by HA fragments in part by signaling of TLR4 [80]. On the other hand in human monocytes, HMW-HA via its engagement with CD44 and TLR4 is a positive regulator of IL-1R-associated kinase-M (IRAK), which is thought to be a negative regulator of inflammatory TLR signaling [81]. HA of different sizes can also signal through the lymphatic vessel endothelial hyaluronan receptor 1 (LYVE 1) and the hyaluronan receptor for endocytosis (HARE). HARE has a complex structure including several HA and other GAG binding motifs. The binding of human or rat HARE with HA of an optimum size of 140 kDa has been shown to stimulate the activation of NF-κβ [82]. In aggregate, affinity for receptors, receptor clustering and uptake will differ depending on HA size, which may affect downstream signaling cascades. Cell type may also be a driver of differences in HA signaling.

Binding of HA with tumor necrosis factor-alpha stimulated gene-6 (TSG-6) is involved in the mediation of lymphocyte migration during inflammation. This binding results in the formation of fibrils that are pro-adhesive to lymphocytes which prevents direct contact of inflammation promoting receptors and elastases with the underlying tissues [83–86] (Figure 2.3). HA cables synthesized by mouse or human airway smooth muscle cells can also form independently without

the presence of TSG-6. These cables are capable of binding a large number of leukocytes and can sequester pro-inflammatory chemokines through interactions with CS and DS chains [87,88].

An investigation on airway responses in sheep showed that the preventive inhibitory effects of inhaled HA (3, 6, 7 or 15 mg in 3 ml phosphate buffered saline (PBS)/ sheep) against human NE-induced bronchoconstriction, could extend for at least 8 hours. Both LMW-HA and MMW-HA showed a dose-dependent inhibition of the inflammatory responses, however above 150 kDa, dose and not molecular weight was the key for effective protection [11]**.** It has been proposed that

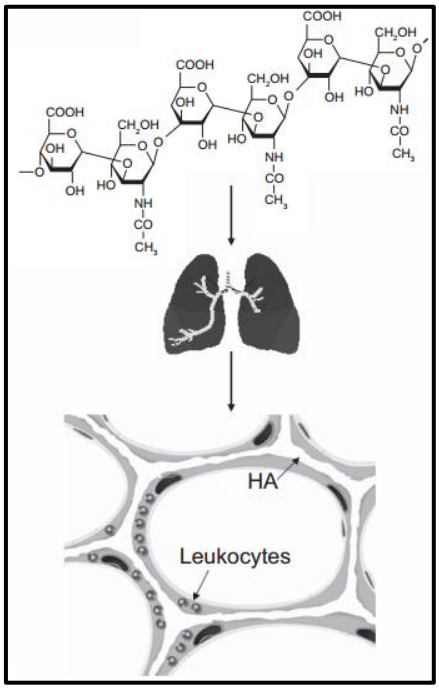

Figure 2.3 Binding of HA to alveolar septal elastic fibers upon intratracheal administration may prevent their degradation by elastases [86]

this protective effect of HA may be accompanied by an improvement in pulmonary mechanics due to HA's special ability to retain water which may help increase the elasticity of lung elastic fibers

[12]. Furthermore, lipopolysaccharide-induced TNF-α, IL-6, and interleukin-1 beta (IL-1β) in human macrophages have been dose-dependently suppressed by different doses of 2,700 kDa HA (0.01, 0.1 and 1 mg/ml). HA (800 kDa) showed no significant effect even at 3 mg/ml. The same study proposed injection of HA into arthritis joints as an anti NF-κβ agent [89].

Due to its biocompatibility, biodegradability, non-immunogenicity, water binding properties and receptors (CD44, RHAMM, TSG-6, HARE, LYVE 1), HA has drawn attention in the field of biopharmaceutics. HA-drug conjugates may be used to increase the solubility, permeability and bioavailability of several anti-cancer and anti-inflammatory drugs [90].

Iovu and others have thoroughly reviewed the anti-inflammatory activity of CS in osteoarthritis. CS and/or its disaccharides reduce inflammation (TNF-α, IL-1β, ROS and nitric oxide) in joint chondrocytes and synovial membrane through the inhibition of NF-κβ nuclear translocation [91]. The role of CS in synovial angiogenesis modulation has been suggested by Lambert and others in a study using biopsies from normal and inflammatory osteoarthritic membranes. Synovial biopsies from inflamed areas expressed pro-angiogenic phenotypes promoted by IL-1β and CS (10, 50, 200 μg/ml) dose-dependently reversed this effect [92]. In a psoriasis model using normal human keratinocytes, CS (200 or 1000 μg/ml) effectively downregulated the NF-κβ and signal transducer and activator of transcription 3 (STAT3) pathways [93]. These effects limited the release of key psoriatic pro-inflammatory cytokines such as TNF-α, IL-8, IL-6 and the cutaneous T cell-attracting chemokine (CCL27). HA, CS and DS extracted from fish have been shown to reduce gliadin-mediated inflammation, in a celiac disease model using human Caco-2 cells, through a decrease in the production of IL-1β [94]. The biological

functions of CS and DS have also been reviewed in the light of their structural interactions with microbes, cell adhesion molecules and growth factors [95]. Octasaccharides of over-sulfated CS can inhibit herpes simplex virus infections and a specific CS sequence has also been shown to be a potential target for the treatment of malaria [96,97]. Highly sulfated CS and DS bind strongly with key liver regeneration growth factors and therefore may be potential candidates for development of therapeutics [95]. Tissue regeneration properties in the central nervous system have also been attributed to CS disaccharides [98]. Regarding tumor growth, it has been shown in vivo that cisplatin-CS liposomes are avidly internalized by highly metastatic liver cancer cells which results in cell death [99]. It has also been reported that sulfated GAG-rich wound fluids markedly inhibit the antibacterial action of the antibacterial peptide LL-37 through specific GAG-LL-37 hydrophobic interactions and hydrogen bonding [100]. Finally, HA and the sulfated GAGs might also be therapeutic agents in other diseases with strong inflammatory components such as inflammatory bowel disease, atherosclerosis, Parkinson's and Alzheimer's diseases, multiple sclerosis, lupus, rheumatoid arthritis and CF [10,101–103].

2.3.4. Degradation

The human body produces thousands of dollars' worth of HA daily, however the action of HAses and ROS with aging and during diseases make its abundance and molecular weight decrease [2,3,9,104]. HAases were first termed as such in 1971 by Karl Meyer who also classified them in three distinct types based on biochemical analyses and generated end products. The first class constitutes a family of enzymes derived from animal venoms, urine, blood and sperm, among others. They are responsible for the fragmentation of HA of all sizes into short chains, down to tetra-saccharides. The second class of HAases has not been studied, however they are known as the leech HAases due to their presence in blood sucking organisms like leeches, bed bugs, ticks,

flies, mosquitoes and certain crustaceans. Microbial HAases are the third type and they decrease the permeability of the ECM to facilitate invasion of pathogens and spreading of toxins. Fungal HAases have not been characterized yet [67,105]. Higher levels of HAase expression and activity have been documented in many diseases. A type 1 HAase has been shown to have an important regulatory role in bladder cancer and increases in its relative abundance lead to increased tumor growth and proliferation [106,107]. There have also been indications that HAases are involved in the turnover of HA during early phases of lung injury and might play important roles in the pathogenesis of lung fibrosis [108]. Acute exacerbations of chronic obstructive pulmonary disease (COPD) are associated with increased HAase activity in BAL, which may contribute to airway inflammation and lung function decline [109].

The molecular weight of HA may be altered by oxidative damage [110]. The size of HA in cigarette smoke exposed mice is significantly smaller (70 kDa less in average) than HA of mice not exposed to smoke [111]. Several previous studies have reported hydroxides as the primary and sole species responsible for HA degradation [112–115]. Moreover, inhibition of ROS induced HA degradation was linked to a reduction of inflammation in bleomycin and asbestos-induced models of pulmonary fibrosis [116,117]. A murine model of allergic contact dermatitis demonstrated that an increased production of ROS is accompanied by HA breakdown to pro-inflammatory LMW fragments in the skin [118]. Other non-enzymatic reactions that may degrade HA (acidity, alkalinity, ultrasound and heat) have been reviewed in detail by Stern and others [119].

2.3.5. Sources

GAGs have a great variety of structures and biochemical features which vary depending on the source, type of tissue, age, physiological conditions and extraction methods, among others.

This variability makes GAG chains or fragments versatile to interact with many kinds of receptors and bioactive proteins. This heterogeneity however, complicates the reproducibility of yields and clinical effects.

HMW-HA was extracted from fresh cattle vitreous humor in 1934 with a reported yield of 0.25 g from 100 eyes [65]. Currently, a well-established source of HA is chicken combs. Severo da Rosa and others extracted 15 μg hexuronic acid/ mg dry tissue, which is equivalent to approximately 2.4 μg hexuronic acid/ mg wet chicken combs. The extraction of the total GAGs was conducted through acetone dehydration and choloroform: methanol delipidation followed by papain digestion and precipitation by a series of NaCl and ethanol washes [120]. These results from 42-day old animals are lower than the values reported by Nakano and others in rooster comb (4.0 μg uronic acid/ mg wet tissue) from 52-week old animals following a method in which samples were dehydrated with acetone prior to papain digestion, tricholoroacetic acid (TCA) deproteinization and dialysis [121]. Higher HA content values in rooster combs were also reported by Nakano and Sim in 1989 and the concentration was also estimated to be two-fold greater in the comb than in the wattle [122]. HA was also extracted from rooster combs by Kang and others using a method that aimed to reduce time and cost to accommodate a large-scale process. Frozen comb samples (500 g) were ground and defatted/dehydrated with acetone to yield 80 g of dry material that was extracted with sodium acetate and purified with ethanol followed by dialysis. Finally, the HA was precipitated with ethanol and heat treated to yield 1 μg dry HA/ mg wet tissue of an average molecular weight of 1200 kDa [123]. The rooster comb extraction process is facing a growing concern over the use of animal derived components in biomedical and pharmaceutical applications [33].

Fish and fish eyeballs are also a valuable source of HA GAGs. Swordfish (*Xiphias gladius*) and shark (*Prionace sp.*) vitreous humor was decomposed and clarified by centrifugation before ultrafiltration, electrodeposition and alcoholic precipitation in a process optimized by Murado and others. The reported yields were 0.055 and 0.3 g HA/ Kg of vitreous humor in swordfish and shark, respectively. In the same study, HA concentrations for pig synovial fluid (0.5-6 g HA/ L) and pig vitreous humor (0.04 g HA/ Kg) were reported [124]. GAGs have also been isolated from haddock (*Theragra chalcogramma*) by papain digestion, TCA deproteinization, dialysis, and cetylpyridinium chloride (CPC) precipitation. The Fourier transform infrared spectroscopy (FT-IR) absorption spectra of the purified haddock extracts fitted the main characteristics of GAGs and suggested the presence of CS and DS, but mainly HA [94]. Chicken (42 d old) keel cartilage has been reported to be a good source of CS following extraction with magnesium chloride. Results showed a yield of 33 mg GAGs/ g wet keel cartilage and 75.5% of the GAGs were CS with an average molecular weight of 48.5 kDa [125].

Despite the abundance of animal sources of HA, currently the main production method is microbial fermentation due to lower costs and environmental impact. Microbial HA production on an industrial scale was first achieved by Shiseido Group (Tokyo, Japan) in the 1980's and since then significant advances have been made to increase fermentation efficiency. Culture conditions (pH, temperature, culture media, agitation speed, shear stress, dissolved oxygen, bioreactor type) and batch modes (batch vs continuous) have been extensively studied to increase HA yields instead of promoting cell growth. *Streptococcus* sp. is the main producer, however the industry is facing issues due to its pathogenicity [33,104]. Recently, the production of HA by *Streptococcus equi*

subsp *zooepidemicus* in media formulated from fish by-products was investigated. The process yielded more than 2 g HA per liter with a molecular weight of 1730-1900 kDa and remarkable cost savings (>50% less than commercial media) [126]. Similarly, the yield of HA from the same bacterial strain using commercial media was 2.83 g/L with a protein content of 23.08% and average molecular weight of 538 kDa. The FT-IR spectrum showed the characteristic stretches of HA standards and excellent wound healing properties in a rat model [127].

Addressing the drawbacks of bacterial fermentation and animal sources, Novozymes (Copenhagen, Denmark) recently launched HA production by *Bacillus subtilis* using a water based process and a growth medium free of animal ingredients or toxins. Moreover, defined molecular weights can be produced [128]. Other bacteria used for recombinant HA production include *Lactococcus lactis* [129], *Agrobacterium sp.* [130], *and E. coli* [131] with yields of 0.65, 0.3 and 2.0-3.8 g/L, respectively. Recombinant HA production yields are generally lower than bacterial fermentation yields.

2.4. Cystic Fibrosis

2.4.1. Introduction

CF is a life-limiting condition that affects ~29,000 individuals in the United States and ~70,000 worldwide with an estimated frequency of 1 in 2,500 births [30,132,133]. The disease affects primarily those of European descent, however it has been reported in all races and ethnicities [15]. It is an autosomal recessive disorder specifically related to abnormalities in the expression and function of the CFTR resulting in abnormal ion transport across epithelial surfaces in the sweat glands, gastrointestinal, reproductive and respiratory systems. The abnormal salt and water transport results in viscous secretions in the airways of the lungs and pancreas ducts, leading

to obstructions that cause inflammation, tissue damage and finally failure of the organ systems [15,134]. Achieving and maintaining an optimal nutrition status is a critical component of CF care [135], however obstructive lung disease is the primary cause of morbidity and is responsible for ~80% of the mortality [15]. The median survival age has increased significantly from 33.4 years in 2003 to 40.7 years in 2013 [136] due to currently available therapies that address the CFTR defect consequences (pancreatic enzyme supplements, antibiotics, anti-inflammatory drugs and sputum thinners) or the CFTR basic defect (CFTR potentiators) [134,137].

2.4.2. History of Cystic Fibrosis

The first description of this disease in the United States was published by Dorothy Andersen, M.D. in 1938 as a pancreatic affection, however it was until 1951 that a connection was made between CF of the pancreas and widespread abnormality in epithelial salt transport [134]. In 1953, Sant'Agnese and colleagues reported that Na^+ and Cl^- levels were markedly elevated in the sweat of CF patients and pointed towards a disturbance in the sweat glands [138], leading to the development of the sweat test as a reliable diagnostic test for CF in 1959 [139,140]. In the 1980's, a number of studies supported the hypothesis that the disease's basic defect altered Cl^- permeability [141–143] and in 1989 the gene responsible for CF was cloned and called CFTR [144,145]. In the clinics, major advances in treating the symptoms and delaying disease progression have been made over the years, hence improving quality of life and increasing life expectancy. This is a result of a better understanding of the natural course of inflammation and infection which has resulted in strategies to assure prompt diagnosis, timely nutritional supplementation, early treatment of exacerbations and implementation of effective hygienic measures in and outside CF centers, among others [146].

2.4.3. The Cystic Fibrosis Transmembrane Conductance Regulator Protein

CFTR is a member of the adenosine triphosphate (ATP)-binding cassette family of transporters, which use energy from ATP hydrolysis to pump substrates across cellular membranes. It is the major epithelial ion (Cl^-) regulator located primarily in the apical plasma membrane, therefore it is key in transepithelial salt transport and fluid flow [137,147]. The amino acids of CFTR form five domains: two membrane spanning domains (MSD-1 & MSD-2), two nucleotide binding domains (NBD-1 & NBD-2) and a regulatory domain (RD). The opening of the anion pathway in CFTR requires phosphorylation of the channel by cyclic adenosine monophosphate-dependent protein kinase A (cAMP-PKA). Once the CTFR RD is phosphorylated, channel gating is regulated by ATP hydrolysis in the NBDs. The RD is dephosphorylated by protein phosphatases to return the channel to its inactive state (Figure 2.4) [134,139,147].

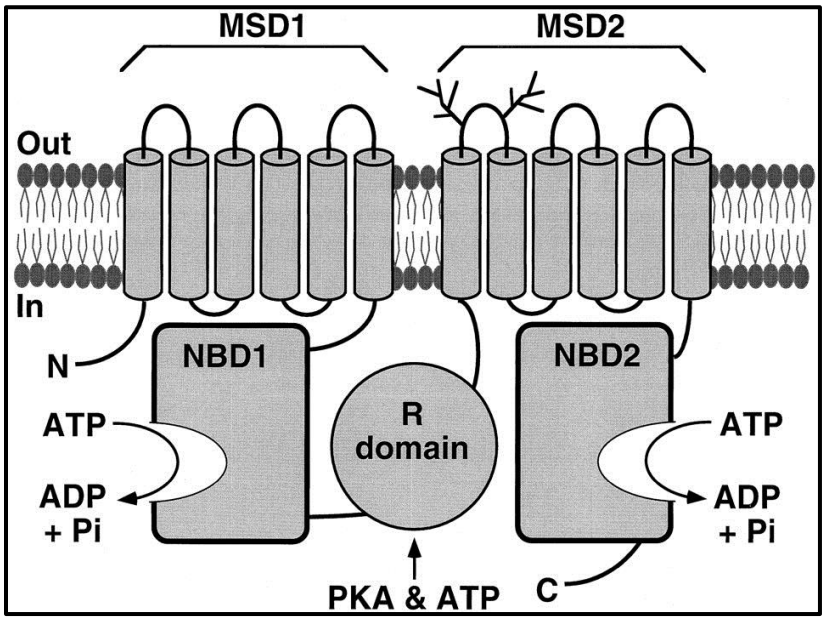

Figure 2.4. Model showing the proposed domain structure of the CFTR [147].

In addition to regulation of CTR function by nucleotide binding and phosphorylation, the amount and quality of CFTR production are also tightly regulated in the endoplasmic reticulum [148].

The CFTR is directly responsible for CF and a person must have two abnormal CFTR genes to manifest the disease. According to the CFTR Mutation Database (http://www.genet.sickkids.on.ca/), there are six classes of CFTR mutations which include 2,006 different mutations [149] that result in a particular phenotype (Figure 2.5).

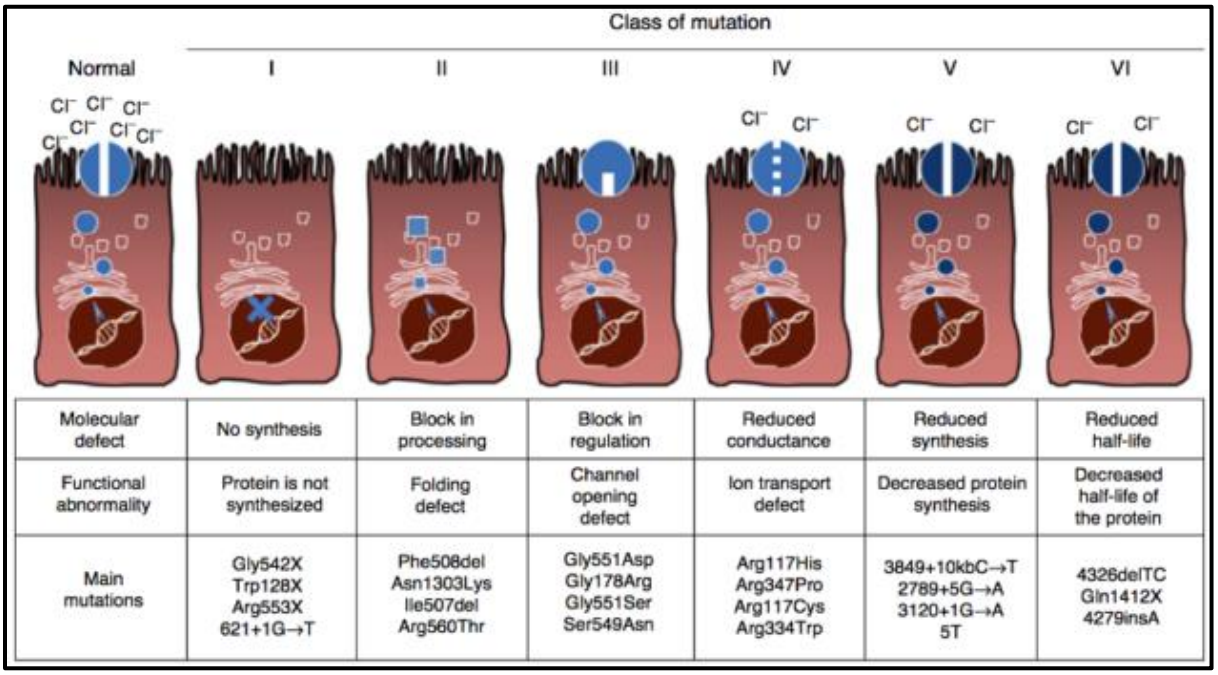

	Normal	I	II	III	IV	V	VI
Molecular defect		No synthesis	Block in processing	Block in regulation	Reduced conductance	Reduced synthesis	Reduced half-life
Functional abnormality		Protein is not synthesized	Folding defect	Channel opening defect	Ion transport defect	Decreased protein synthesis	Decreased half-life of the protein
Main mutations		Gly542X Trp128X Arg553X 621+1G→T	Phe508del Asn1303Lys Ile507del Arg560Thr	Gly551Asp Gly178Arg Gly551Ser Ser549Asn	Arg117His Arg347Pro Arg117Cys Arg334Trp	3849+10kbC→T 2789+5G→A 3120+1G→A 5T	4326delTC Gln1412X 4279insA

Figure 2.5. Classification of CFTR mutations [150].

The F508del mutation is associated with severe CF and it is the most common mutation occurring in ~86.4% of patients in one or both alleles. This is a class II mutation in which the CFTR protein is created but misfolded, keeping it from reaching the cell surface, specifically due to a phenylalanine residue deletion in the 508 position [145]. Other CFTR mutation classes include

nonsense mutations (Class I), altered gating mutations despite expression of full length protein (Class III), misense mutations resulting in lowered Cl^- permeability (Class IV), insufficient synthesis of CFTR (Class V) and reduced CFTR half-life in the apical membrane mutations (Class VI) [133,134,150]. These dysfunctions in the CFTR disrupt ion transport in the epithelia of various organs which results in the many manifestations of the disease, from airway disease and pancreatic failure to male infertility and elevated electrolyte levels in sweat [138,151–153].

In addition to its role in Cl^- transport, the CFTR in its active state negatively regulates the epithelial Na^+ channel (ENaC). Since Cl^- conductance is defective in CF, ENaC currents are not inhibited resulting in increased Na^+ absorption in the airway epithelium and depletion of the airway surface liquid (ASL) which is known as the "low-volume hypothesis" [154–157] (Figure 2.6).

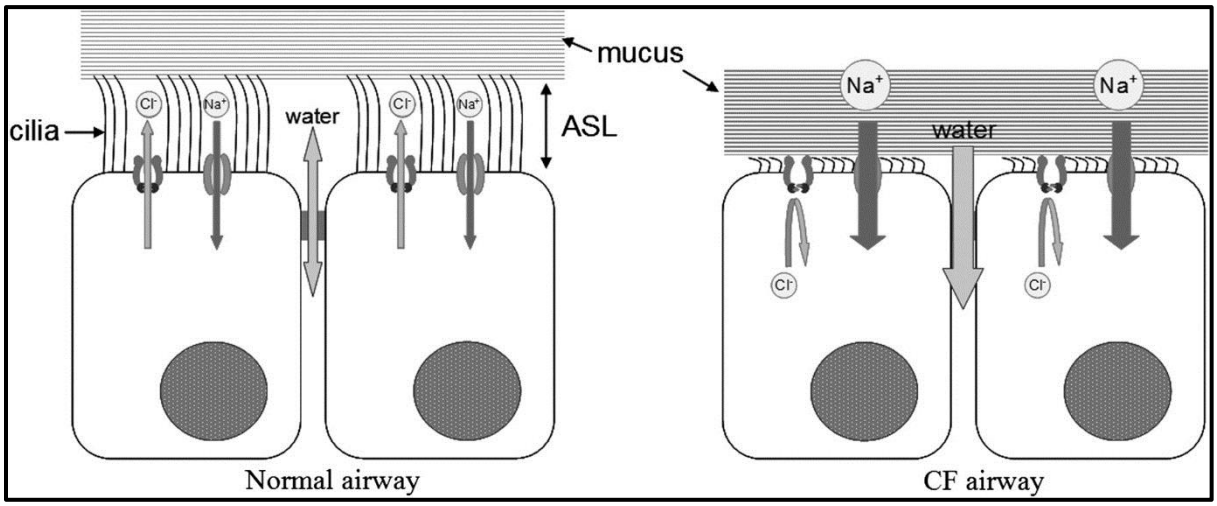

Figure 2.6. Low volume hypothesis for CF [158].

2.4.4. Diagnosis

Nationwide newborn screening for CF has been in place since 2010 and even earlier in some states. As a result, a growing proportion of people are now diagnosed in infancy and in 2014, 63.7% of new diagnoses were detected within the first year of life and often before the onset of symptoms [133,136]. There is consensus that CF is diagnosed based on evidence of CFTR abnormality (sweat test or genotyping) and characteristic phenotypic features or family history. There has been a decrease in the use of sweat electrolyte testing due to an increased reliance on genetic testing, however the challenges of using genetic analysis alone are that it does not provide information about the gene product or function and all of the mutations might not be identified [139,159,160]. Early diagnosis and treatment have led to better lung function and nutritional outcomes later in life, however the disease continues to be characterized by a number of life threatening symptoms.

2.4.5. Airway Pathophysiology in Cystic Fibrosis

Abnormal CFTR expression in the human bronchus affects predominantly the submucosal glands. [161,162]. Clinicians often describe CF as a vicious cycle of airway inflammation, obstruction and infection in which each of these components contributes to the progression of the lung disease [163]. The main cause of death is due to chronic inflammation and persistent infections with *Pseudomonas aeruginosa* and other pathogens. This section focuses only on the pulmonary aspects of this genetic disease and does not include other important aspects of this illness including gastrointestinal, endocrine and metabolic manifestations.

CF leads to severe pathological changes in the airway epithelium as it induces an early, intense and constitutive inflammatory process even before the onset of bacterial infection [21].

This congenital pro-inflammatory phenotype is caused by an innate increase in ROS promoted by misfolded protein stress and TGAse-driven defective autophagy of misfolded or damaged CFTR aggresomes [164–166]. It has also been demonstrated in human CF epithelial cell lines and in adult CF mice (F508del) that TGAse is a driver of inflammation in CF airways and it can be upregulated by ROS [29]. This inflammatory process leads to the increased expression of NF-κβ and pro-inflammatory cytokines as well as a large recruitment of neutrophils [17–20]. Moreover, the excessive production of the serine protease NE, overwhelms the normal anti-proteinase capacity and results in irreversible airway structural damage which overwhelms the normal repair pathways [167,168]. Although NE's physiological role is to degrade phagocytosed proteins, it also degrades structural proteins like elastin, collagen, fibronectin and proteoglycans causing damage to the airway epithelia [169,170] and contributing to bronchiectasis progression. NE is also the most significant predictor of bronchiectasis in early-life CF [171]. It has been reported that neutrophils from CF patients release significantly more ROS that neutrophils from healthy individuals [172], thus further perpetuating the inflammatory response. Furthermore, the lysis of neutrophils results in large amounts of DNA that contribute to the increased viscosity and adhesiveness of lung secretions and formation of mucous plugs [173].

The airway tissue damage and the ion transport defects in CF epithelia cause deficiencies in mucociliary clearance (MCC) that result in airway obstruction. Sodium hyper-absorption and defective chloride secretion drive increased water absorption by osmosis which reduces mucus clearance and increases mucus adherence resulting in a reduced ASL height [158]. The ASL consists of two layers above the epithelial surface: a mucus layer and a perciliary liquid layer [174] and it has been suggested in mouse, human and in vitro studies that its hydration status predicts

the outcome of therapeutic interventions [156,175,176]. Understanding of this pathological condition is critical as MCC is recognized as the primary physiologic defense mechanism and it is used as an outcome measure in the development of new physical and pharmacological therapies for patients with CF. Moreover, for normal MCC to occur it is necessary that the airway epithelial cells are intact [177] and as discussed previously this is compromised in CF airways due to the exaggerated expression of NE. It has been demonstrated in vitro that mucus transport is lost within 24 h in CF cultures, compared to up to 72 h in normal airways, mainly as a result of increased absorption of liquid from the culture surface [178]. A study in mice with airway-specific overexpression of ENaC, demonstrated that the lungs are normal at birth, however there is an early surface dehydration, increased mucus concentration and increased mucus adhesion that produce mucus plugging which triggers airway inflammation and is associated with early mortality [179]. In humans, large volumes of viscous mucopurulent sputum are accumulated putting patients at a higher risk of developing lung infections [180]. A long term clinical study measured a significant reduction in pulmonary exacerbations, compared to a control group, upon the administration of hypertonic saline solution twice daily during 48 weeks (4 ml of 7% saline) [181]. Likewise, Donaldson and others reported an improvement in MCC after a 14-day saline treatment (5 ml of 7% saline) four times daily. Despite improvement in treatments, decreased lung function and COPD have been and continue to be the leading cause of CF morbidity and mortality [182–184].

Along with obstructive pulmonary disease, chronic infections represent a serious problem for most individuals with CF and it is considered a paradox that the large numbers of neutrophils present in the CF airways fail to effectively kill colonizing bacteria [167]. Bactericidal activity has been reported in CF epithelia at low NaCl concentrations, however the CF ASL has a high NaCl

concentration which reduces bactericidal activity [151]. More recently, Pezzulo and others (2012) showed that the lack of CFTR reduces bacterial killing in newborn pigs and in primary epithelial cultures. This result was linked to a lower ASL pH in CF pigs compared to their wild-type counterparts and further linked to a HCO_3^- transport deficiency. CFTR facilitates HCO_3^- secretion, therefore its absence or malfunction causes the ASL pH to fall which inhibits antimicrobial function, reduces MCC and finally facilitates bacterial colonization [185,186]. Similarly, Nordin and others (2013) investigated the expression pattern and activity of the antibacterial growth factor midkine in CF lung tissue. Midkine was present at 100-fold higher levels in CF sputum when compared with sputum from healthy control subjects, however it was subject to increased degradation into smaller fractions by NE which impaired its bactericidal properties against *P. aeruginosa*. Increased salt and acidity also impaired its bactericidal properties in vitro [187].

Bacterial infections in CF frequently have an age-dependent sequence (Figure 2.7). In 2014, the CF Foundation reported that early infections are most frequently caused by *Staphylococcus aureus, P. aeruginosa and Haemophilus influenzae,* however *P. aeruginosa* is by far the most significant pathogen throughout the life of CF patients [133,188]. There is evidence indicating that in young children with CF, early *P. aeruginosa* infection gradually declines lung function and increases the risk of morbidity and mortality [189,190]. Additionally, Aaron and others (2015) constructed a statistical model to assess the 1-year risk of death for CF patients using data from 1970 up to 2010 and concluded that having *Pseudomonas* plays a critical role especially when a patient's overall health is moderately to severely compromised [191]. Even though the prevalence of *P. aeruginosa* continues to decrease due to prevention of initial infection, there is still a prevalence of multi-drug resistant *P. aeruginosa* (18.1% of CF patients in 2014). A five-fold

increase in prevalence of methicillin resistant *S. aureus* has also been reported which becomes critical as *S. aureus* isolation has been proposed as a risk factor for initial *P. aeruginosa* infection in young CF patients [192].

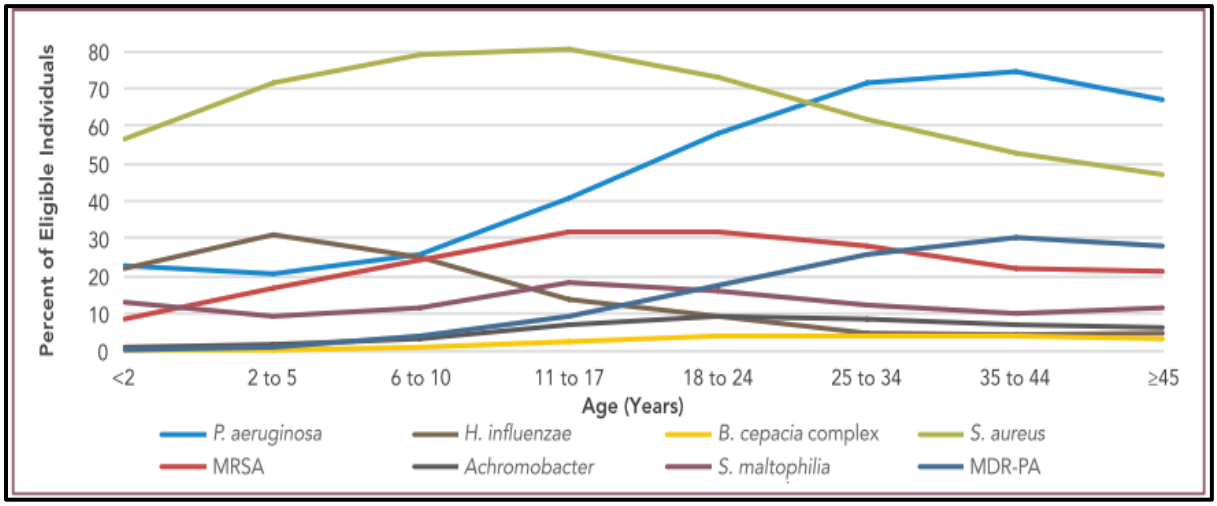

Figure 2.7. Prevalence of Respiratory Microorganisms by Age Cohort, 2014 [133].

In CF patients *P. aeruginosa* has demonstrated a very high level of adaptation and mutability to establish a persistent infection, likely caused by the large diversity of infecting organisms, ineffective host defenses and ongoing antibiotic therapies [188,193,194]. Among the organisms identified later in the course of CF disease are: the *Burkholderia cepacia* complex, *Strenotrophomonas maltophilia*, *Achromobacter*, *Aspergillus* and other non-tuberculous mycobacteria [195–200]. Of these, the *B. cepacia* complex is the most dangerous because of its rapid progression to death through high fevers and bacteremia [188].

2.4.6. Current Treatment

Current CF clinical practice guidelines recommend individuals ages 6 and older to visit care centers at least four times per year to conduct microbiological cultures, perform pulmonary

function tests, receive an influenza vaccine, measure liver enzyme levels and blood levels of fat-soluble vitamins [136]. CF is a disease that requires more intensive treatments as the disease progresses, therefore the availability of multiple pulmonary therapies is beneficial. Typically, chronic pulmonary therapies with dornase alfa, hypertonic saline, ibuprofen and/or tobramycin, among others, are a major component of the treatment regime [133,201,202] (Figure 2.8). DeWitt and others (2008) estimated the United States mean annual cost of care for patients with CF with mild impairment in lung function to be over $43,000. These costs are driven by medications, but also include hospitalization costs, emergency room and home nursing visits and indirect costs associated with missed school or work days [203]. More recently, similar costs (€26,335 - €76,271) were reported for patients in the United Kingdom depending on the severity of the disease [204].

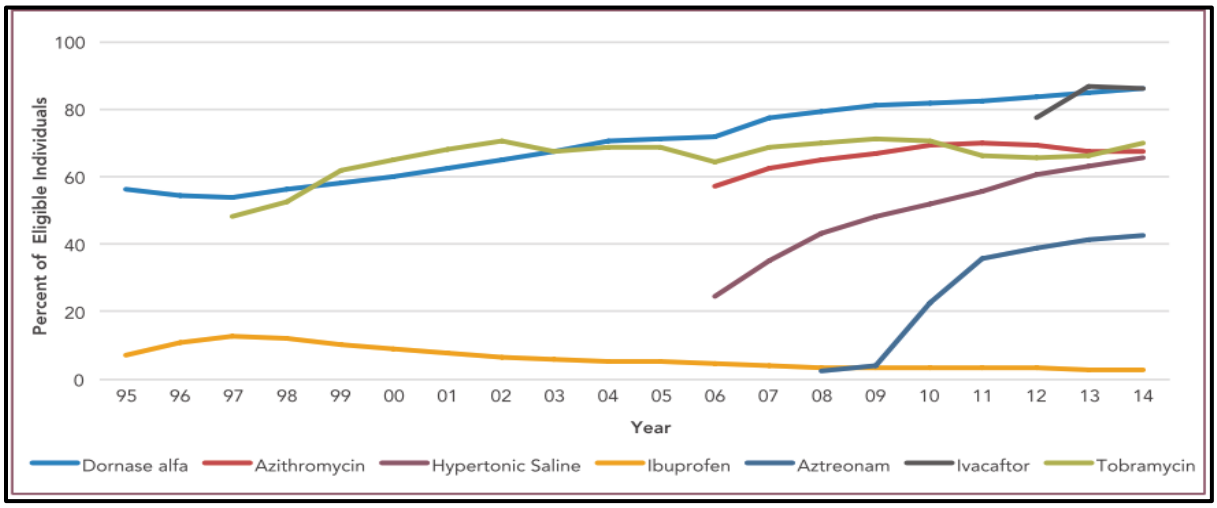

Figure 2.8. Chronic Medication Use in CF Patients, 1995-2014 [133].

Dornase alpha is an orphan drug described as a recombinant human deoxyribonuclease (DNase) that hydrolyzes DNA present in the sputum of CF patients, reducing the lung viscosity and improving MCC [205,206]. The nebulized use of this DNase is prescribed for the majority of

the population and more than half is prescribed hypertonic saline either in place of, or in addition to dornase alpha [133]. In a multicenter study of 48 CF patients, 18 months treatment (2.5 mg/day) with dornase alpha reduced DNA load in BAL [207]. A 3-year multicenter study with 105 patients reported on the positive influence of dornase alpha on airway inflammation. It was shown that neutrophil content, NE activity and IL-8 remained stable in patients treated with DNase compared to control and untreated subjects [208]. Two week dornase alpha treatment has also been shown to improve forced expiratory volume in 1 second (FEV_1) in 67% of patients independently of weight, age or baseline FEV_1 [205]. More recently, it was reported that DNase treatment (25 µl of 1 mg/ml) in mice eliminates lung neutrophil extracellular traps and improves lung mechanics, however it does not prevent airway inflammation [209].

Hypertonic saline (HTS) is also available to CF patients as a means to restore ASL. HTS is defined as a solution possessing an osmotic pressure greater than that of physiologic isotonic NaCl solution (0.9%) and popularity of its use has increased on the basis of a number of studies [210]. Inhalation of HTS has been reported to increase airway antioxidant levels, improve MCC, increase ASL hydration, and inhibit ENaC, among other positive effects. In a study on adult CFTR knockout mice, nebulized 7% sterile HTS (2 mL/mouse) promoted an increase in glutathione, an airway antioxidant that can protect the airways from hypochlorous acid mediated injury [211]. A long term (48 weeks) clinical study with 164 CF patients showed that patients treated with 7% HTS (4 ml twice daily) had significantly higher forced vital capacity (FVC) and FEV_1, as well as fewer pulmonary exacerbations than control patients. Furthermore, significant improvements in quality of life were observed [181]. HTS at a concentration of 3% or higher is used to create an osmotic gradient that draws water into the airway surface, therefore improving ASL and

facilitating MCC [212]. The findings of a human study by Hebestreit and others indicate a significant inhibition of luminal sodium conductance by HTS which may be associated with improved fluid transport across the respiratory epithelium, improved MCC and increased lung function [213]. There is also increasing evidence suggesting that HTS is beneficial through its anti-inflammatory properties due to reduction of IL-8 concentrations and neutrophil chemotaxis in CF airways [210]. Moreover, HTS has the ability to reduce bacterial activity and biofilm formation [214,215]. Finally, the tolerability and pleasantness of 7% HTS can be significantly improved when administered together with 0.1% HA, thus improving adherence to HTS therapy due to reduced cough, throat irritation and saltiness [24,32].

Symptomatic therapies to treat CF patients include non-chronic use of high-dose ibuprofen (25-30 mg/kg) [133,216]. Ibuprofen administered twice daily for four years (50-100 μg/ml in plasma) to CF patients (5-39 years old) with mild lung disease resulted in a slower annual rate of change in FEV_1 compared to patients assigned to placebo [217]. Similarly, a long term clinical study with children and adolescents with CF concluded that ibuprofen treatment significantly slowed the rates of FEV_1 decline compared to untreated subjects [218]. In both studies the side effects were not serious or the apparent benefits of ibuprofen therapy outweighed the small risks. Despite its apparent benefits, ibuprofen is infrequently used due to the need to measure plasma levels and because of the potential renal and gastrointestinal side effects [146].

Anti-infective pulmonary therapies with inhaled tobramycin, inhaled aztreonam or azithromycin are also widely used in 69.8%, 42.5% and 67.5%, respectively, of CF patients ($\geq$ 6 years) infected with *P. aeruginosa* [133]. Tobramycin is the established standard of antibiotic care

in CF. It is an aminoglycoside antibiotic that has shown a sustained improvement in FEV_1 upon chronic inhaled administration over 2 years [219]. In a multicenter study of 520 patients, intermittent administration of inhaled tobramycin for 6 months showed significant improvement in lung function after two weeks and the effects were maintained throughout the study [220]. Tobramycin exerts its antimicrobial activity by binding to the bacterial ribosome and inhibiting protein synthesis, thus inhibiting growth and division of the bacteria [221]. A recent study showed that the combination therapy of HA plus tobramycin is effective in the treatment of bacterial rhinosinusitis in CF [31]. Long-term treatment with azithromycin is also included in the current guidelines for CF patients older than 6 years. Although it is not active against *P. aeruginosa*, azithromycin can interfere in some bacterial activities and make them more susceptible to antibiotic treatment [222]. Aztreonam was recently approved (2010) for the treatment of CF and an aztreonam vs tobramycin comparative study demonstrated that aztreonam patients had fewer respiratory hospitalizations [223]. Early anti *P. aeruginosa* antibiotics have been demonstrated to successfully prevent chronic infection and improve clinical outcomes, however there is still debate on the side effects of long term treatment, most importantly the development of antibiotic resistance in airway pathogens.

GAGs have been investigated as potential molecules for the treatment of CF and airway disease symptoms due to their water-retaining, re-epithelizing and anti-inflammatory properties, among others. Nebulized 300-500 kDa HA (0.5 mg HA/animal/day for 7 days) was effective in controlling inflammation in vivo in mice CF airways as well as in vitro in human airway epithelial cells (100 μg HA/ml for 24 h) [10]. Adult sheep treated with nebulized 150 kDa or 300 kDa HA (3-15 mg/ewe), dose dependently improved their pulmonary resistance after challenge with human

NE [11]. Moreover, seven days after treatment of cultured ovine tracheal cells with HA, ciliary beat frequency increased by 16% which may be indicative of the late expression of an HA-binding receptor in this particular culture [224]. Researchers have also proposed the pivotal role of HA in mucosal host defense by stimulating ciliary beating through its interaction with ciliary RHAMM [79]. Finally, intranasal use of sodium hyaluronate (9 mg twice daily for 30 days) in patients undergoing functional endoscopic sinus surgery for nasal polyposis significantly improved MCC and other important clinical parameters [225].

The anti-inflammatory and tissue regeneration properties of sulfated GAGs have been reviewed in various diseases, however the results have not been promising in relation to symptomatic treatment of CF. For example, a pilot clinical study demonstrated no evidence of improved FEV_1, MCC or inflammation markers with a dose of 50,000 IU of heparin twice daily for two weeks [226]. Furthermore, it has been shown that high expression of CS and HS in normal and CF human lung tissue, facilitate the binding of IL-8 protecting it from proteolysis and prolonging its activity [227,228].

2.4.7. Markers of Inflammation in Cystic Fibrosis

Dysregulated inflammation is an early event in CF and it has a direct link to defective CFTR. The CFTR mutations lead to an increase in TGAse levels and activity which result in the cross-linking and proteasome degradation of the peroxisome proliferator-activated receptor-γ (PPARγ), a key negative regulator of inflammatory gene expression [30]. This defect perturbs the regulation of the NF-κβ pathway causing excessive production of inflammatory mediators [229]. It has also been shown that the most characteristic feature of airway inflammation in CF is

a persistent influx of neutrophils and an increased NE burden, driven by host and bacterial chemo-attractants [16,230]. IL-8 is the major neutrophil chemo-attractant and its levels are elevated in the BAL, sputum and serum of CF patients [231–233]. In healthy tissues, IL-8 is barely detectable, but it is rapidly increased in response to pro-inflammatory cytokines, *P. aeruginosa* or cellular stress [234,235]. Increased concentrations of other pro-inflammatory cytokines, such as IL-1β, TNF-α and IL-6 have also been detected in CF airways [236–238]. Furthermore, the high NE load in CF airways has been hypothesized to trigger the senescence of epithelial cells which can be in a pro-inflammatory state. Three different senescence biomarkers were shown to be increased in CF airways compared to control subjects, therefore contributing to the perpetuation of chronic inflammation [239]. Most research focuses on increased activation of inflammatory responses, however there is also an inability to resolve inflammation due to deficiencies in the expression of anti-inflammatory molecules including interleukin-10 (IL-10), nitric oxide and lipoin-A_4 [240]. IL-10 is not thought to be under direct control of NF-kB, however it terminates acute inflammatory responses, downregulates production of TNF-α, IL-6, IL-1β and IL-8 by macrophages, inhibits pro-inflammatory transcription factors and induces neutrophil apoptosis [236,240,241].

CHAPTER 3
MATERIALS AND METHODS

3.1. Experimental Design and Statistical Analysis

A completely randomized block design (CRBD), with three GAG extractions (repetitions) as the blocking units, was used to test equality of means among treatments. The null (H_o: $\mu_1 = \mu_2 = \mu_3 = \mu_4$) and alternate ($H_a$: some μ_i is different) hypotheses were stated and all experiments and analyses were conducted in triplicates. Analyses of variance (ANOVA) using Proc GLM were conducted along with post-ANOVA Tukey pairwise tests using the Statistical Analysis System (SAS®) version 9.4 Results were reported as means ± standard deviations (SD) and differences were considered significant at $p \leq 0.05$.

The gene expression analysis experiments were carried out in triplicate and statistical analysis was performed using the SABiosciences PCR Array Data Analysis Web-based software which calculated fold-regulation *p-values* using a Student's t-test on the fold-change values for each gene in the treatment group compared to the control group ($p \leq 0.05$). ANOVA and post-ANOVA Tukey pairwise tests using the Statistical Analysis System (SAS®) version 9.4 were conducted to evaluate RNA purity and PCR control gene expression. Results are presented as means ± standard error (SE) ($p \leq 0.05$).

3.2. Materials

Butyl alcohol (Cat. No. W217820), 2-mercaptoethanol (Cat. No. M-7154), absolute etanol for molecular biology (Cat. No. E7023), porcine pepsin (Cat. No. P7125), L-cysteine (Cat. No. W326305), ethylenediaminetetraacetic acid (EDTA) (Cat. No. E9884), sodium chloride (Cat. No.

793566), crystalline carbazole (Cat. No. C5132), sodium tetraborate decahydrate (Cat. No. B9876), HAase type 1 from bovine testes (607 U/mg) (Cat. No. H3506), ChrAse ABC from *Proteus vulgaris* (Cat. No. C3667), CS-A from bovine trachea (Cat. No. C9819), Stains-All 95% (Cat. No. E9379), gel loading buffer (Cat. No. G2526), single use micro DispoDialyzers™ (50 kDa molecular weight cut-off (MWCO)) (Cat. No. D9187) and dialysis cellulose tubing (14 kDa MWCO) (Cat. No. D9402) were purchased from Sigma Aldrich (St. Louis, MO). Absolute ethanol 200 proof (Cat. No. 111000200) was purchased from VWR (Radnor, PA). Sodium hydroxide (Cat. No. S318-3), acetic acid (Cat. No. UN2789), urea peroxide (Cat. No. ACS241020010), EMD Millipore ACS grade sulfuric acid (Cat. No. MSX1244PC5), hydrochloric acid (HCl) ACS grade (Cat. No. S25838), monobasic anhydrous sodium acetate (Cat. No. BP3331), Invitrogen™ Novex™ sharp pre-stained protein standard (Cat. No. LC5800) and HA standard from *Streptococcus* sp. (94%) (Cat. No. AC251770010) were obtained from Fisher Scientific (Pittsburgh, PA). Papain (Cat. No. 102566) was acquired from MP Biomedicals (Santa Ana, CA). UltraPure™ agarose (Cat. No. 16500500) and tris borate-EDTA (TBE) buffer (Cat. No. 15581044) were obtained from Thermo Fisher Scientific (Waltham, MA). Select-HA™ low polydispersity HA standards HiLadder (1648, 1138, 940, 667, 509 kDa) and LoLadder (509, 310, 213, 111, 30.2) (Cat. No. HYA-HILAD-20 and HYA-LOLAD-20) were purchased from Hyalose (Oklahoma City, OK). Bovine serum albumin (BSA) (Cat. No. SC-2323) was purchased from Santa Cruz Biotechnologies Inc. (Dallas, TX). Sodium phosphate (Cat. No. 0571), sucrose (Cat. No. 0335), and ultrapure grade Tris-HCl (Cat. No. 0234) from Amresco (Solon, OH).

For the CF *ex-vivo* mice study retinoic acid (Cat. No. R2625), insulin (Cat. No. 91077c), transferrin (Cat. No. T8158), cholera toxin (Cat. No. C8052), bovine pituitary extract (Cat. No.

P1476), pronase from *Streptomyces griseus* (Cat. No. 10165921001) and DNase 1 from bovine pancreas (Cat. No. DN25) were purchased from Sigma Aldrich (St. Louis, MO). Corning™ Nu-Serum growth medium supplement (Cat. No. CB-51000), Y-27632 ROCK inhibitor (Cat. No. BDB562822), rat tail collagen I (Cat. No. CB-354249), Corning™ fetal bovine serum (FBS) (Cat. No. 11648647), methyl sulfoxide (>99.8%) (Cat. No. AC327182500), phosphate buffered saline solution (pH 7.4) (Cat. No. 10010031), recombinant mouse epidermal growth factor (Cat. No. PMG8041), Dulbecco's Modified Eagle Medium (DMEM)/Ham's F-12 (1:1) (HEPES) (Cat. No. 11330-032), Gibco™ penicillin-streptomycin (10,000 U/ml; 10,000 mg/ml) (Cat. No.15-140-122), Corning™ Primaria™ tissue culture dishes (Cat. No. 08-772-4A), Corning™ Costar™ Transwell™ clear polyester membrane inserts for 12-well plates (Cat. No. 07-200-161) and Falcon™ 6-well tissue culture plates (Cat. No. 0877233) were obtained from Fisher Scientific (Pittsburgh, PA).

3.3. Extraction of GAGs from Alligator Carcasses, Feet and Backstraps

Farmed AFT (2 anterior & 2 posterior) and ABS were collected from Vermilion Gator Farm Inc. in Abbeville, Louisiana and waste ACS were provided by Jacques' Croc's and Farm Pride (Scott, LA). All animals were between 12 and 18 months old at the time of slaughter and samples were kept at -20°C until used for GAG extraction at the Louisiana State University School of Nutrition and Food Science (Baton Rouge, LA).

A Baader® 693 bone separator (Indianola, MS) was used to process ACS and separate bones from meat. Three passes through a perforated stainless steel drum (Ø = 3 mm) were performed at increasing belt pressures (20, 30 and 40 bar). Only bones including connective tissue were used for GAG extraction from ACS. AFT and ABS were ground in a Hobart HCM450

grinder-mixer (Troy, OH) prior to GAG extraction. The extraction process (Figure 3.1) was developed by adapting methods previously reported by Ogawa and others [242], Losso and others [243], Kittiphattanabawon and others [244], Severo da Rosa and others [120] and Garnjanagoonchorn and others [245]. To remove non-collagenous proteins and bleach skin pigments, the ACS, AFT or ABS were mixed with 0.2N NaOH at a sample: solution ratio of 1: 2.5 (w/v), in addition to 0.5% (w/w) urea peroxide. The mixture was stirred intermittently for 12 h with a solution change after 6 h. The deproteinized samples were defatted with 20% butyl alcohol (1:2.5 w/v) for 3 h and for removal of inorganic compounds samples were soaked in a 0.2N HCl solution (1:2.5 w/v) for 3 h with manual stirring once every hour. Samples were filtered through cheese cloth and washed in running tap water after every step. For collagen proteolysis, the deproteinized, defatted and demineralized samples were finely ground with 1M acetic acid (1:2 w/v) and mixed with pepsin (0.3% w/w). Pepsin proteolysis was conducted for 4 h at 40°C, followed by addition of papain (0.3% w/w) for 12 h at 60°C. Prior to use, papain was activated in 1:1 (w/v) digestion buffer (100 mM Na acetate, 5 mM L-cysteine, 5 mM EDTA). A double layer of cheesecloth was used to filter the resulting clear solution and the filtrate was collected, centrifuged (7,000 rpm/ 20 min/ 20°C) and filtered again using filter paper (Whatman No. 4). Samples were dialyzed at 4°C using a 14 kDa MWCO cellulose membrane against distilled water for 24 h, with solution changes every 8 h. The dialyzed samples were mixed (1:1 v/v) with a solution composed of 2M NaCl: absolute ethanol (5:1). Absolute ethanol was added (1:2 v/v) and GAGs were precipitated for 12 h at -20°C. The pellet was dissolved in distilled water prior to a heat treatment (90°C/ 5 min) to inactivate enzymes and disinfect samples. Finally, samples were centrifuged to discard the pellet and collect the supernatants which were freeze dried in a VirTis

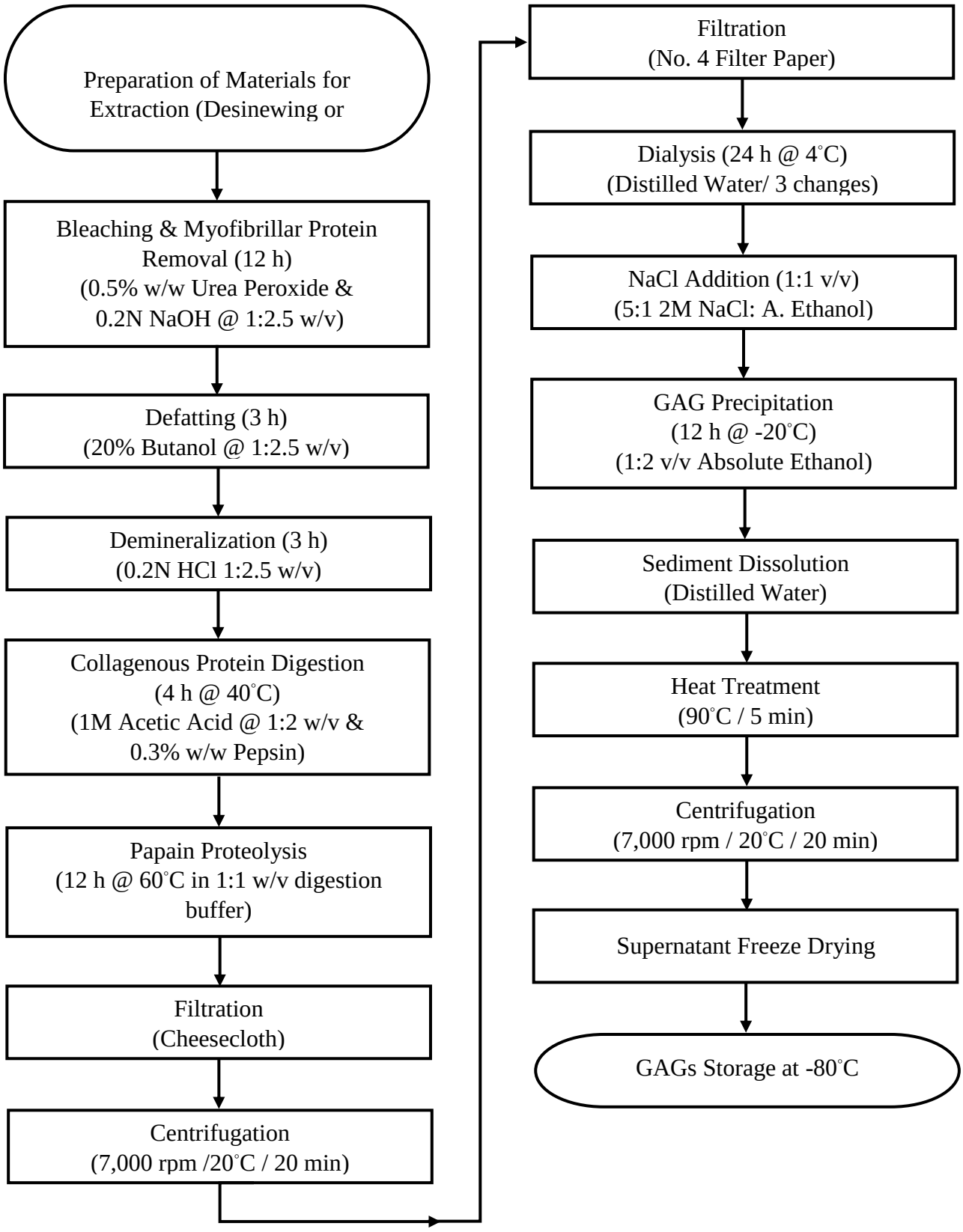

Figure 3.1. Process diagram of GAG extraction from alligator ACS, AFT and ABS.

Genesis 35XL pilot lyophilizer (Stone Ridge, NY) during 24 hours. Dry samples (< 5.0% moisture content) were stored at -80˚C until analyzed.

3.4. Extraction of GAGs from Alligator Eyeballs

Farmed AEB were manually collected from heads at Vermilion Gator Farm Inc. in Abbeville, Louisiana. Alligator eyeball GAGs were obtained as reported by Murado and others with modifications [124]. AEB were cut vertically in half using a sharp scalpel blade to extract the vitreous humor (Figure 3.2). Subsequently, the vitreous humor was dissolved in distilled water (1:1 v/v) and homogenized in order to deconstruct it. Subsequently, the humor was clarified by centrifugation at 7,000 rpm (20 min / 4 °C). Two clear phases were obtained: dark sediment of impurities and a majority of vitreous humor supernatant. The supernatant was collected and protein

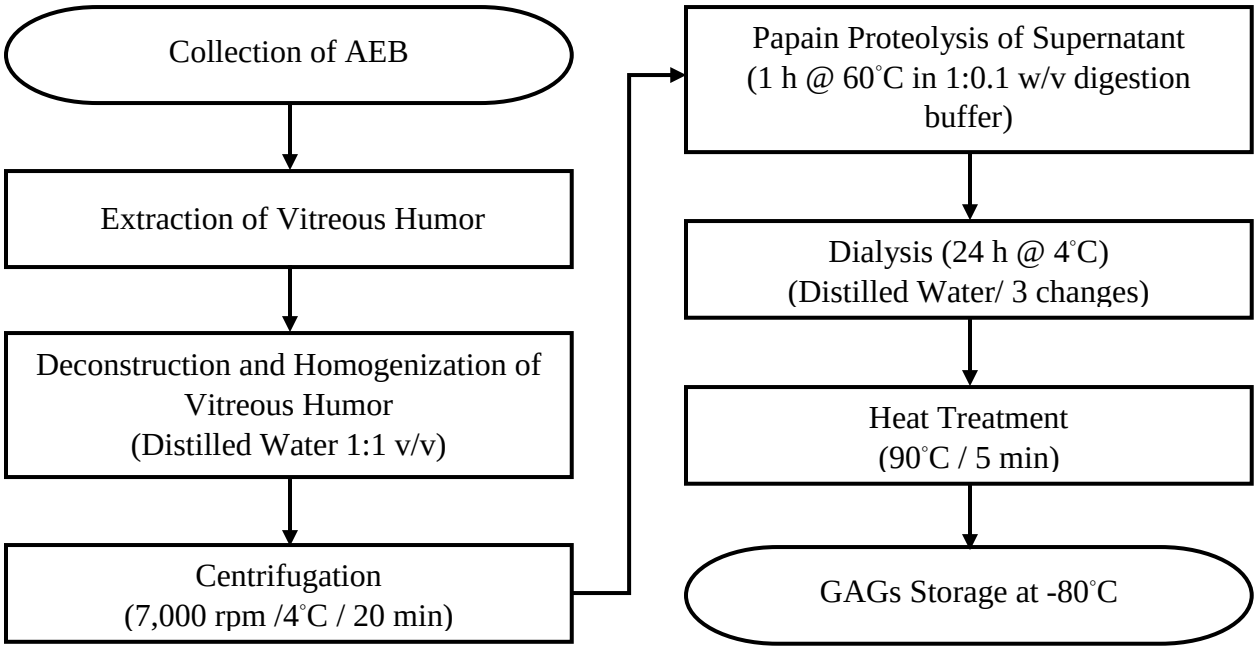

Figure 3.2 Process diagram of GAG extraction from AEB.

hydrolyzed using papain in digestion buffer as described previously. Samples were dialyzed at 4°C using a 14 kDa MWCO membrane against distilled water for 24 h, with solution changes every 8 h. Finally, the samples were heat-treated (90 °C/ 5 min) and stored at -80°C until used.

3.5. Determination of Sulfated GAGs, HA and Total GAGs Content

The content of sulfated GAGs was determined using a Chondrex Inc. (Redmond, WA) dimethylmethylene blue (DMB) assay (Cat. No. 6022) as reported by Garnjanagoonchorn and others [245]. Calibration curves were developed using a chondroitin-6-sulfate standard and samples were solubilized and diluted with PBS to fit the standard range. One hundred microliters of standards, samples and sample blanks were added in triplicates to a 96-well plate. Subsequently, a 1,9-DMB solution (100 µl) was added into the standard and sample wells, while PBS (100 µl) was added into the sample blanks. The plate absorbance was read at 525 nm within 5 min of DMB addition in a Bio-Rad Benchmark Plus Microplate Spectrophotometer (Philadelphia, PA). The content of sulfated GAGs was calculated by regression analysis. HA content was measured using an Echelon® competitive ELISA kit (50-1600 ng/ml) (K-1200, Echelon Biosciences Inc., Salt Lake City, UT) which detected molecules as small as 6.4 kDa. Manufacturer protocol instructions were followed. Briefly, 100 µl of HA standards and diluted samples were added into a 96-well incubation plate followed by 50 µl of detection solution, prior to incubation for 1 h at 37°C. Following the incubation step, samples (100 µl) were transferred into a detection plate for competitive binding at 4°C for 30 min. The plate was then washed three times with 200 µl PBS-Tween (PBST), before addition of an enzyme-linked antibody and substrate solution. Colorimetric detection at 405 nm was used to detect the enzyme-substrate system comprised of alkaline phosphatase/ pNPP phosphatase substrate. The colorimetric signal was inversely proportional to the HA content in the sample and the concentration. A standard curve with the known amounts of

HA was used to determine concentration of HA. The total GAG content of the extracted materials was calculated by addition of the two analyses described above and further confirmed using a carbazole reaction to measure uronic acid after hydrolysis of GAGs with sulfuric acid, as previously reported [246–248]. The absorbance of samples was measured at 550 nm and GAG content was calculated by regression analysis using a HA sodium salt standard curve.

3.6. GAGs Size Analysis

The molecular weight of GAGs was evaluated by agarose gel electrophoresis based on the method of Cowman and others with modifications [249]. Agarose gels (0.75% w/v) were prepared by dissolving 0.3 g of agarose in 36 ml of water using 1.5 min of heating in a microwave oven. The agarose solution was cooled under running tap water for 3 min and then mixed with 4 ml of 10X TBE buffer to make the final gel volume of 40 ml. Gels of 10 x 6.2 cm were cast in a casting accessory using an 8-tooth well-forming comb. Before electrophoresis, gels were allowed to set for at least 1 h. To load samples, the comb was removed and the gel plate was transferred to a Bio-Rad (Hercules, CA) Mini-Sub® Cell GT system which was filled with 290 ml of pre-chilled 1X TBE buffer. Cells were loaded with samples (3 ug GAGs/ well in ultrapure water) and GAG standards (HA & CS) which were mixed with 4 µl of 2 M sucrose loading buffer and sample volume made up to 24 µl with ultrapure water. Select-HA™ HiLadder (5 µl) and LoLadder (5 µl) were mixed with deionized water (10 µl) and loading buffer (4 µl) before being loaded into a well. Electrophoresis was carried out at room temperature at a constant voltage of 70 V for 2.5 h using a Bio-Rad PowerPac™ power supply. The loading buffer tracking dye migrated about 80% of the gel during this time period. Immediately after the run the gel was placed in approximately 250 ml of a staining solution containing 0.005% Stains-All in 50% absolute ethanol (stored protected from light). The gel was stained overnight under light-protective cover at room temperature. For

destaining, the gel was transferred to a 10% ethanol solution and stored in the dark for 8 h with at least one change of destaining solution. Final destaining of any residual background was accomplished by placing the gel on a light box for a few minutes.

Agarose gel electrophoresis was also performed on all samples after an alternative final dialysis step using single use micro DispoDialyzers™. Briefly, GAG dry samples were dissolved in distilled and deionized water (100 µl) and placed in a floating sample chamber that separated the low molecular weight GAGs (<50 kDa) through a cellulose membrane and into the dialysis buffer (tap water). Samples were dialyzed with constant stirring for 48 h in 200 ml of buffer with changes every 2, 5, 15, 30 and 45 h. Samples were recovered into a micro centrifuge tube by centrifugation (1-2 s) at 1500 rpm. Electrophoresis was performed as described above.

3.7. Digestion of GAGs by Type-1 Hyaluronidase and Chondroitinase ABC

Digestion of ACS, AFT, ABS and AEB samples by a type 1 bovine testes HAase was conducted to prove that the stains seen on the previously described agarose gels were truly GAGs. Phosphate Buffer (300 mM sodium phosphate, pH 5.35 at 37°C) was used to prepare a 0.5 mg/ml GAG solution which was completely dissolved and kept at 37°C in a water bath. Immediately before use, a 24,000 U/ml HAase stock solution was prepared by dissolving the enzyme in enzyme diluent (20 mM sodium phosphate with 77 mM sodium chloride and 0.01% (w/v) BSA, pH 7.0 at 37°C). Ultrapure water was used and pH was adjusted with 1 N NaOH or 1 N HCl. The stock solution was diluted with enzyme diluent to obtain additional working solutions of 12,000 U and 6,000 U. The final HAase assay concentrations (48, 24 and 12 U/µg sample) were obtained by mixing 0.5 ml of each GAG solution with 0.5 ml of enzyme solution (24,000, 12,000 or 6,000 U/ml). Incubation was conducted at 37°C with continuous swirling during exactly 20 hours. HAase

was heat inactivated on a boiling water bath for 10 minutes prior to centrifugation at 10,000 rpm for another 10 min. Supernatants were collected and stored at -80°C until used.

An enzymatic assay using ChrAse ABC was conducted on ACS GAGs to further confirm the identity of the purple stains in agarose gels stained with 0.005% Stains-All solution. A GAG solution in sample diluent (250 mM Tris-HCl and 300 mM sodium acetate with 0.05% (w/v) BSA, pH 8.0 at 37°C) and a ChrAse ABC solution (0.4 U/ml) in 0.01% BSA were prepared. Working enzyme solutions (0.2 U/ml and 0.1 U/ml) were prepared from dilutions of the stock solution. The final ChrAse assay concentrations (0.2, 0.1 and 0.05 U) were obtained by mixing equal parts of ACS sample solution and enzyme stock or working solutions. Digestion was conducted at 37°C during 8 h with constant swirling, after which samples were boiled for 10 min, centrifuged at 10,000 rpm during 10 min and stored at -80°C until used. The results of the HAase and ChrAse ABC assays were evaluated by running all samples in 0.75% agarose gels and staining with 0.005% Stains-All as described previously.

3.8. Determination of Protein and Mineral Content

Protein content of the solubilized purified GAG extracts was quantified by measuring absorbance at 562 nm using a Pierce™ Bicinchoninic Acid (BCA) Protein Assay (Philadelphia, PA). A series of dilutions of known concentrations of bovine serum albumin were used as standards and assayed alongside the GAG samples. GAG extract samples were prepared for mineral content by dilution of 100 mg in deionized water (10 ml) and filtration through a 0.22 µm syringe filter. Concentration determination of the filtered samples was carried out using inductively coupled plasma atomic emission spectrometry (ICP-AES) at the Louisiana State University Soil Testing and Plant Analysis Laboratory.

3.9. Structure Characterization by FT-IR Spectroscopy

A Bruker (Billerica, MA) Tensor 27 FT-IR spectrometer with a MIRacle™ single reflection diamond/ZnSe attenuated total reflectance cell (Pike Technologies, Madison, WI) was employed to obtain FT-IR spectra of lyophilized ACS, AFT, ABS and AEB GAGs. Commercial HA and chondroitin-4-sulfate powders were analyzed and used as standard spectra. The spectrum of each compacted dry sample was obtained over 50 scans in the range of 650-4000 cm^{-1}, against a background spectrum recorded from the clean empty cell at room temperature. Spectral data analysis was conducted using the OPUS data collection software version 7.2 (Bruker, Ettlinger, Germany). Atmospheric and baseline corrections were applied to the data which was presented as wavenumber (cm^{-1}) versus normalized absorbance (min = 0.0 and max = 2.0).

3.10. Cystic Fibrosis *Ex-Vivo Scnn1b*-Tg Mice Pilot Study

3.10.1 Transgenic Mice Generation and PCR Genotyping

All animal protocols were approved by the Louisiana State University's Institutional Animal Care and Use Committee. The transgenic mice used for this experiment were *Scnn1b*-Tg, a well-established murine model of CF and COPD [179,250,251]. This C57BL/6N congenic mice line over-expresses the β-subunit of the ENaC channel which leads to ASL depletion and CF-like mucus obstruction. Moreover, *Scnn1b*-Tg mice recapitulate many key features of CF including high MIP-2, TNF-α, high TGAse activity, and neutrophilia among others [10,164,179,252,253]. Genomic DNA extraction from mice tail tissue was performed and transgene-positive animals were identified by polymerase chain reaction (PCR) as previously published [179].

3.10.2 Animal Husbandry

All the *Scnn1b*-Tg mice used in this study were maintained in hot-washed, individually ventilated cages on a 12-hour dark/light cycle and were fed regular diet and water *ad libitum*. Mice were euthanized after establishment of chronic pulmonary disease, on post-natal day 38.

3.10.3 Trachea Harvesting

Mice (4 females) were euthanized by avertin injection (300 µl/mice) before being laid down (abdomen up) and disinfected (abdomen, thorax and neck) with 70% ethanol. Using clean surgical instruments, a horizontal cut from abdomen to neck skin was performed to expose the thoracic and neck regions prior to exsanguination via dissection of the abdominal aorta and puncturing of the diaphragm. Trachea were exposed by removal of surrounding tissue and were removed by dissecting just below the vocal cords and at the carina bifurcation. All trachea were placed into a 50 ml conical tube containing 10 ml of cold Ham's F12 media containing antibiotics. In a sterile laminar flow hood, the trachea and Ham's F12 media containing antibiotics were transferred into a 100 mm Petri dish for removal of extraneous tissue (thyroid gland, esophagus, etc.). Trachea were transferred to a new Petri dish containing Ham's F12 with antibiotics (10 ml) and cut open lengthwise to expose the lumen. Finally, trachea were placed in a 50 ml conical tube containing 10 ml of a solution prepared by mixing 9 ml of cold Ham's F12 with antibiotics and 1 ml of a filter-sterilized 1% pronase stock solution. The tube was incubated on a rocker overnight at 4°C. Subsequently, MTEC isolation and primary cell cultures were conducted as previously described by Lam and others [254] as well as other researchers [255–257] with modifications.

3.10.4 MTEC Isolation

After overnight incubation, 10 ml of Ham's F12 media containing 20% FBS and antibiotics were added to the tube which was then rocked 12 times and let to stand 30 min on ice. Tracheas were then transferred to a new conical tube containing 10 ml of Ham's F12 media with 20% FBS and antibiotics using a Pasteur pipette and rocked 12 times. This step was repeated two more times and finally the remaining tissue was discarded. The pronase solution along with the three supernatants were pooled (50 ml total) and kept on ice at all times prior to centrifugation at 500 x g for 5 min at 4°C in a Heraeus Megafuge 16R centrifuge (Thermo Scientific, Kalkberg, Germany). The supernatant was discarded and the pellet gently re-suspended and incubated 5 min on ice in 1 ml of a filter-sterilized DNase solution (0.5 mg/ml) prepared by dissolving 1.0 mg of DNase in 1.8 ml of Ham's F12 media containing antibiotics and 200 µl BSA stock solution (10 mg/ml). After incubation, the suspension was centrifuged (500 x g for 5 min at 4°C) to discard the supernatant and gently re-suspend the pellet in 5 ml of filter-sterilized MTEC basic media containing 10% FBS (Table 3.1). For the removal of fibroblasts, the suspension was plated on a

Table 3.1

MTEC Basic Media (10% FBS) Formulation

Reagent	Final Concentration
DMEM/Ham's F-12 (HEPES) (1:1)	-
Penicillin-Streptomycin	0.25 µg/ml
HEPES	15 mM
Sodium Bicarbonate	3.6 mM
L-Glutamine	4 mM
Fetal Bovine Serum	10%

Primaria™ tissue culture dish and incubated at 37°C in an atmosphere of 95% air and 5% CO_2 for 4.5 hours. Following incubation, the cell suspension was collected and the plate was rinsed twice with 4 ml MTEC basic media containing 10% FBS. The cell suspension and washes were pooled together in a 50 ml conical tube and centrifuged (500 x g for 5 min at 4°C) to discard the supernatant and re-suspend the pellet in 4.4 ml of filter-sterilized MTEC media containing Y27632 ROCK inhibitor (10 µM) (MTEC+Y27632). Cells were counted (10 µl cell suspension + 10 µl trypan blue) in a Bio-Rad TC20™ automated cell counter (Bio-Rad Laboratories, Hercules, CA).

3.10.5 MTEC Submerged Culture

Six Transwell™ polyester membrane inserts were coated with 50 µg type I collagen dissolved in 165 µl of a solution prepared by mixing 0.02N sterile acetic acid and collagen stock (8.31 µg/µl). The inserts were air-dried in a hood overnight and then exposed to ultraviolet light for 30 min before being seeded with 300 µl of the previously prepared cell suspension (9.5×10^4 cells/insert). MTEC+Y27632 media (1 ml) (Table 3.2) was fed basally and cells were incubated overnight at 37°C in an atmosphere of 95% air and 5% CO_2. On the first day post-seeding, the apical media and non-adherent cells were aspirated. The inserts were then washed twice with 1 ml PBS and transferred to a 6-well plate with previously autoclaved teflon rings. The cultures were fed every other day with 2.5 ml MTEC+Y27632 media basally and 50 µl apically until confluent (7 days). The apical surface was washed gently once a week by adding 0.5 ml of PBS to the insert and carefully aspirating with a Pasteur pipette.

3.10.6 MTEC Differentiation in Air-Liquid Interface Culture

Once confluent, cell cultures were changed to an air-liquid-interface (ALI) in a fresh 6-well tissue culture plate for differentiation. The cells were fed basally with 2.5 ml of MTEC media

Table 3.2

MTEC+Y27632 Media Formulation

Reagent	Final Concentration
DMEM/Ham's F-12 (HEPES) (1:1)	-
Penicillin-Streptomycin	100 U/ml: 100 mg/ml
Insulin	10 µg/ml
Epidermal Growth Factor	25 ng/ml
Transferrin	5 µg/ml
Bovine Pituitary Extract	30 µg/ml
Retinoic Acid	$5x10^{-8}$ M
Fetal Bovine Serum	5%
Cholera Toxin	0.1 µg/ml
Y-27632 ROCK inhibitor	10 µM

containing Nu-Serum growth medium supplement (MTEC+NuSerum) every other day during 21 days (Table 3.3). Fresh retinoic acid ($5x10^{-}8$) was also supplemented to the MTEC+NuSerum media every other day during the last 14 days of ALI culture. The apical surface was washed gently once a week by adding 0.5 ml of PBS to the insert and carefully aspirating with a Pasteur pipette.

3.10.7 MTEC Treatment with AEB GAGs

Once cells were differentiated (day 21 of ALI culture) the MTEC cultures were treated apically with 350 µl of a solution containing 1.43 mg AEB GAGs/ml in 0.9% saline (0.5 mg AEB GAGs/insert). MTEC cultures treated only with the normal saline (350 µl) were used as a control. The volume applied apically (350 µl) has been reported in ALI primary tracheal mice [179] and the treatment solution was sterilized by autoclaving at 121°C for 5 min as previously reported [258,259]. The GAG concentration to be used for this treatment was estimated using as a guideline

Table 3.3

MTEC+NuSerum Media Formulation

Reagent	Final Concentration
DMEM/Ham's F-12 (HEPES) (1:1)	-
Penicillin-Streptomycin	100 U/ml: 100 mg/ml
Retinoic Acid	$5x10^{-8}$ M
Nu-Serum	2%

the successful concentrations reported by Gavina and others (100 µg HA/ml for 24 h in-vitro and 0.5 mg/mice/day for 7 days in-vivo) [10] and Lieb and others (100 µg HA/ml) [224]. Cultures were maintained at 37°C in an atmosphere of 95% air and 5% CO_2. The treatment was terminated by aspiration of the supernatant after 24 h and the supernatants were stored at -80°C for further analysis.

3.10.8 Cell Lysis and RNA Purification

RNA was extracted from MTEC cultures using the RNeasy® Plus Mini Kit (Cat. No. 14134) from Qiagen (Valencia, CA) following the manufacturer's instructions in an Air Clean® 600 PCR Workstation (BioExpress, Kaysville, UT). Appropriate RNA handling techniques were applied to avoid contamination. Briefly, cells were disrupted and lysates homogenized using QIAshredder spin columns (Qiagen Cat. No. 79654) placed in 2 ml micro-centrifuge tubes which were centrifuged for 2 min at maximum speed in a Thermo Scientific Sorvall™ ST 16R Centrifuge (Kalkberg, Germany). The homogenized lysates were transferred to gDNA eliminator spin columns in 2 ml collection tubes and centrifuged for 30 s at 8,000 x *g*. The flow-through was saved and one volume of 70% ethanol was added and mixed gently by pipetting. The samples were then transferred to an RNeasy spin column in a collection tube and centrifuged for 15 s at 8,000 x *g* to

discard the flow-through and elute the RNA from the column by centrifugation with 40 µl of RNase-free water. RNA concentration (260 nm) and purity (A_{260} /A_{280}) in the eluate (1 µl) were measured by UV spectrophotometry using the NanoDrop 2000 from Thermo Scientific (Wilmington, DE) blanked with RNase-free water. RNA samples (2 ng/µl) were submitted to the LSU School of Veterinary Medicine GeneLab for RNA integrity number calculation (RIN) and 18s and 28s fragment visualization using a Fragment Analyzer™ (Advanced Analytical Technologies Inc., Ames, IA).

3.10.9 cDNA Generation and PCR Microarray

Purified RNA (0.33 µg) was used to generate cDNA using the RT^2 First Strad Kit from Qiagen which consisted of a genomic DNA elimination step and reverse transcription at 42°C for exactly 15 min. SYBR® Green based real-time PCR was performed using a murine CF RT^2 Profiler PCR Array which profiles the expression of 84 key CF genes involved in neutrophil chemotaxis, inflammation, immune response and oxidative stress, among others (Table 3.4) in a 96-well plate format. The arrays included a genomic DNA (GDC), reverse-transcription (RTC) and positive PCR controls (PPC). Manufacturer protocols were followed. PCR was conducted in a CFX96 Real-Time System equipped with CFX Manager™ Software and automatic threshold cycle (C_T) calculation from Bio-Rad Laboratories (Hercules, CA). The real-time cycler was first programed to cycle for 10 min at 95°C to activate the HotStart DNA Taq Polymerase. This cycle was followed by 40 cycles of annealing for 15 s at 95°C and elongation for 1 min at 60°C with fluorescence data collection. The temperature ramp rate was adjusted to 1°C/s. Finally, a melting curve (65°C to 95°C at 0.5°C /s for 5 s) analysis was conducted to verify PCR specificity, evident by a single peak appearing in each reaction at temperatures greater than 80°C. C_T values for all wells were processed with the SABiosciences PCR Array Data Analysis Web-based software. The

software calculated ΔC_T (C_T Gene of Interest - C_T Housekeeping Gene) based on the *B2m* housekeeping gene and then calculated the normalized gene expression values using the formula $2^{\wedge -\Delta C_T}$. The fold-change values were then converted to fold-regulation. The software also performed a hierarchical cluster analysis of the dataset to generate a gene expression heat map (fold-regulation >1.5 and $p \leq 0.05$) with dendrograms indicating co-regulated genes across arrays. A heat map for all the 84 genes analyzed was also generated.

Table 3.4
Murine CF RT2 Profiler PCR Array Gene List*

Gene ID	Official Name
	CF Modifier Genes
Adipor2	adiponectin receptor 2
Gstm2	glutathione S-transferase, mu 2
Ifrd1	interferon-related developmental regulator 1
Msra	methionine sulfoxide reductase A
Nos3 (eNOS)	nitric oxide synthase 3, endothelial cell
Tcf7l2	transcription factor 7 like 2, T cell specific
	CFTR Interactors
Ahsa1	AHA1, activator of heat shock protein ATPase 1
Canx	Calnexin
Cftr	cystic fibrosis transmembrane conductance regulator
Dnaja1	DnaJ heat shock protein family (Hsp40) member A1
Dnajc5	DnaJ heat shock protein family (Hsp40) member C5
Ezr	ezrin
Gopc	golgi associated PDZ and coiled-coil motif containing
Hsp90aa1 (Hspca)	heat shock protein 90, alpha (cytosolic), class A member 1
Hspa4 (Hsp70)	heat shock protein 4
Nme1 (NM23A)	NME/NM23 nucleoside diphosphate kinase 1
Pdzk1	PDZ domain containing 1
Ppp2r4	protein phosphatase 2 regulatory subunit 4
Prkaa1 (Ampk)	protein kinase, AMP-activated, alpha 1 catalytic subunit
Prkaa2	protein kinase, AMP-activated, alpha 2 catalytic subunit
Slc26a3	solute carrier family 26, member 3
	CFTR Interactors
Slc9a3r1	solute carrier family 9 (sodium/hydrogen exchanger), member 3 regulator 1
Slc9a3r2	solute carrier family 9 (sodium/hydrogen exchanger), member 3 regulator 2
Snap23	synaptosomal-associated protein 23

(Table 3.4 continued)

Gene ID	Official Name
	CFTR Interactors
Stx1a	syntaxin 1A
Stx8	syntaxin 8
Tjp1	tight junction protein 1
Vcp	valosin containing protein
	Neutrophil Chemotaxis
Ccl12 (MCP-5, Scya12)	chemokine (C-C motif) ligand 12
Cxcr2 (IL-8rβ)	chemokine (C-X-C motif) receptor 2
Edn1	endothelin 1
Ednra	endothelin receptor type A
IL-1β	interleukin 1 beta
Itgb2	integrin beta 2
	Inflammatory Response
Ace	angiotensin I converting enzyme
Adrb2	adrenergic receptor, beta 2
Alox12b	arachidonate 12-lipoxygenase, 12R type
Cxcl1 (Gro1)	chemokine (C-X-C motif) ligand 1
Cxcl3	chemokine (C-X-C motif) ligand 3
Defb1	defensin beta 1
IL-10	interleukin 10
IL-6	interleukin 6
Mbl2	mannose-binding lectin (protein C) 2
Pla2g5	phospholipase A2, group V
Ptgs2 (COX)	prostaglandin-endoperoxide synthase 2
S100a8	S100 calcium binding protein A8
S100a9	S100 calcium binding protein A9
Serpina1e	serine (or cysteine) peptidase inhibitor
Tgfb1	transforming growth factor, beta 1
Tlr2	tool-like receptor 2
Tlr4	tool-like receptor 4
Tlr5	tool-like receptor 5
Tnf	tumor necrosis factor
Tnfrsf11a (Rank)	tumor necrosis factor receptor superfamily, member 11a, NF-κβ activator
Tnfrsf1a (Tnfr1)	tumor necrosis factor receptor superfamily, member 1a
	Immune Response
Clu	clusterin
Icam1	intercellular adhesion molecule 1
Lcn2 (NGAL)	lipocalin 2
Mapk1 (Erk2)	mitogen-activated protein kinase 1
NF-Kβ1	nuclear factor of kappa light polypeptide gene enhancer in B cells 1, p105

(Table 3.4 continued)

Gene ID	Official Name
	Immune Response
NF-Kβia (IKβα, Mad3)	nuclear factor of kappa light polypeptide gene enhancer in B cells inhibitor, alpha
Prkce	protein kinase C, epsilon
Tnfsf10 (Trail)	tumor necrosis factor (ligand) superfamily, member 10
Fas (Tnfrsf6)	Fas (TNF receptor superfamily member 6)
IL-7r	interleukin 7 receptor
	Unfolded Protein Response
Calr	Calreticulin
Hspa1a (hsp70A1)	heat shock protein 1A
Hspa8	heat shock protein 8
Hsph1 (hsp105)	heat shock 105kDa/110kDa protein 1
	Ion Binding & Transport
Adk	adenosine kinase
Kcne1	potassium voltage-gated channel, Isk-related subfamily, member 1
Nr4a2 (Nurr1)	nuclear receptor subfamily 4, group A, member 2
Scnn1b	sodium channel, nonvoltage-gated 1 beta
Scnn1g	sodium channel, nonvoltage-gated 1 gamma
	Oxidative Stress
Dusp1 (Ptpn16)	dual specificity phosphatase 1
Gclc	glutamate-cysteine ligase, catalytic subunit
Sftpb	surfactant associated protein B
	Other CF Genes
Epsti1	epithelial stromal interaction 1 (breast)
Igfbp5	insulin-like growth factor binding protein 5
Itga2	integrin alpha 2
Kit (CD117)	kit oncogene
Met	met proto-oncogene
Prtn3	proteinase 3
Slpi	secretory leukocyte peptidase inhibitor

*Genes might be relevant in more than one CF pathway.

3.10.10 Transglutaminase Activity Assay

Extracellular TGAse activity in MTEC was measured spectrophotometrically (450 nm) using the TGAse Assay Kit from Sigma-Aldrich (Cat. No. CS1070). Manufacturer's protocols were followed. The assay is based on the TGAse catalysis of a covalent bond formation between a free amine group of poly-L-lysine, which is covalently bonded to a 96-well plate surface, and

the γ-carboxamide group of a biotin substrate buffer. The amount of immobilized biotin was proportional to the amount of active TGAse.

CHAPTER 4
RESULTS AND DISCUSSION

4.1. Yields of Sulfated GAG, HA and Total GAG from Alligator By-products

Waste by-products of farmed alligators 12 to 18-months old with approximate snout to tail length of 4-feet, had mean weights as reported in Table 4.1. These values represent results from 80 ACS, 400 AFT, 100 ABS and AEB from 200 gator heads. Alligators from different farms and/or development stage may or may not conform to this data.

Table 4.1

Alligator By-product Processing Results

By-product	ACS (n = 80)	AFT (n = 100)*	ABS (n = 100)	AEB (n = 200)
Weight (g)	942.00 ± 109.12	105.84 ± 6.93	68.44 ± 12.46	2.67 ± 0.19
Meat Yield (% w/w)	74.34 ± 2.72	-	-	-
Bone Yield (% w/w)	22.46 ± 3.88	-	-	-
Vitreous Humor Yield (% w/w)	-	-	-	25.85 ± 2.24

Means ± SD are shown. ACS = alligator carcasses, AFT = alligator feet, ABS = alligator backstraps, AEB = alligator eyeballs. *Average weight of two anterior and two posterior feet is reported.

The data presented in Table 4.1 can be used by alligator processors to estimate the value of their by-products if used for GAG extraction and estimate the number of alligators needed to meet a particular sales need. To the best of our knowledge, this is the first work that reports the desinewed meat yield (74.34 ± 2.72%) from ACS. This meat, which contained 17.32 ± 0.02% fat (wet basis) as determined by accelerated hexane extraction, might be a business opportunity if incorporated into dry protein snacks, sausage, hamburger or pet treat formulations.

Purified GAGs from farmed alligator by-products were obtained by a series of optimized physical and chemical processes including removal of myofibrillar proteins and fat, enzymatic hydrolysis of collagenous protein and purification by dialysis, as well as NaCl-ethanol precipitation, heat treatment and lyophilization. The sulfated GAG yields (Table 4.2) as determined by the DMB assay were highest ($p \leq 0.05$) in ABS (0.22 ± 0.01 mg/g wet ABS), followed by AFT, ACS and AEB, in that order. The calibration curve for this assay showed a linear relation between the absorption at 525 nm of the chondroitin sulfate-DMB complexes versus concentration of CS in the solution, with a correlation coefficient (R^2) of 0.975 as shown in Figure 4.1.

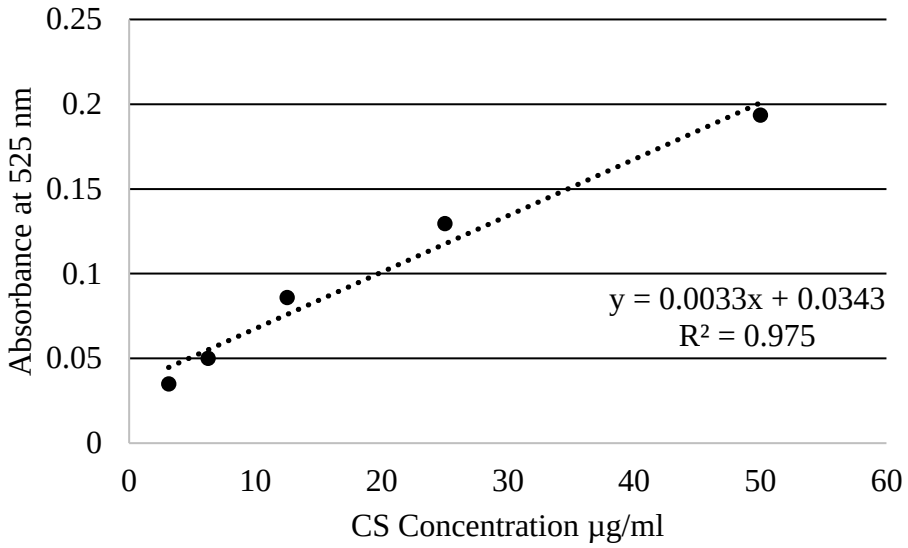

Figure 4.1. Standard curve for sulfated GAG assay.

A quantitative analysis of the GAGs extracted from chicken combs demonstrated a sulfated GAG concentration (0.2 mg sulfated GAGs/ g wet comb) very similar to our ABS results. The content was characterized to be mainly DS and CS [120]. In contrast, a study conducted by Luo and others, evaluated the CS yield of chicken keel cartilage and it was shown that every gram of wet keel cartilage yielded approximately 24.84 mg of dry CS [125]. Some of the differences that

might account for the lower sulfated GAG yields obtained in our study compared to keel cartilage include: sample type (cartilage only), species, slaughter age, extraction process and purification methods. For instance, the chicken keel cartilage study used a 3.5 kDa MWCO membrane which might retain more of the typically low molecular weight sulfated GAGs compared to the 14 kDa MWCO membrane used in our study. Moreover, hyoid, rib, sternum and trachea cartilages from four year-old Thailand crocodiles have also been found to be rich in CS with contents ranging from approximately 2.58 to 3.99% on a wet basis [245]. On this research, Garnjanagoochorn and others performed an enzymatic cartilage hydrolysis with papain and CS purification using NaCl and CPC. Heat treatment (90-95 °C for 10 min) of cartilage samples was conducted beforehand to remove meat and connective tissue [245].

Quantitation of HA concentrations by ELISA using a standard curve generated by non-linear regression analysis (Figure 4.2) revealed yields of 0.60 ± 0.00, 4.62 ± 0.06, 15.31 ± 0.26 and 0.78 ± 0.01 mg per gram of wet ACS, AFT, ABS and AEB, respectively (Table 4.2). The addition of sulfated GAG and HA concentrations is also presented in Table 4.2 as total GAGs (mg/g by-product). The total concentration of GAGs was calculated to be 0.60 ± 0.00 (0.06% w/w), 4.72 ± 0.05 (0.47% w/w), 15.53 ± 0.27 (1.55% w/w) and 0.79 ± 0.01 (0.08% w/w) mg/g of wet ACS, AFT, ABS and AEB, respectively. Non-sulfated HA accounted for 97.87 – 99.48% of the extracted GAGs and the highest yield per gram was obtained from ABS, followed by AFT, AEB and ACS. Similar results have been reported for Mediterranean mussels (*Mytilus galloprovincialis*), in which ~97% of the extracted GAGs were HA [260]. Based on the average by-product weight data reported in Table 4.1 and the average yields reported in Table 4.2 (average by-product weight x average total GAG yield), the estimated total GAG yields from one farmed alligator (~4 ft.) are

Table 4.2

Composition of Alligator GAGs

By-product	Sulfated GAGs (mg/ g of wet by-product)	HA Content (mg/ g of wet by-product)	Total GAGs (mg/ g of wet by-product) †	Total GAGs (mg/ g of wet by-product) ††
ACS	$0.00 \pm 0.00^{c*}$	0.60 ± 0.00^{d}	0.60 ± 0.00^{d}	0.63 ± 0.03^{c}
AFT	0.10 ± 0.01^{b}	4.62 ± 0.06^{b}	4.72 ± 0.05^{b}	4.98 ± 0.73^{b}
ABS	0.22 ± 0.01^{a}	15.31 ± 0.26^{a}	15.53 ± 0.27^{a}	16.66 ± 2.34^{a}
AEB	0.01 ± 0.01^{c}	0.78 ± 0.01^{c}	0.79 ± 0.01^{c}	0.83 ± 0.04^{c}

Means ± SD are shown. ACS = alligator carcasses, AFT = alligator feet, ABS = alligator backstraps, AEB = alligator eyeballs.

* Means that do not share a letter within a column are significantly different *($p \leq 0.05$)*.

† Total GAGs (mg) = Sulfated GAGs (mg) + Hyaluronic Acid (mg)

†† Total GAGs measured by the 96-well carbazole reaction.

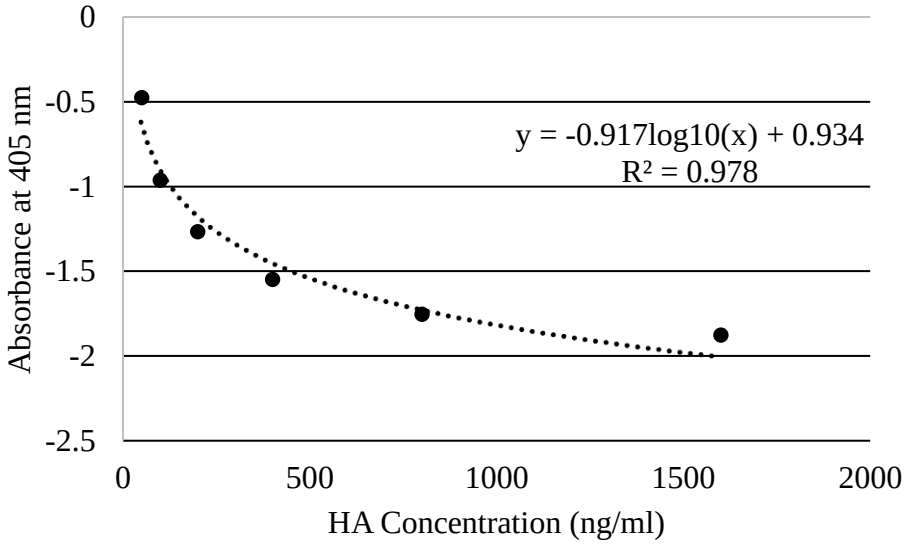

Figure 4.2. HA competitive ELISA standard curve

highest in ABS (1.06 g/backstrap), while ACS (0.57 g/carcass) and AFT (0.50 g/4 feet) have similar contents, and AEB (0.004 g/2 eyes) have the lowest yield. These results are equivalent to approximately 2.13 g GAGs from each alligator. In 2014, a total of 341,887 farmed alligators were

slaughtered in Louisiana [39] which means that an estimated 0.73 tons (728.22 Kg) of GAGs could have been extracted with over 97% accounting for HA.

The 96-well assay for uronic acid carbazole reaction has been reported to be a sensible and reproducible method for the determination of complex uronic acid containing GAGs [248]. In our samples, the carbazole assay further confirmed the presence of uronic-acid containing polysaccharides (Table 4.2), however there was a slight (4.76 - 6.78%) overestimation of the total GAG content compared to the additive procedure (sulfated GAG concentration + HA concentration). A study by Frazier and others highlighted the reproducibility of the 96-well carbazole assay, however it observed that it may overestimate GAGs in the presence of salts [261]. This salt effect might account for the difference in total GAG results due to an increase in background absorbance. The calibration curve of the HA standard performed in a 96-well plate is shown in Figure 4.3.

Vertebrate tissues and invertebrate species have been largely studied as rich sources of sulfated and non-sulfated GAGs [65,120,122–125,245,247,262–264]. For instance, several publications have reported yields from chicken combs ranging from 1 to 4 mg hexuronic acid/ g wet tissue [120,121,123]. Our higher yields per gram from AFT and ABS indicate that these by-products are promising when compared to this well-established source of HA. GAGs have also been successfully extracted from marine by-products such as shark fin cartilage (~2.45% on a wet basis) and ray cartilage (~1.83% on a wet basis). Differences in the yields compared to our research are mainly driven by the fact that cartilages were manually separated and cleaned prior to GAG extraction which results in higher yields compared to our direct processing of samples as collected

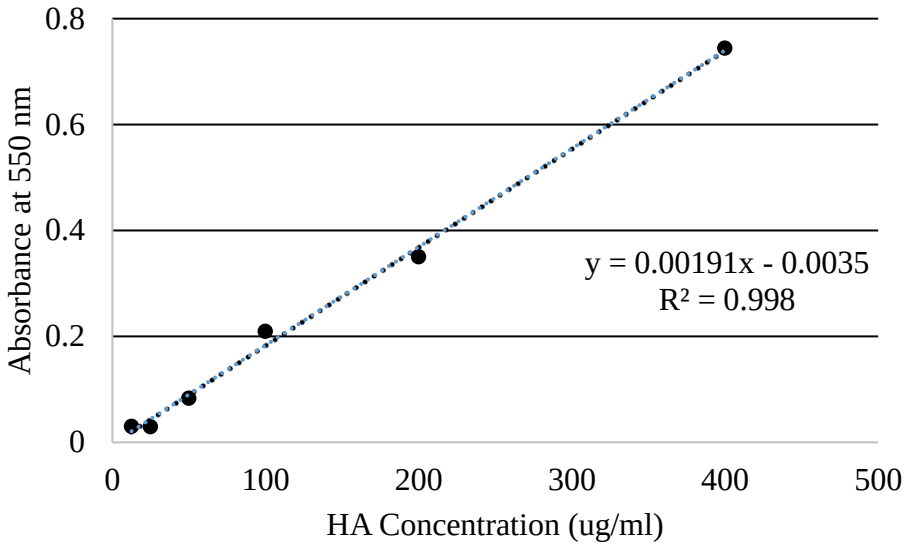

Figure 4.3. Calibration curve for HA standard carbazole reaction

from the alligator facilities [245]. Comparison of yields to other marine sources such as salmon nasal cartilage (24% w/w on a dry basis) and dogfish cartilage (1.5% w/w on a wet basis) face the same constraint [265,266]. Furthermore, in Mediterranean mussels the dry weight yield of GAGs was estimated to be 6.1 mg/g (0.6% w/w). These were obtained after defatting with organic solvents, extracting by proteolytic treatment and precipitation with NaCl and ethanol [260]. Recent work on marine sources of GAGs, reflects that processes for marine GAG extraction are focused on obtaining sulfated GAGs [263,264], however lumpsucker fish (*Cyclopterus lumpus*) dorsal humps have a yield of ~40% purified GAGs from wet starting mass and the majority of the extract was dominated by non-sulfated high molecular weight HA [247]. Attempts have also been made to determine the concentration of GAGs in the body wall of sea cucumbers (*Stichopus japonicus*). Kariya and others reported it to be only 0.03% [267]. In the light of the currently available data for animal by-product sources, the process proposed for GAG extraction from ACS, AFT and ABS is promising due to the high abundance of these by-products in Louisiana, to the high percentage of

non-sulfated HA in the extracts and the high yields per gram obtained particularly in ABS and AFT. The main by-product disposed from alligator processing by weight is ACS, therefore its high availability in addition to the potential added-value of desinewed meat justify its use for GAG extraction despite its lower yield compared to ABS and AFT.

Even with a lower GAG content per alligator, AEB must be considered a viable source of HA due to its highly pure abundance in the vitreous humor which facilitates its extraction and purification, compared to ACS, AFT and ABS. Moreover, the AEB HA yield obtained in this study (0.78 mg/g eyes or ~3.02 mg/g vitreous humor) is much higher than the concentrations reported by other studies. This result is at least two times higher than reported contents in bovine vitreous humor (0.3 mg/g), swordfish vitreous humor (0.055 mg/g), shark vitreous humor (0.3 mg/g) and pig vitreous humor (0.04 mg/g) [124,268]. The differences in GAG contents are thought to be mainly due to differences between species and extraction procedures.

4.2. Agarose Gel Electrophoresis of Alligator GAGs

The molecular weight of GAGs is an important determinant of its biological activity. To estimate the molecular weight of ACS, AFT, ABS and AEB GAGs, agarose gel electrophoresis was performed following an improved method reported by Cowman and others with slight modifications [249]. Figure 4.4 shows the separation of GAG standards and the polydisperse molecular weight nature of ACS, AFT, ABS and AEB GAGs on a 0.75% agarose gel stained with Stains-All. We observed a primarily blue staining on all samples (lanes 2-5) indicating the presence of HA. The polydisperse distribution of molecular weight in HA from animal tissues was evident in ACS (~110-1600 kDa), AFT (~70-510 kDa), ABS (~15-1100 kDa) and AEB (~25-1600 kDa) GAGs. CS was visualized on ACS (<70 kDa) as a purple-reddish smear. The characteristic staining

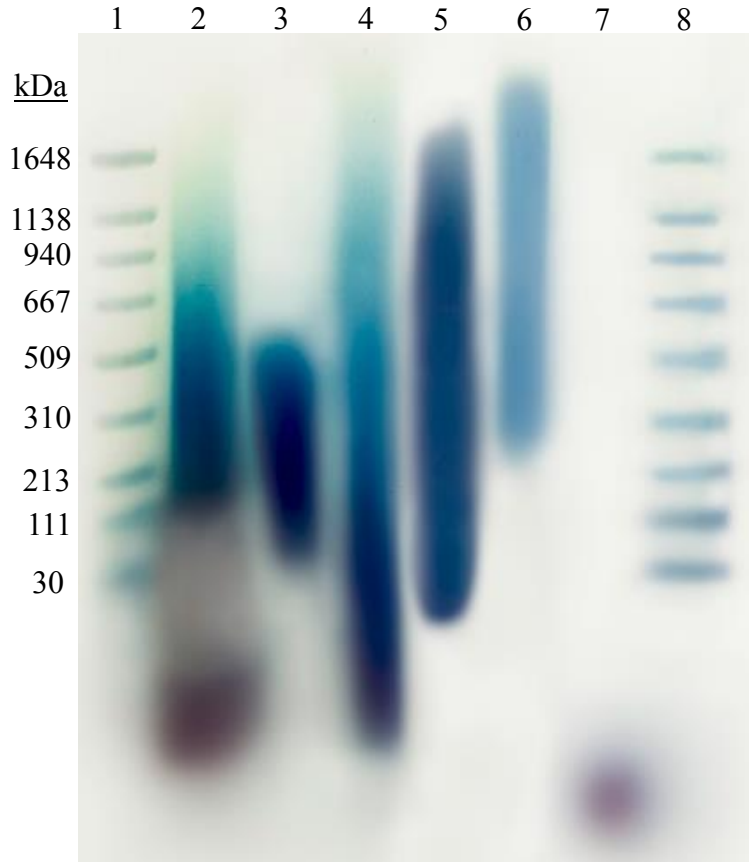

Figure 4.4. Electrophoresis of ACS, AFT, ABS and AEB GAGs on a 0.75% agarose gel. Lane 1: mixture of Select-HA HiLadder and LoLadder (1648, 1138, 940, 667, 509, 310, 213, 111 and 30.2 kDa); lane 2: ACS GAGs; lane 3: AFT GAGs; lane 4: ABS GAGs; lane 5: AEB GAGs; lane 6: HA salt; lane 7: Chondoitin-4-sulfate salt from bovine trachea; lane 8: mixture of Select-HA HiLadder and LoLadder.

of sulfated GAGs with Stains-All has been previously reported [269]. The presence of sulfated fractions was not observed in AFT, ABS or AEB which might indicate that they migrated faster due to their low molecular weight and ran off the gel. Sulfated GAGs from sea cucumbers have a molecular weight of 18 kDa [267].

Agarose gel electrophoresis of the GAG samples was also conducted after dialysis in a small volume (100 µL) sample chamber with a cellulose membrane against water. Figure 4.5 indicates that dialysis during 48 hours successfully removed HA below ~28 kDa and LMW sulfated GAGs from all samples (see arrow on Figure 4.5). Based on the target market requirements, further purification and specific molecular weight separation can be conducted using size exclusion chromatography. Our results show that ACS, AFT, ABS and AEB contain HA of molecular weights comparable to the HA sizes reported from other animal and microbial sources. The molecular weights of HA purified from Mediterranean mussels and eggshells was estimated to be about 200 kDa and 50-250 kDa, respectively [246,260,270]. HMW-HA has been reported in vitreous humor from fish (1600-2000 kDa) [124]. HA from rooster combs has been reported to have a size ranging from 750 to 1200 kDa [123,271]. Microbial fermentation sources report HA molecular weights of 538-900 kDa, with wound healing properties proven in the 538 kDa fractions [127,246]. Due to their content of beneficially bioactive HMW-HA and MMW-HA, alligator by-products have a significant commercial potential.

4.3. Enzymatic Assays

Alligator GAG samples were digested with HAase from bovine testes as negative controls to prove that the stainings seen on Figure 4.4 are truly representative of GAGs. Our results (Figure 4.6) show that increasing concentration of HAase resulted in increasing depolymerization of the

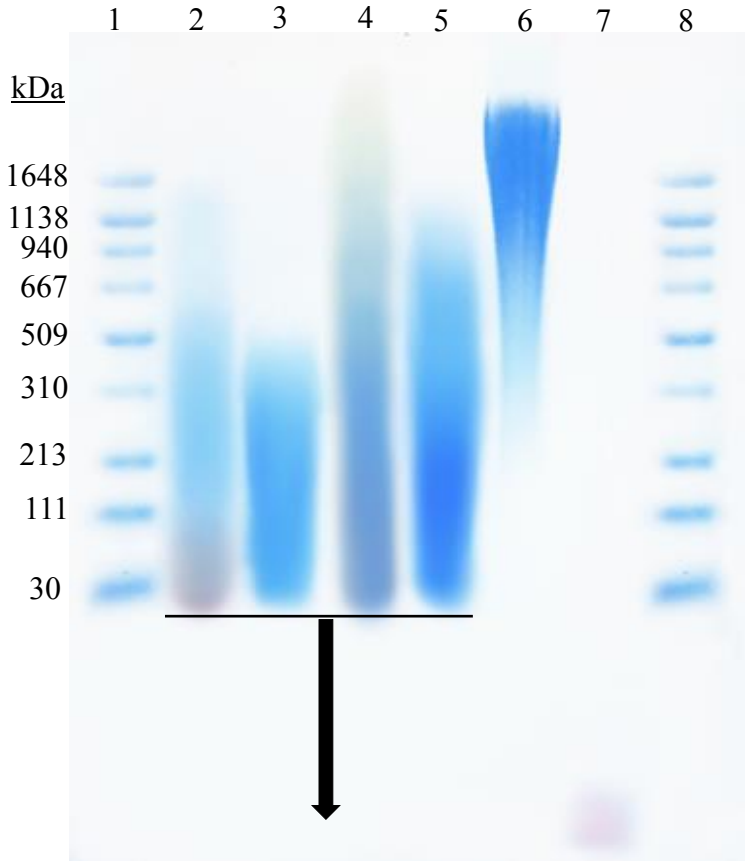

Figure 4.5. Electrophoresis of ACS, AFT, ABS and AEB GAGs on a 0.75% agarose gel after dialysis (50 kDa MWCO). Lane 1: mixture of Select-HA HiLadder and LoLadder (1648, 1138, 940, 667, 509, 310, 213, 111 and 30.2 kDa); lane 2: ACS GAGs; lane 3: AFT GAGs; lane 4: ABS GAGs; lane 5: AEB GAGs; lane 6: HA salt; lane 7: Chondoitin-4-sulfate salt from bovine trachea; lane 8: mixture of Select-HA HiLadder and LoLadder.

GAG samples which proves the presence of HA and CS in the extracts. HAase randomly hydrolyzes 1,4-linkages between GlcNAc and GlcA in HA and 1,4-linkages between GalNAc or sulfated GalNAc and GlcA in all types of CS at an optimum pH of 4.5-6.0 [272]. HA degradation patterns were similar in all samples with increasing concentrations of HAase resulting in increased HA hydrolysis seen as stains with lower molecular weight or lighter colored bands (downward

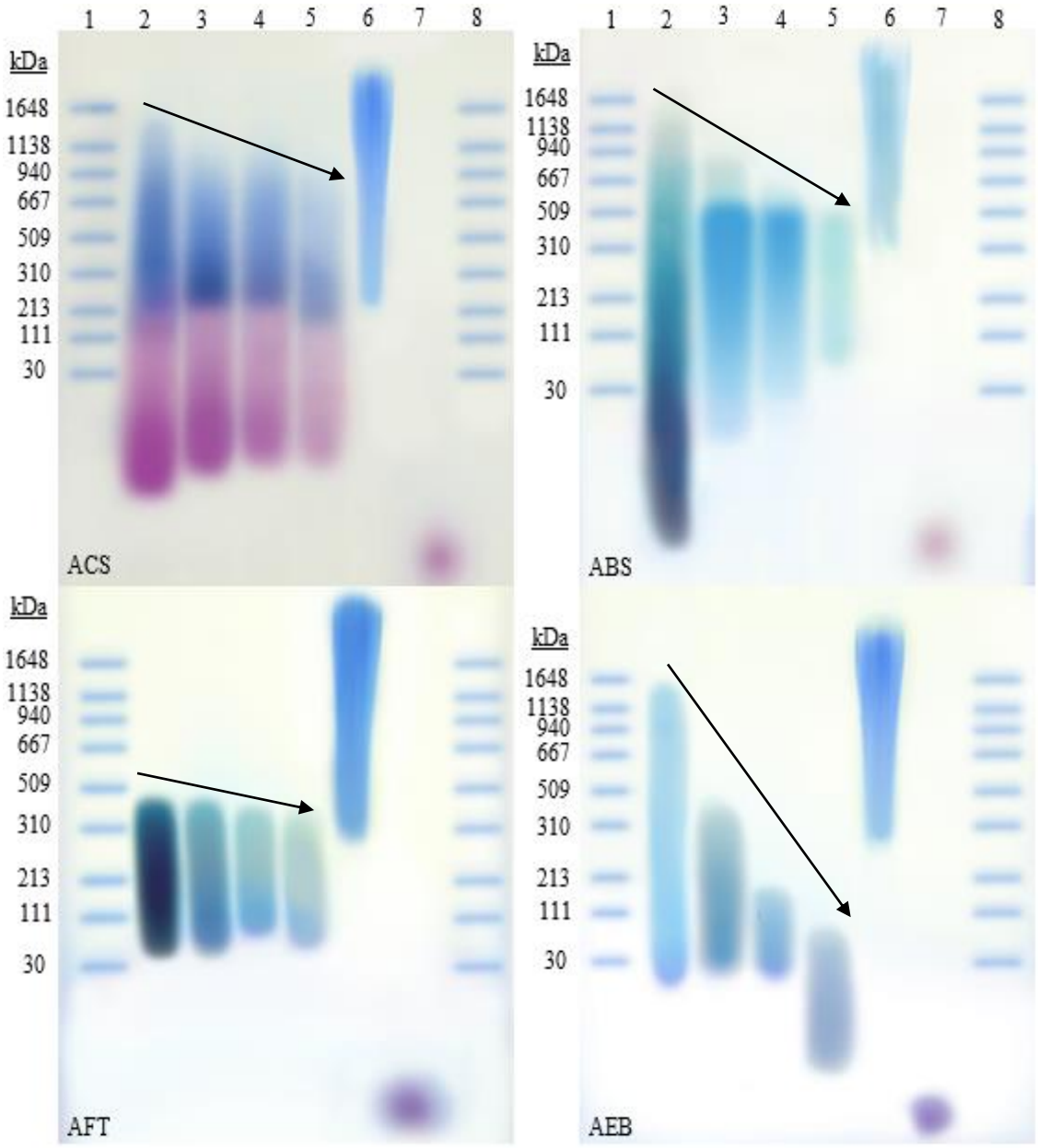

Figure 4.6. Electrophoresis of ACS, AFT, ABS and AEB GAGs on a 0.75% agarose gel after HAase digestion. In all gels lane 1: mixture of Select-HA HiLadder and LoLadder; lane 2: 0 U/µg sample; lane 3: 12 U/µg sample; lane 4: 24 U/µg sample; lane 5: 48 U/µg sample; lane 6: HA salt; lane 7: Chondoitin-4-sulfate salt from bovine trachea; lane 8: mixture of Select-HA HiLadder and LoLadder.

arrows on Figure 4.6). ABS showed overall HA degradation above 700 kDa and below 33 kDa, however some concentration was seen around 300-400 kDa in the 12 and 24 U/µg treatments (ABS

lanes 3 and 4). This might be due to accumulation of hydrolyzed HA chains in that particular molecular weight or due to transglycosylation. Transglycosylation activity of HAse in the presence of 6 to 12 monomer HA units has been previously reported to yield HA oligosaccharides at a pH ~7 and salt content below 0.5M [273,274].

ChrAse ABC was used to catalyze the degradation of polysaccharides containing 1,4 and 1,3 linkages. This effect was observed on both non-sulfated and sulfated GAGs in ACS (downward arrows on Figure 4.7). The GAGs hydrolyzed by ChrAse ABC include C4S, C6S, DS and HA [275,276]. Even though HA is degraded at a lower rate, this effect was clear in our assay (Figure 4.7). ChrAses A, C, AC and ABC act upon HA, however ChrAse B is specific for cleavage of DS [277]. Our results show that the purple stains observed in the agarose gels corresponded to some type of CS. Moreover, dialysis or size exclusion chromatography might be better options to preserve HMW and MMW HA during the elimination of LMW GAGs.

4.4. Protein and Mineral Contents of Alligator By-product GAGs

Extracts from ACS, AFT, ABS and AEB were analyzed for presence of residual protein by using the BCA assay at 562 nm. Most of these by-products are high in muscle and/or collagenous protein content [245]; therefore, a sequential pepsin and papain methodology was conducted to yield a clear solution after a total of 16h at 40˚C and 60˚C, respectively. The protein content results in the different GAG extracts are shown in Figure 4.8. Previously reported protein content values for GAG extracts from animal sources using diverse proteolysis methods are varied. The protein content of GAGs purified from chicken keel cartilage by papain digestion (44 mg papain/g dry matter)

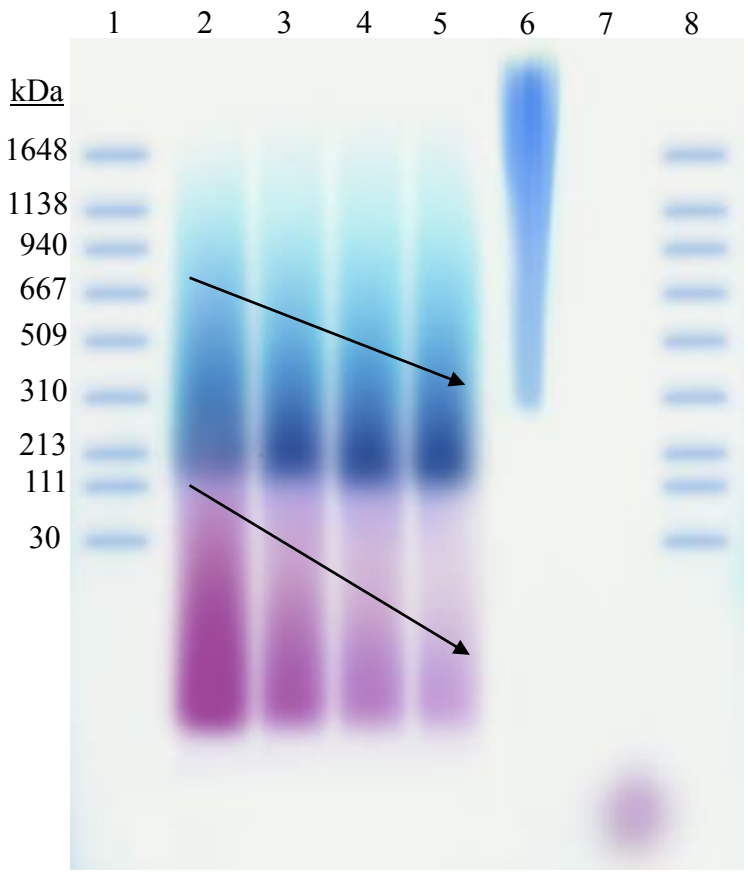

Figure 4.7. Electrophoresis of ACS GAGs on a 0.75% agarose gel after ChrAse digestion. Lane 1: mixture of Select-HA HiLadder and LoLadder (1648, 1138, 940, 667, 509, 310, 213, 111 and 30.2 kDa); lane 2: ACS GAGs + 0 U ChrAse; lane 3: ACS GAGs + 0.05 U ChrAse; lane 4: ACS GAGs + 0.1 U ChrAse; lane 5: ACS GAGs + 0.2 U ChrAse; lane 6: HA salt (1500-2200 kDa); lane 7: Chondoitin-4-sulfate salt from bovine trachea; lane 8: mixture of Select-HA HiLadder and LoLadder.

during 6 h at 60˚C, has been estimated to be 1.8 g/100 g dry product (1.8%) [125]. Furthermore, GAGs isolated from the body wall of sea cucumbers by proteolytic digestion using actinase at a concentration of 50 mg/g of body wall protein, yielded extracts with 3.1% protein content [267]. These results are within the range of the ones obtained in our study. Moreover, extraction of low protein and high purity HA from fish eyeballs has been reported using a combination of optimized

steps including: ultrafiltration-diafiltration, protein electrodeposition, resolubilization in a hydroalcoholic medium and precipitation in alkaline hydroalcoholic solution. AEB extracts in our

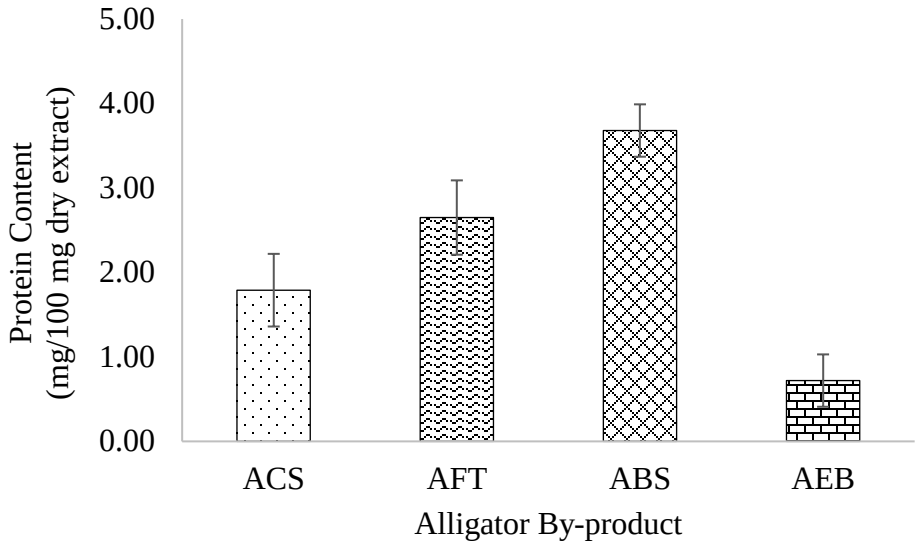

Figure 4.8. Protein content in alligator by-product GAG extracts

study are similarly of low protein content and high purity (~99%). The AEB protein content is also similar to the results of Vijayabaskar and Vaseela which reported the protein content of brown marine algae (*Sargassum tenerrimum*) sulfated GAG extracts to be 0.86 ± 0.42% [278]. Protein contents of up to 23.08% have been reported in HA salt from *S. zooepidemicus* and its wound healing properties have been demonstrated [127].

The main problem in HA purification is the elimination of diverse proteins that may be allergenic in some applications [279]. For injection applications (dermal fillers), the ideal final protein concentration should be around ~5-10 μg of protein/ mg HA and standards become more tolerant for topical, perfusion or oral intake applications [124]. Although the specifications of the

European and British Pharmacopoeia require 0.1-0.3% protein in HA [246,280], in the United States commercially available HA has been reported to contain up to 4.7% protein [281]. Based on this information, AEB may have potential for use in osteoarthritis visco-supplements, ophthalmic viscoelastic adjuvants, aesthetic surgery adjuvants, eye drops and topical preparations for wound and burn healing, among others. With the current protein contents, ACS (1.8%), AFT (2.65%) and ABS (3.68%) GAG extracts could be used for research applications and potentially animal nutrition applications. An evaluation of the impurities in HA from different sources was conducted by Shieldlin and others. HA powders isolated from rooster comb, bovine vitreous humor, and human umbilical cord were purchased from Sigma Chemical Company. All the samples contained some amount of protein. The highest levels were detected in HA from human umbilical cord (47.7 µg/mg HA) and bovine vitreous humor (36.2 µg/mg HA) [281]. The protein content in commercial human umbilical cord HA is ~30% higher than in ABS which has the highest protein content among alligator samples. ACS, AFT and AEB also have lower protein impurities than the ones reported for commercial HA from human umbilical cord and bovine vitreous humor. To the best of our knowledge, there is currently no standard of identity or reference standards for HA or sodium hyaluronate in the United States, however protein contents in alligator GAGs might need to be further reduced to comply with European medical grade or cosmetic grade standards.

The process described in Figure 3.1 includes four unit operations that mainly influence the final protein concentration. Namely, removal of muscle proteins with 0.2N NaOH, pepsin and papain digestion, dialysis filtration and NaCl-ethanol precipitation of GAGs. This process could be further optimized or new processes such as electrodeposition, filtration through activated

charcoal or size exclusion chromatography could be incorporated keeping in mind up-scalability and economic feasibility. It must be kept in mind that further processing is likely to reduce the molecular weight of the extracted materials. For instance, LMW-HA (125 kDa) with no protein content has been extracted and purified from commercial eggshells (5.3 mg HA/ g eggshell) using acetic acid extraction, isopropanol precipitation and silica gel-activated charcoal purification [246].

Mineral contents in alligator by-product GAGs are predominantly sodium as measured by ICP-AES (Figure 4.9). The contents were similar in ACS (13.92 ± 0.20 mg/100 mg dry extract), AFT (10.64 ± 0.20 mg/100 mg dry extract) and ABS (11.03 ± 0.20 mg/100 mg dry extract) with sodium accounting for over 97% in all three extracts. These results were expected in the extracts due to the separation of GAGs with NaCl (Figure 3.1). This is in close agreement with what is reported in current product specifications from Sigma-Aldrich (St. Louis, MO) for hyaluronic acid sodium salt from bovine vitreous humor (3-10% Na). The usage rate of NaCl (2M) in this study (Figure 3.1) was determined based on the efficiency of GAG recovery. Addition rates of 1M, 1.5M, 2M and 4M were evaluated, however no significant increases in GAG yields were observed after 2M. NaCl (4M) and CPC (10%) were also evaluated in combination and no increase in GAG recovery was observed (data not shown). Murado and others reported that NaCl concentrations higher than 1.5M should be used for optimal GAG recovery. Lower values of NaCl might lead to extracts with higher protein concentrations [124]. AEB GAGs purified without NaCl precipitation, as reported in Figure 3.2, had lower total mineral contents (0.27 ± 0.03 mg/100 mg dry extract) and cations (Na^+ and K^+) were the predominant minerals. Physiologically, HA is found in the salt form bound to cations [282]. Trace levels of other minerals such as Phosphorus, Sulfur and

Calcium were also detected in all samples. The origin of these is thought to be the bones, claws and calcified scales in ACS, AFT and ABS, respectively.

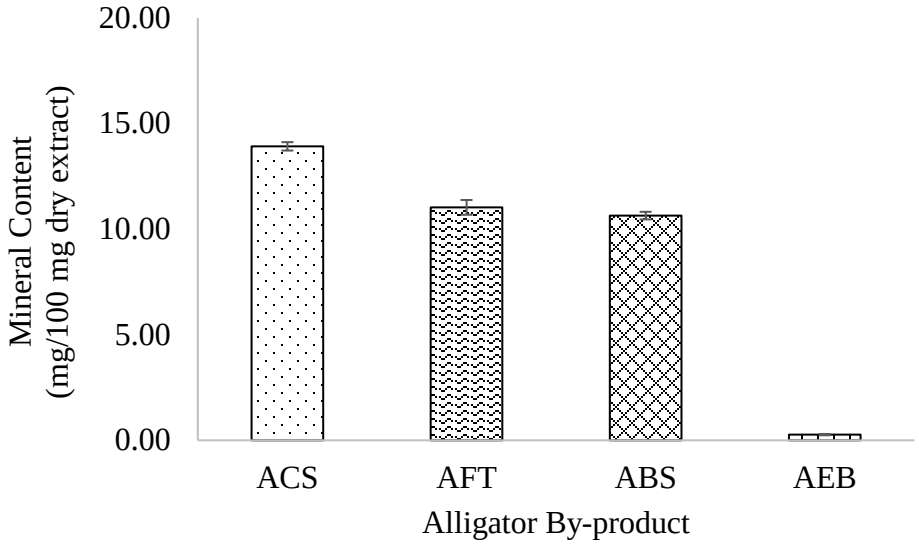

Figure 4.9. Mineral content in alligator by-product GAG extracts

4.5. FTIR Spectra of Alligator By-product GAGs

The FTIR-ATR spectra in the spectral range of 650-4000 cm^{-1} for GAGs from ACS, AFT, ABS and AEB are presented in Figure 4.10. The assignment of FTIR bands for the various samples is given in Table 4.3. Commercial *Streptococcus sp.* HA and bovine trachea CS standards were used as references for data analysis and peak identification. All samples and standards displayed a strong absorption peak in the range of 3258 cm^{-1} to 3289 cm^{-1} suggesting the stretching of -NH or -OH in the uronic acid COOH group as expected in GAGs [94]. Lower absorption peaks near 3078 cm^{-1} for samples and 3099 cm^{-1} for standards have been previously identified as the -NH and C=O combination in the amino sugar of GAGs while minor stretches at the range of 2890 and 2980 suggest -CH stretching [127,246,283,284]. The FTIR spectra of alligator samples also revealed the presence of characteristic C=O vibrations associated with primary amides between 1627 cm^{-1} and

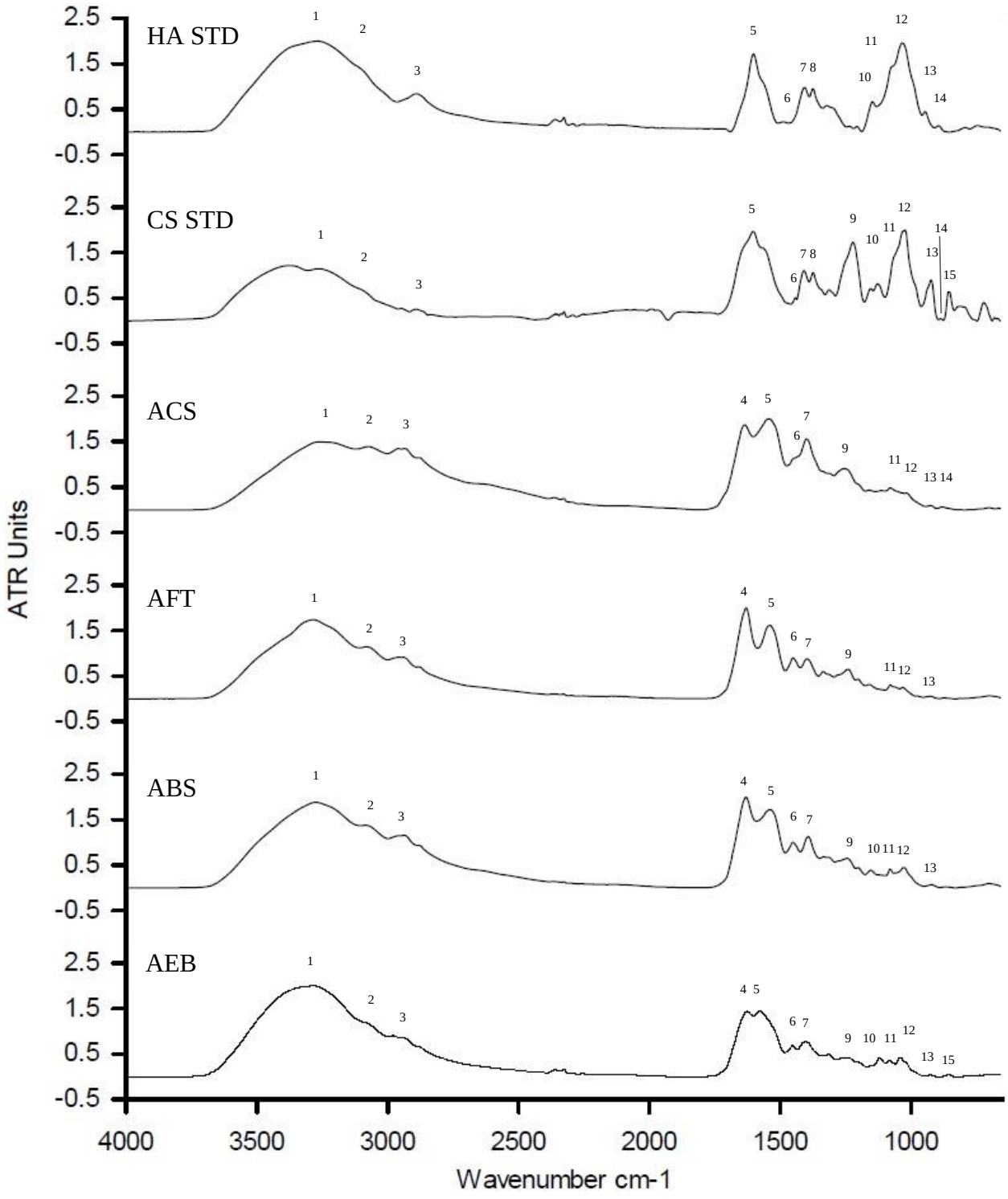

Figure 4.10. FTIR-ATR spectra of alligator GAGs

Table 4.3

Assignment of FTIR Bands for Standards and Alligator GAGs

FTIR Bands	Functional Groups	Wavenumber (cm^{-1})					
		HA STD	CS STD	ACS	AFT	ABS	AEB
1	O-H or N-H stretching	3271*	3267	3258	3285	3272	3289
2	N-H with C=O combination	3095	3099	3078	3078	3079	3078
3	C-H stretching	2890	2891	2935	2959	2937	2980
4	C=O carboxyl amide I	-	-	1635	1631	1632	1627
5	Amide II	1602	1604	1546	1539	1538	1575
6	N-H deformation	1490	1442	1452	1452	1452	1453
7	C-O with C=O combination	1407	1409	1399	1399	1393	1404
8	C-O-H deformation	1375	1375	-	-	-	-
9	S=O stretching	-	1222	1255	1241	1245	1243
10	C-O-H stretching, C-O and C-O-C	1148	1155	-	-	1154	1121
11		1080	1080	1080	1080	1080	1081
12		1034	1023	1030	1029	1028	1042
13	O-H deformation	947	923	922	921	921	925
14	C-O-C stretching	895	887	882	-	-	-
15	C4S Sulfate group	-	855	-	-	-	855

*Peak absorbance wavenumbers (cm^{-1}) are shown. HA STD = hyaluronic acid standard, CS STD = chondroitin sulfate standard, ACS = alligator carcasses, AFT = alligator feet, ABS = alligator backstraps, AEB = alligator eyeballs.

1635 cm^{-1}. Although these peaks were not observed in the HA or CS standards, they have been reported in haddock (*Theragra chalcogramma*) and other marine species GAGs as C=O stretching in N-acetyl groups of amino sugars or C=O stretching in peptide residues [94,284,285]. The secondary amide peaks were centered around 1600 cm^{-1} for HA and CS standards and were found at lower wavenumbers for alligator samples (1538 cm^{-1} to 1575 cm^{-1}). A peak in the range of 1222 cm^{-1} and 1255 cm^{-1} was observed mainly in the CS standard while alligator samples showed minor absorption in this region which is supported by the quantified sulfated GAGs content reported in Table 4.1. Accordingly, absorption in the 1200 cm^{-1} to 1250 cm^{-1} range was not observed in the HA standard [94,284]. Peaks in the range of 1000 cm^{-1} and 1200 cm^{-1} (C-OH, C-O and C-O-C) have been reported to be fingerprints of pyranose rings which are the building blocks of GAGs [286,287]. Below 1000 cm^{-1}, -OH deformations and C-O-C stretches were suggested by Alkrad and others [283]. Absorption at 855 cm^{-1} confirms the presence of chondroitin-4-sulfate [245]. In aggregate, the fingerprint functional groups and structures related with GAGs were identified in the 650-4000 cm^{-1} FTIR spectra. Moreover, the FTIR fingerprints of ACS, AFT, ABS and AEB reveal broad similarities between them and the findings are comparable with the spectra reported in past studies on animal sourced GAGs.

AFT GAG samples were also submitted to Thermo Fisher Scientific for collection of FTIR spectra (Figures 4.11 and 4.12). The FTIR spectra presented a high similarity to the one depicted in Figure 4.10, however a sharper definition of the fingerprint region may be due to the use of newer and more sensitive equipment. Quenching of some fingerprint signals and the presence of amide peaks was thought to be due to presence of residual collagen protein or peptides.

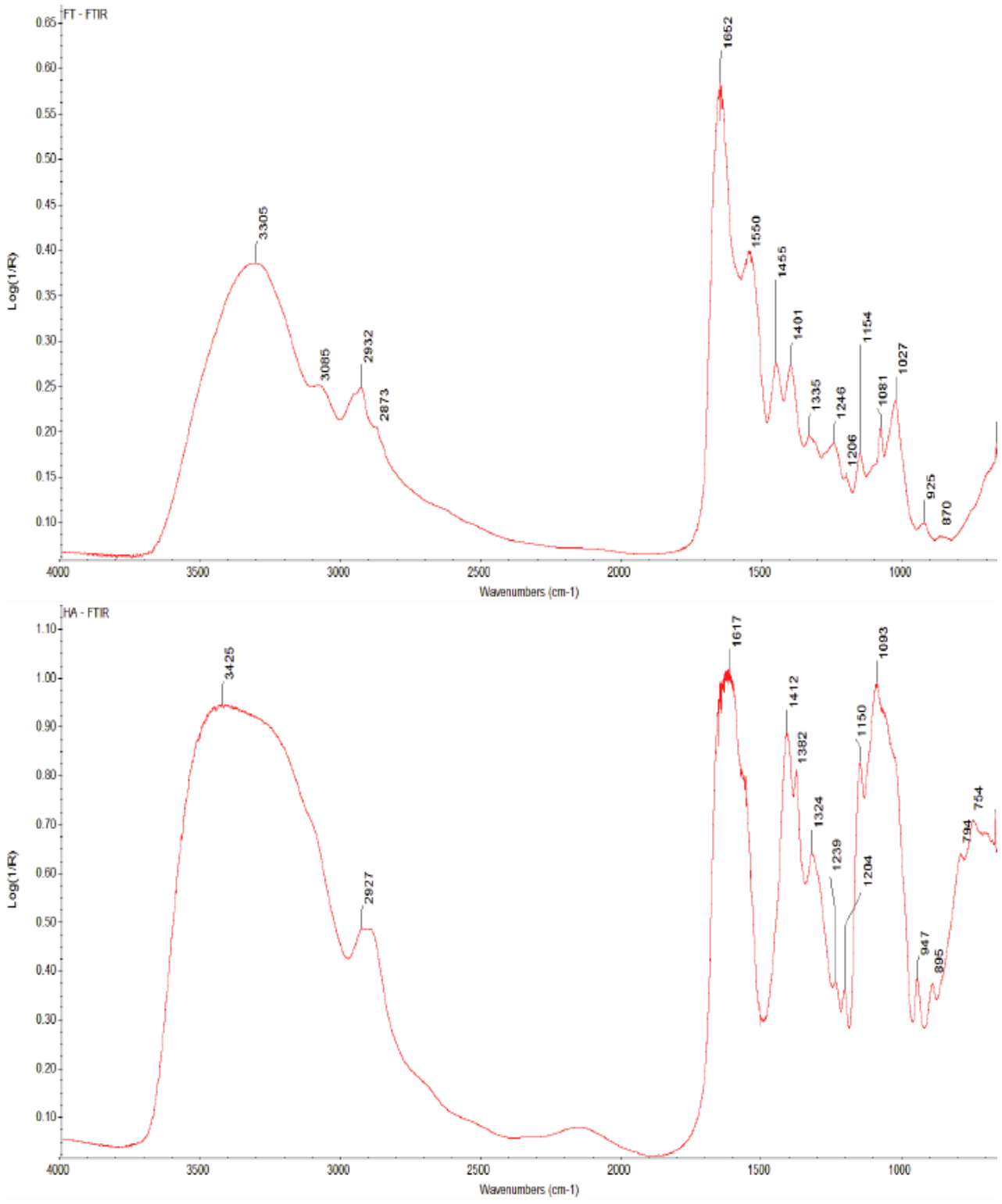

Figure 4.11. FTIR spectra of AFT GAGs (top) and streptococcal HA-salt (bottom).

4.6. *Scnn1b*-Tg MTEC Gene Expression Analysis

To evaluate the potential of AEB GAGs (Figure 4.12) to regulate gene expression in CF-like MTEC *ex-vivo* cultures, we took advantage of the well-established *Scnn1b*-Tg mice line that over-expresses the β-subunit of the ENaC channel and presents constitutive airway inflammation. The isolation of *Scnn1b*-Tg MTECs yielded $3.49x10^5$ live cells/trachea which were successfully proliferated in a submerged culture and differentiated at ALI into an intact monolayer with a cobblestone morphology as previously reported [281]. Murine epithelial primary cultures with these characteristics are suitable for the investigation of airway diseases and evaluation of novel therapies [257]. The ALI Transwell™ culture system allowed culturing of the MTEC in conditions closer to the in-vivo physiological orientation which is an advantage compared to conventional media submerged cultures [254].

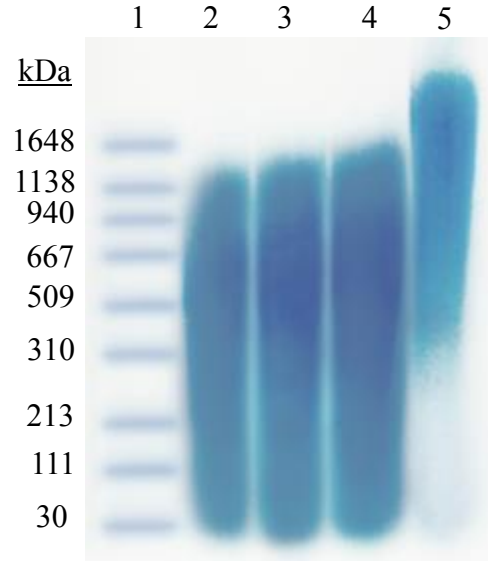

Figure 4.12. Electrophoresis of AEB GAGs used for MTEC treatment after dialysis (50 kDa MWCO) and autoclaving (121.1°C for 5 min). Lane 1: mixture of Select-HA HiLadder and LoLadder (1648, 1138, 940, 667, 509, 310, 213, 111 and 30.2 kDa); lanes 2-4: AEB GAGs (10 μg/lane); lane 5: HA salt

RNA free of any major contaminants was successfully purified from MTEC control and treated cultures as indicated by the A_{260}/A_{280} of 2.07 ± 0.00 and 2.08 ± 0.01, respectively (Table 4.4). These RNA quality parameters impact downstream reverse transcription procedures the most [289]. High RIN results (Table 4.4) in addition to sharp peaks and bands of rRNA 5S, 18S and 28S fragments are indicators of RNA with very low degradation (Figure 4.13). RIN values above 5.5 have been reported to yield high quality outcomes in rt-PCR [290]. Quality control assays of the cDNA generation efficiency, genomic DNA contamination, and overall PCR performance were passed by all samples. All the arrays presented similar ($p \leq 0.05$) reverse-transcription efficiencies (average RTC – average PPC ≤ 5) which indicate that the generated data is suitable for comparison (Table 4.4). Genomic DNA contamination did not contribute to the fluorescence signals captured during real-time PCR (GDC $C_T \geq 35$) and the overall PCR reproducibility within and between arrays passed the manufacturer's approval parameters (Table 4.4).

Table 4.4.

RNA Extraction and PCR Control Results

Reagent	Control (saline)	AEB GAGs Treated
RNA A_{260}/A_{280} Ratio[‡]	2.07 ± 0.00*[a]	2.08 ± 0.01[a]
RIN[††]	9.03 ± 0.06[a]	8.93 ± 0.15[a]
C_T GDC[§]	>35	>35
Reverse-Transcription Efficiency[φ]	3.93 ± 0.06[a]	4.11 ± 0.26[a]
PCR Array Reproducibility[Ω]	Pass	

[*] Means that do not share a letter within a row are significantly different.

[‡] A ratio of ~2 is generally accepted as "pure".

[††] Values range from 1 (totally degraded) to 10 (intact). RIN ≥7 is ideal.

[§] GDC $C_T \geq 35$ is equal to "Pass".

[φ] Average RTC C_T - Average PPC $C_T \leq 5$ is equal to "Pass".

[Ω] If average PPC C_T within an array is 20±2 and average PPC C_T of any two arrays is not more than 2 different from one another, then the sample receives a "Pass".

The gene expression analysis of PCR microarray data was conducted by setting a lower limit of detection (C_T< 35), a ΔRn threshold above the automatically calculated background signal,

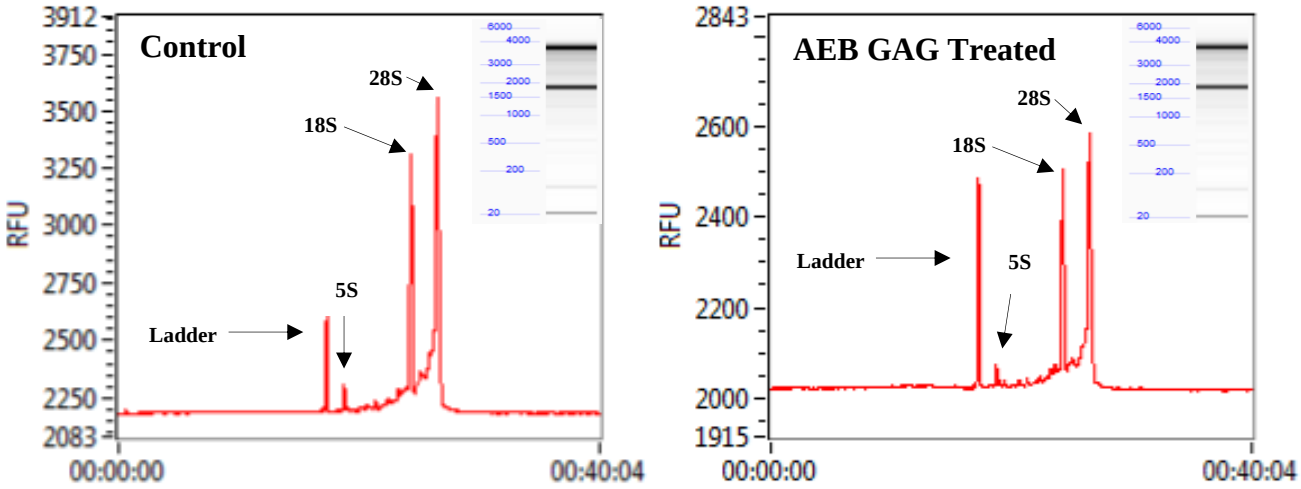

Figure 4.13. Capillary electrophoresis electropherograms and gels of RNA extracted from control and AEB-GAG treated Scnn1b-Tg MTEC.

a fold-regulation threshold (1.5) and normalization to the *B2m* housekeeping gene which was the most stably expressed across the evaluated samples (ΔAverage C_T <1). The genes that were not detected (9.52%) in at least one of the microarrays were not included in the analysis, namely *Alox12b, Ccl12, Cxcr2, Il1b, Il10, Il6, S100a8, Serpina1e, Slc26a3*. Seventy five (89.29%) of the genes analyzed were detected and a heat map depicting their differential expression in MTEC cultures is shown in Figure 4.14. After treatment with 0.5 mg AEB GAGs, MTEC gene expression was differentially regulated when compared to controls. Without a fold-regulation threshold, 32.00% (24 genes) of the genes were significantly ($p \leq 0.05$) down-regulated and 4.00% (4 genes) up-regulated, while the rest of the genes was not significantly ($p > 0.05$) down (42.67%) or up-regulated (21.33%) (Figure 4.15A). The overall shifts observed in the expression of 75 genes are indicative of the multiple signaling properties associated with HA in murine lungs through the

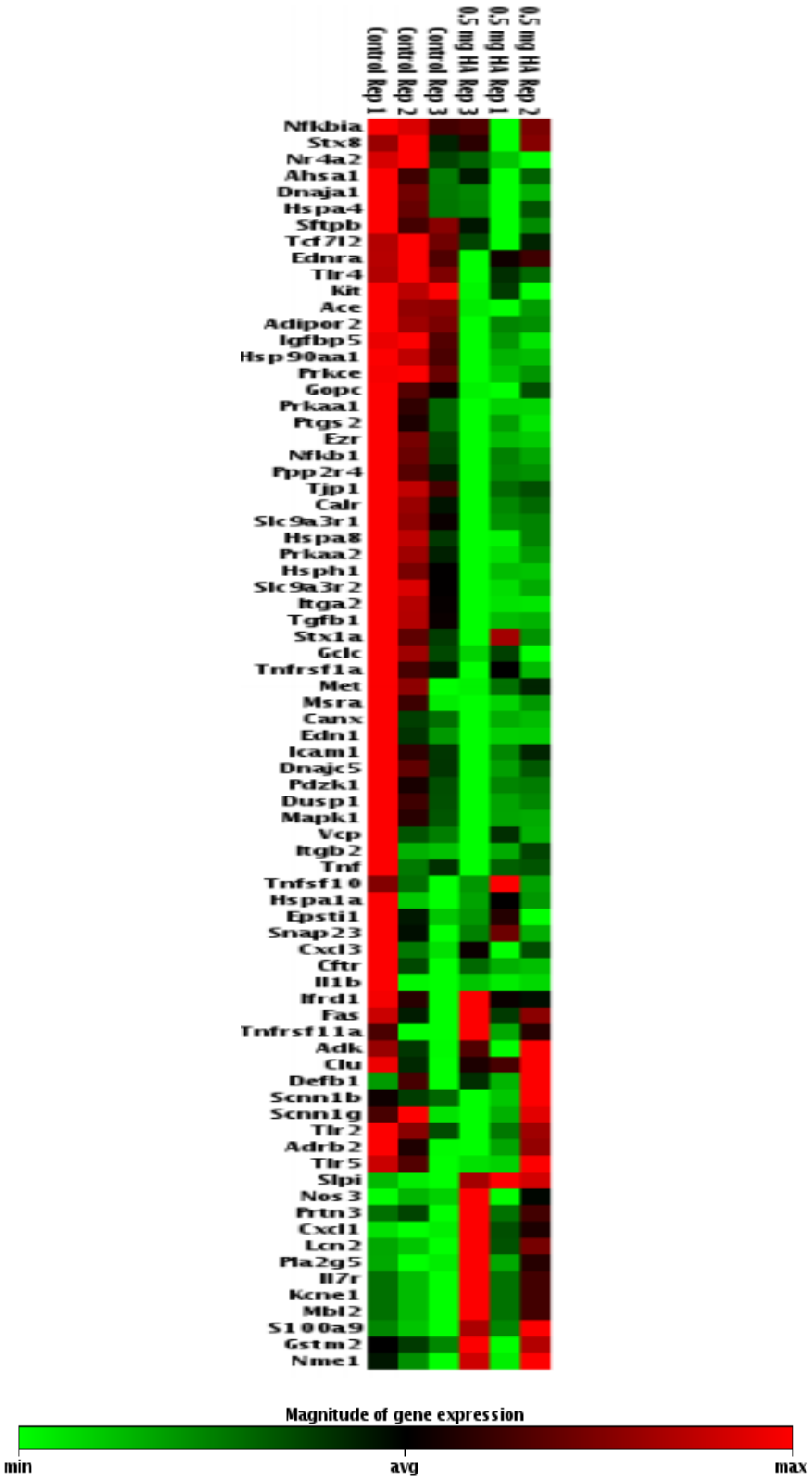

Figure 4.14. Non-supervised hierarchical clustering heat map of the differentially expressed genes in treated and untreated (control) Scnn1b-Tg MTEC in ALI culture.

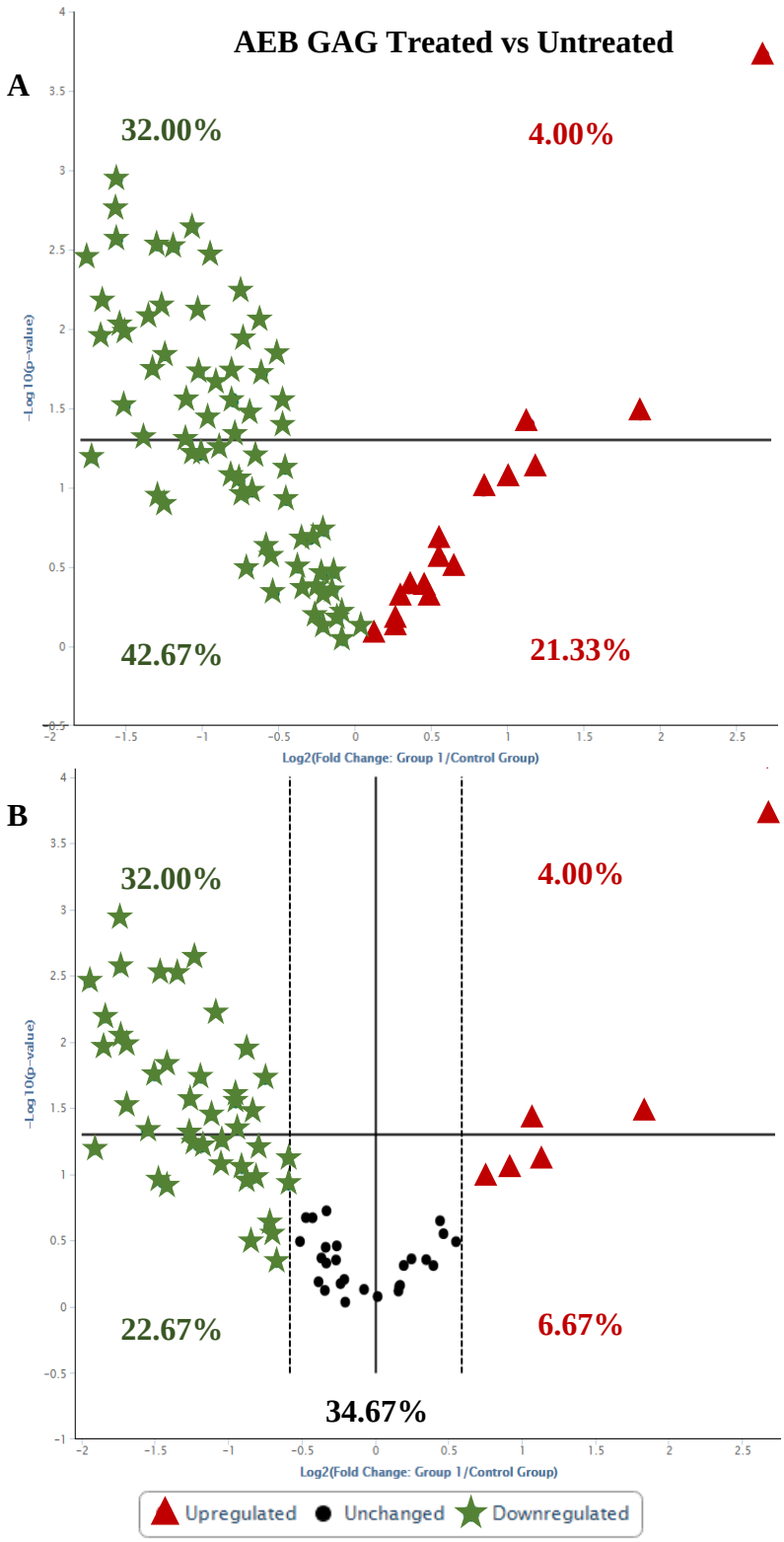

Figure 4.15. Distribution of gene regulation due to AEB GAGs treatment of Scnn1b-Tg MTEC in ALI culture. A) Plot of significantly ($p \leq 0.05$) and not significantly regulated genes. B) Plot of significantly ($p \leq 0.05$) and not significantly regulated genes with a 1.5-fold regulation threshold.

CD44, RHAMM and/or TLR4 [78,79,291,292], however for a more significant view of the potential effects of AEB GAGs in gene expression, a volcano plot including a 1.5 fold-regulation threshold is shown in Figure 4.15B. Under this criteria, 34.67% of the genes remained unchanged after AEB GAG treatment and the percentage of significantly ($p \leq 0.05$) regulated genes remained unchanged. Evaluation of the gene expression of wild-type MTEC cultures is important for further confirmation and understanding of these results. Figure 4.16 presents a non-supervised hierarchical clustering heat map with dendrograms which graphically presents differences in the gene expression patterns between treated and control cell cultures. Genes are clustered based on similarities in their expression patterns and not according to known functional similarities. In order of regulation magnitude, the significantly ($p \leq 0.05$) up-regulated (>1.5-fold) genes were the *Slpi, Cxcl1,* and *Lcn2* (Table 4.5). Following the same criteria, the down-regulated genes were *Kit, Hsph1, Itga2, Ace, Hsp90aa1, Tgfb1, Slc9a3r2, Ezr, Nfkb1, Slc9a3r1, Igfbp5, Tjp1, Adipor2, Prkaa1, Gopc, Prkce, Prkaa2, Ppp2r4, Hspa8, Sftpb, Nr4a2, Tlr4, Calr,* and *Tcf712*. Other genes with non-significant ($p > 0.05$) fold-regulation above 2- fold included *S100a9* (2.18-fold; *p-value= 0.0778302*), *Ptgs2* (-3.78-fold; *p-value= 0.065190*), *Edn1* (-2.69-fold; *p-value= 0.123140*), *Dusp1* (-2.28-fold; *p-value= 0.062676*), and *Dnajc5* (-2.07-fold; *p-value= 0.056502*). Preliminary interpretations of these gene expression regulations suggest potential anti-protease, anti-inflammatory, and ion-transport homeostatic effects of AEB GAG treatment on *Scnn1b*-Tg MTEC *ex-vivo* cultures.

The 6.38-fold upregulation of *Slpi* in AEB GAG treated cells compared to control untreated cultures was the highest and most significant ($p = 0.0019$) gene regulation observed in this study (Table 4.5). In human vaginal epithelial cells, Dusio and others reported a marked increase in *Slpi*

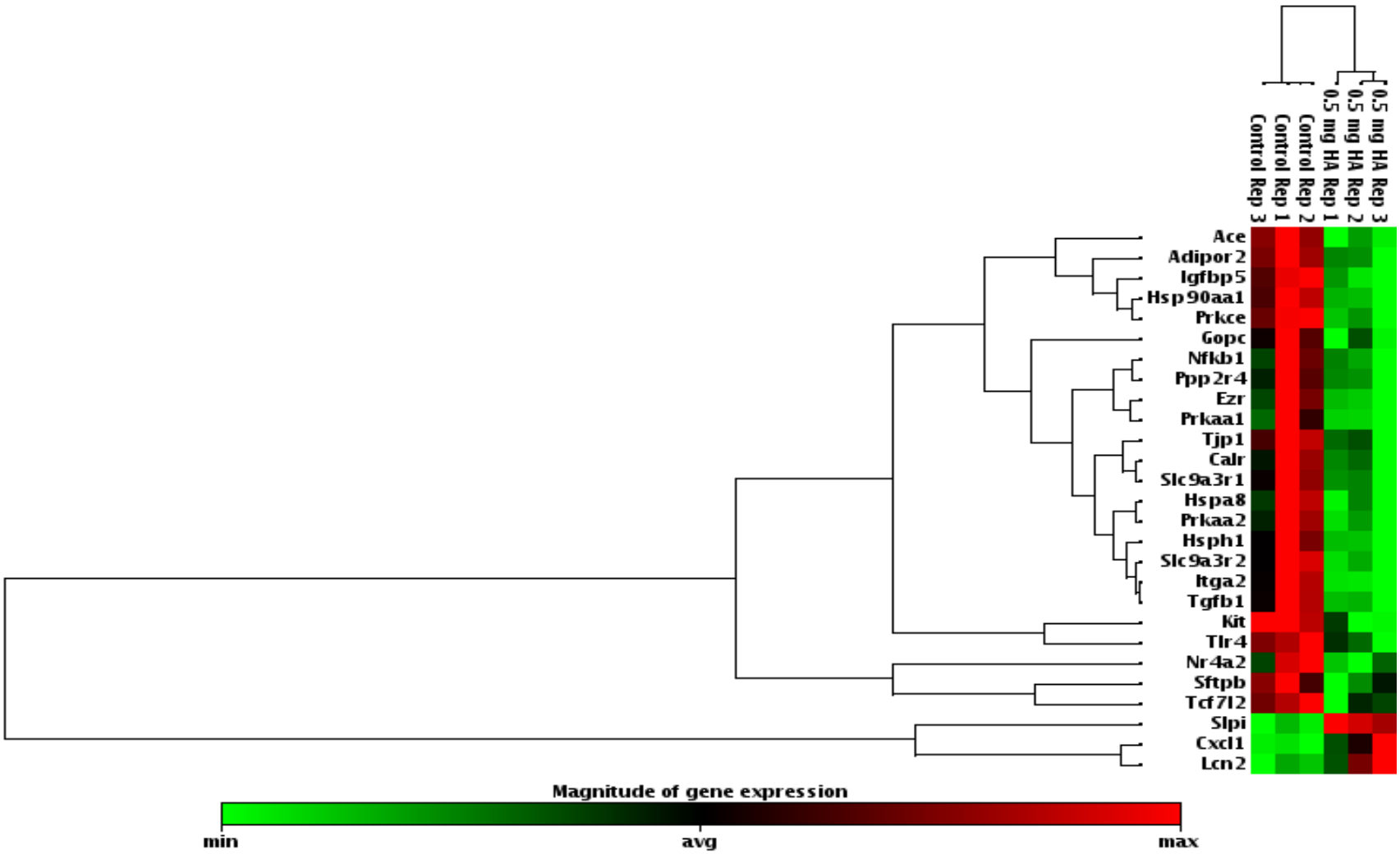

Figure 4.16. Non-supervised hierarchical clustering heat map with dendrograms indicating co-regulated genes of the significantly ($p \leq 0.05$) regulated (>1.5 fold) genes in treated and untreated (control) Scnn1b-Tg MTEC in ALI culture.

Table 4.5.

Genes differentially expressed in HA treated vs untreated Scnn1b-Tg MTEC*

Gene	Function	*p*-value	Fold-regulation
	Up-Regulated		
Slpi	Protection of epithelial tissues from serine proteases	*0.0019*	6.38
Cxcl1	Antimicrobial gene. Neutrophil chemoattractant	*0.0349*	3.54
Lcn2	Antibacterial activity & oxidative stress protection	*0.0398*	2.10
	Down-Regulated		
Kit	MAST cell adhesion to airway epithelia	*0.0036*	-3.88
Hsph1	Stress response	*0.0110*	-3.61
Itga2	Matrix metalloproteinase-1 positive regulation	*0.0066*	-3.59
Ace	Vasoconstrictor & pro-inflammatory mediator	*0.0011*	-3.35
Hsp90aa1	Endoplasmic reticulum stress response	*0.0027*	-3.35
Tgfb1	Fibrosis development & inflammatory response	*0.0094*	-3.33
Slc9a3r2	Trans-epithelial sodium/hydrogen absorption	*0.0105*	-3.25
Ezr	Actin linking to the apical membrane & mucin secretion	*0.0305*	-3.23
Nfkb1	Positive regulator of inflammation	*0.0471*	-2.96
Slc9a3r1	Trans-epithelial sodium/hydrogen absorption	*0.0181*	-2.84
Igfbp5	Fibrosis development & ECM production	*0.0030*	-2.78
Tjp1	Regulation of cell polarity & tight junction regulation	*0.0148*	-2.69
Adipor2	Regulation of AMPK & PPAR-alpha metabolisms	*0.0031*	-2.56
Prkaa1	Metabolic regulation	*0.0498*	-2.42
Gopc	Ion channel binding	*0.0277*	-2.41
Prkce	Immune response modulation	*0.0023*	-2.35
Prkaa2	Metabolic regulation	*0.0188*	-2.28
Ppp2r4	Homeostatic balance of cell metabolism & signaling	*0.0359*	-2.18
Hspa8	Protein folding & cellular homeostasis	*0.0290*	-1.94
Sftpb	Surfactant surface formation	*0.0273*	-1.94
Nr4a2	Modulation of inflammation & metabolism	*0.0458*	-1.92
Tlr4	Modulation of inflammation & immunity	*0.0114*	-1.85
Calr	$Ca2^{+}$ binding & regulation of surface protein expression	0.0333	-1.79
Tcf7l2	Glucose metabolism & type 2 diabetes susceptibility	*0.0193*	-1.69

* Genes with significant (*$p \leq 0.05$)* fold-regulation greater than 1.5-fold are presented.

transcription after LMW-HA (<200 kDa and 0.2% w/v in media) treatment for 18 h [293]. The secretory leukocyte protease inhibitor is a serine anti-protease encoded by the *Slpi* gene and it is known to inhibit elastase, cathepsins, trypsin and chymotrypsin [294,295]. Defects in airway mucosal defense, including disruption of the homeostatic protease/anti-protease balance, contribute to the pathogenesis of obstructive pulmonary disease in CF [296], therefore offsetting this imbalance is one of the therapeutic goals in CF management [297,298]. Therapeutic approaches have included administration of *Slpi* and synthetic anti-proteases [295,296]. An *in-vivo* study with sheep exposed to human elastase reported a blockage of elastase-related airway responses after treatment with aerosolized HA (150 and 300 kDa) [11]. It has also been reported that a single aerosol exposure (20 mg/mice for 50 min) to streptococcal HA (100 kDa) reduced elastase-induced airspace enlargement in mice and prevented elastic fiber injury in-vitro [300]. Overall, positive results regarding HA protection of airway fibers and regulation of acute lung injury have been reported [301], however there are no known reports of HA regulation of the *Slpi* gene in airway epithelial cells as observed in our results. HA has also been reported to immobilize and regulate other important components of the airway defense mechanism such as the serine protease tissue kallikrein and lactoperoxidase. Regulation of these enzymes is important for homeostasis at the apical mucosal surface [79]. The down-regulation of *Itga2* (-3.59-fold) further supports the potential capacity of AEB GAG treatment to mediate the protease/anti-protease imbalance characteristic of CF. Integrin α2β1 is a positive gene expression regulator of the MMP-1 [302] which is a serine collagenase known to be differentially upregulated during acute and chronic lung diseases compared to healthy patients [303,304]. Inhibition of expression or activation of MMPs has been proposed as a therapeutic strategy in lung CF and other chronic lung diseases [303,305,306].

Tgfb1 was down-regulated -3.33-fold in AEB GAG treated MTEC (Table 4.5) and it encodes the transforming growth factor-β which promotes fibrosis through the deposition of ECM, promotes inflammation and modulates immune responses in a cellular and environmental context-dependent manner [307]. Polymorphisms in the *Tgfb1*gene have been associated to an accelerated decline in lung function of patients with CF [308]. Microarray analyses with cDNA have shown that *Tgfb1* upregulation alters the expression of multiple genes important for the initiation of acute lung injury in nickel exposed mice [309]. A recent (2016) review highlights the fact that fibrosis is generally viewed as failed wound healing and that it can eventually lead to loss of lung function [310]. This supports the positive implications of *Tgfb1* and *Igfbp5* (-2.78-fold) downregulation in treated cells (Table 4.5). Studies have demonstrated the increased expression of *Igfbp5* in mice lung tissue after bleomycin-induced fibrosis [311], idiopathic pulmonary fibrosis in human lung sections [312], and severe emphysema of smokers in a chromosomal region strongly linked to FEV_1 [313]. The results discussed so far and the currently available literature point towards an important role of AEB GAGs in *Snn1b*-Tg epithelial tissue protection from excessive degradation by proteases and excessive remodeling in airway diseases [314]. The prominent roles of *Slpi* anti-protease activity and *Tgfb1*-related inflammation in wound healing and skin diseases like psoriasis suggest that AEB GAGs might also have potential in the treatment of inflammatory skin diseases [315–317].

In addition to protease inhibition, the secretory leukocyte protease inhibitor encoded by *Slpi*, has also been shown to inhibit inflammatory responses via a number of different mechanisms including competition with p65 for binding of NF-κβ which in turn prevents its activation and inhibition of neutrophil degranulation [296,318]. In our study, anti-inflammatory effects were

observed in epithelial cells treated with AEB GAGs which could be dependent or independent of *Slpi* regulation. Down-regulation of *Ace* (-3.59-fold), *Nfkb1* (-2.96-fold), *Nr4a2* (-1.92-fold), and *Tlr4* (-1.85-fold) (Table 4.5) and directionally but not significantly ($p>0.05$) of *Ptgs2* (Cyclooxygenase-2) (-3.78-fold) support this observation. Angiotensin II is a vasoconstrictor related to hypertension, however independently from this role it is also a potent pro-inflammatory mediator and inhibition of its converting enzyme encoded by *Ace* has been beneficial in mice pulmonary disease models and for patients with inflammatory diseases [319,320]. Asthmatic patients report higher ($p\leq0.05$) serum levels of angiotensin II converting enzyme compared to controls and it has been proposed that regulating this imbalance may aid in recovering the system's inflammatory and ROS homeostasis [321]. Interestingly, an association has been reported between the severity of CF and the undesirable effects of the *Ace* gene in Tunisian CF patients [322]. Furthermore, angiotensin II is associated with activation of NF-κβ-mediated genes in lung injury [323,324]. There is consensus in the fact that NF-κβ-mediated chronic inflammation is a prominent feature of CF lung disease and its downstream activation of IL-8 secretion and neutrophil influx promote progression of COPD and emphysema [325,326]. Our data further suggests potential anti-inflammatory properties of AEB GAGs through the modulation of *Prkce* (-2.35-fold) and *Nr4a2* (-1.92-fold) (Table 4.5). Protein kinase C encoded by *Prkce* is involved in many signal transduction events for several pathways including immune response, bacterial induced inflammation, development of COPD and formation of neutrophil extracellular traps (NET) [327–330]. The protein kinase C dependence for formation of NETs and the pro-inflammatory potential of excessive NET formation in CF has been demonstrated [328,331,332]. Therefore the *Prkce* downregulation observed in our study is valuable in supporting the anti-inflammatory effects of AEB GAGs. *Nr4a2* is a nuclear receptor regulated by *Nfkb1*, *Tgfb1*, *Ptgs2*, and *Tlr4* and it

modulates inflammation via MMP regulation [333,334]. In a synoviocyte cell line, microarray analyses showed that *Nr4a2* regulates the transcription of the *Il8* gene (+5.04-fold increase vs control) [335] and it is also a key regulator of inflammation in rheumatoid arthritis in vitro [336]. A highlight of the arthritis study is the remarkable anti-inflammatory effect of streptococcal HA (257 kDa) via the attenuation of mRNA expression of *Nr4a1*, *Nr4a1*, *Nr4a3* and *Mmp* genes. Immune and inflammatory responses can also be mediated by negative regulation of TLRs which play a role in lung inflammation and risk of emphysema development [337–339]. In our study, all TLRs analyzed (*Tlr2, Tlr4,* and *Tlr5*) were downregulated, however only *Tlr4* passed the thresholds for statistical significance ($p \leq 0.05$) and fold-regulation (>1.5-fold). This is of interest in our study due to the report that NE can induce *Il8* gene expression via *Tlr4* in human bronchial epithelial cells [340]. It has also been reviewed that in healthy epithelial cells HMW-HA is sensed by TLR2 and TLR4 and it protects the integrity of the epithelium by preventing apoptosis. On the other hand in injured tissues, HMW-HA is degraded and shorter fragments sensed by TLRs which results in inflammatory gene expression [291]. This offers an insight into the potential use of continued HMW-HA treatment in diseased airways as a novel therapeutic strategy and area of research for the modulation of inflammation.

Kit is a gene that encodes a receptor tyrosine kinase which contributes to mast cell adhesion to structural airway epithelial cells [341] and it showed the largest down-regulation (-3.88-fold) of all the genes differentially expressed in our study (Table 4.5). Targeting the inhibition of mast cell interactions with structural airway cells has been proposed as a novel approach to the treatment of asthma [341]. Chronic mast cell activation has undesirable effects on airway function, inflammation, and re-modelling in asthma pathophysiology through the production of TNF-α, IL-

1β, IL-6 and IL-13 mediated by TLR4 activation [342,343]. In CF and idiopathic pulmonary fibrosis, the concentration of tryptase and chymase positive mast cells were increased in lung areas showing increased inflammation or fibrosis compared to control individuals. These alterations in mast cell concentrations correlated positively to lung function parameters [344]. Moreover, mast cell serine proteases (tryptase and chymase) have the ability to activate MMP-1 [345]. In our study, down-regulation of *Ptgs2* (cyclooxygenase-2), which is upregulated in CF, may also reduce the release of the inflammatory mediator histamine from mast cells [346,347]. The potential positive effects of *Kit* downregulation after AEB GAG treatment are in agreement with the anti-inflammatory and protease/anti-protease balance mediation effects previously discussed. Altogether, these effects may be contributing to the apparent lower stress response in AEB GAG treated MTEC.

Heat shock proteins (HSP) are mammalian stress proteins produced in response to various forms of cellular stress [348]. HSPs also appear to be upregulated with worsening inflammation as previously reported in asthma epithelial cells [349,350]. Our results show that *Hsph1* (HSP105), *Hsp90aa1* (HSP90α) and *Hspa8* (HSP70) were all significantly ($p \leq 0.05$) down-regulated in AEB GAG treated cells by -3.61, -3.35 and -1.94-fold, respectively compared to control cultures (Table 4.5). This a positive outcome given that elevated levels of HSP27. HSP70 and HSP90α in COPD are markers for immune activation and tissue destruction [351]. Accordingly, HSP70 and IL-8 levels in lung epithelial tissues of patients with COPD were significantly increased compared to patients without COPD and the results positively correlated with the severity of the disease [352]. HSP105 exists as a complex associated with HSP70 [348]. AEB GAG treated MTEC might also have been protected against oxidative stress as suggested by Lcn2 upregulation (2.20-fold) (Table

4.5). Under conditions of oxidative stress, upregulation of *Lcn2* has a protective role against free H_2O_2 radicals and its upregulation can be cancelled by the addition of antioxidants which further supports its proposed role [353,354]. In agreement with these findings, *Lcn2* has been reported to be up to 9.8-fold upregulated in bronchial tissues of individuals exposed to sulfur mustard gas compared to controls and an advantageous role in decreasing ROS stress has been proposed [355]. Human neutrophil lipocalin-2 is also a key antibacterial component of the innate immune system [356] and a biomarker of acute exacerbation in CF [357]. We speculate that in the present study the upregulation of *Lcn2* may have been protective as a result of nitrosative and oxidative stresses which can occur in *Scnn1b*-Tg mice as mentioned by Livraghi and others [358]. *Cxcl1* (3.54-fold) was also upregulated in our study (Table 4.5) and its expression is known to be high in non-asthmatic airway smooth muscle cells in vivo which limits mast cell chemotaxis [359]. Marcos and others recently reported that levels of *Cxcl1*are high in BAL of *Scnn1b*-Tg mice compared to wild-type littermates, however there was no correlation between its upregulation and free levels of DNA or parameters of pulmonary obstruction [360]. Furthermore, this chemokine ligand has been reported to contribute to host defense by modulating neutrophil-related bactericidal functions [361]. Increased mRNA expression of several genes related to antimicrobial functions has been reported after HA treatment of vaginal epithelial cells [293]. To evaluate if the observed upregulated antimicrobial gene expressions were not due to contaminants present in the AEB GAG preparations (i.e. lipopolysaccharide), the AEB GAG solution used for treatment was analyzed for E.coli/coliforms and total aerobic counts (data not shown). Aerobic counts (10^0-10^{-3} duplicate plates) of the autoclaved treatment solution showed no growth or presence of coliforms, however aerobic counts of samples prior to autoclaving showed 68 CFU/ml (10^0 dilution). It is possible that

lipopolysaccharides from dead bacteria in the solution may have contributed to the upregulation of *Cxcl1* to some extent [362].

Slc9a3r2 (-3.25-fold) and *Slc9a3r1* (-2.84-fold) were differentially down-regulated by AEB GAG treatment in *Scnn1b*-Tg MTEC (Table 4.5). These genes encode Na^+-H^+ antiporter regulators in the sub-apical membrane of epithelial cells where they play a central role in pH regulation and Na^+ homeostasis. Moreover, CFTR and Na^+-H^+ antiporters in renal epithelial cells have been shown to interact via a regulatory complex that includes ezrin, encoded by *Ezr*, and protein kinase A, encoded by *Prkaa* [363,364]. *Ezr* (-3.23-fold), *Prkaa1* (-2.42-fold) *and Prkaa2* (-2.28-fold) were also downregulated by AEB GAG treatment (Table 4.5). These observations raise the possibility that AEB GAGs may help modulate the increased Na^+ influx in *Scnn1b*-Tg by downregulating Na^+-H^+ antiporter regulators as well as other components of their regulatory complex. In this manner, the airway epithelia could potentially maintain a more optimal ASL [365]. A Joint Location-Scale Test very recently highlighted *Slc9a3r1*, *Slc9a3r2*, and *Ezr* for their previously unknown role in contributing to CF lung disease [366]. Moreover, *Ezr* is highly expressed in the bronchi of humans with chronic airway diseases and it has been demonstrated that it is essential in NE-induced mucin exocytosis which can lead to airway obstruction and bacterial colonization [367]. BAL secreted mucin content is increased in *Scnn1b*-Tg mice [358]. *Prkaa1* and *Prkaa2* encode the adenosine mono-phosphate (AMP)-activated kinase (AMPK). AMPK is an important regulator of cellular energy homeostasis and [368] and it can be activated by hypoxia, oxidative stress , and hyperosmotic stress [369,370]. Altogether, the down regulation of *Slc9a3r1*, *Slc9a3r2*, *Ezr*, *Prkaa1* and *Prkaa2* indicate that AEB GAGs may be mediating Na^+ homeostatic balance and improvements on the condition of *Scnn1b*-Tg MTEC ASL *ex-vivo* [371].

Tight junctions between epithelial cells control paracellular movements of water, ions , and solutes, regulate cell polarity and even play a role in airway protection from bacterial infection [372–375]. It has been proposed that hypertonic saline solutions increase water transport into the ASL which promotes MCC [376]. The suggested mechanism of this action is the opening of the tight junctions between epithelial cells which may increase paracellular water transport into the airway lumen [377]. In the context of an *ex-vivo* model using cells over-expressing Na^+ channels, our observed downregulation of the tight junction protein *Tjp1* (-2.69-fold vs control) (Table 4.5), along with the Na^+ balance regulation previously described, may be another indicator of optimization of the ASL conditions through enhanced paracellular permeability. CF airway epithelial cells in vitro have tighter tight junctions than healthy cells and [378], however like in our study, effects in-vivo in the presence of bacterial insults may cause a different expression of *Tjp1* and other associated proteins [168,372]. Reports on the effects of HA on tight junctions are varied. In human tracheal epithelial cells at ALI, HA (40 KDa) has been reported to enhance Tjp1 expression and functionality [379], however in human tracheal-bronchial epithelial cells exposed to cigarette smoke at ALI, HA (<70 kDa) has been reported to disrupt the tight junctions [380].

Other genes that were downregulated with AEB GAG treatment were: *Adipor2* (-2.56-fold), *Gopc* (-2.41-fold), *Ppp2r4* (-2.56-fold), *Sftpb* (-1.94-fold), *Calr* (-1.79-fold), and *Tcf7l2* (-1.69-fold). *Adipor2* (-2.56-fold) (Table 4.5) which encodes for a receptor of adinopectin, has tissue and environmental-dependent anti- and pro-inflammatory effects [381]. Adinopectin has been proposed as an inflammatory biomarker in COPD due to its rise during exacerbations [382], however human and murine studies are still inconclusive regarding its role in inflammation [383]. *Gopc* also known as the Golgi-associated PDZ is a protein involved in vesicle trafficking and is

also a negative regulator of CFTR membrane surface levels [384]. Suppression of *Gopc* has been proposed as a pharmacological target as an approach to retaining CFTR at the apical membrane [385]. Furthermore, a logistic regression of whole blood gene expression in smoking and non-smoking individuals identified *Gopc* as one of the top five genes that predict smoking status [386]. *Ppp2r4* is a CFTR modifier gene that encodes a regulatory subunit of protein phosphatase 2A and it is associated with CFTR deactivation and correlates positively with a worse progression of FEV_1, lung clearance index and effective specific airway resistance in CF patients [387]. In our study, the role of *Ppp2r4* downregulation remains unclear given the fact that protein phosphatase 2A signaling has shown a critical role in countering inflammatory and proteolytic responses after cigarette smoke exposure in mice [388]. The *Sftpb* gene has shown contradicting results in studies in Chinese and German populations. In the Chinese population it protected subjects from COPD and increased FEV_1 [389], however in Germany a splice variant of *Sftpb* increased risk of acute respiratory failure in COPD [390]. This gene is key to epithelial surfactant homeostasis and is known to be overexpressed in CF chronic rhinosinusitis and lipopolysaccharide-induced injury [391]. In a 3-year study, surfactant protein B concentrations increased 213% from year 1 to 3 in CF patients' BAL and this correlated positively to decrease in lung function. Interestingly, surfactant proteins A, C and D concentrations remained unchanged during the 3-year period but there was a progressive loss of their function [392]. In our *Scnn1b*-Tg *ex-vivo* study, *Sftpb* may have been downregulated due to a better monolayer hydration which might contribute to make surface tension lowering less critical. Calreticulin is a protein encoded by the *Calr* gene and it is involved in Ca^{2+} binding as well as protein folding, maturation and trafficking [393]. In COPD and CF airways, endoplasmic reticulum stress and its Ca^{2+} stores (calreticulin) promote Ca^{2+}-dependent hyper-inflammatory responses [394,395]. Some elements of this response are positive

such as protective Ca^{2+} -enhanced MCC, however others such as Ca^{2+}-dependent IL-8 secretion are undesirable [396]. *Calr* downregulation by AEB GAG treatment of MTEC may further contribute to ameliorating the inflammatory phenotype of these cultures.

The last downregulation ($p \leq 0.05$; >1.5-fold) observed in this study was related to the *Tcf7l2* gene (-1.69-fold) (Table 4.5). This gene confers increased risk of diabetes mellitus on the general population and modifies age of onset in CF [15,397]. *Tcf7l2* is postulated to play a role in the function of the beta cells of pancreatic islets [398] and an in vivo study on mice suggested that decreased expression of *Tcf7l2* confers reduction of diabetic susceptibility via regulation of the metabolism of glucose and lipids [399].

TGAse activity in the MTEC culture supernatants after AEB GAG treatment was evaluated with a method that offers a detection limit of 0.03 mU TGAse/ml. A linear standard curve (R^2=0.992) with triplicate readings in the 0.03 to 0.35 mU/ml range was developed, however no TGAse activity was detected in any of the samples. Further studies are necessary to elucidate the role of TGAse in the airways of *Scnn1b*-Tg mice.

Finally, it is important to mention that the amount of AEB GAGs (0.5 mg/insert of an extract containing >98.5% HA (~30-1600 kDa)) used in our experiment is much higher than the innate concentrations previously reported in mice BAL (<5 ng/ml in healthy ice and 100-120 ng/ml in ozone-exposed mice) [400]. This dose should be enough to compete with any HA present in the MTEC ASL and to gain access to cell surface receptors. Furthermore, it has been reported that concentrations of CS are low and HS is not detectable in airway secretions, and thus it is unlikely

that any innate presence of these GAGs in MTEC ASL contributes or confounds the results reported here [380].

CHAPTER 5
CONCLUSIONS AND FUTURE STUDIES

In this research, GAGs were extracted and characterized for the first time from farmed *Alligator mississippiensis*. The extraction and purification methods applied are commonly used to purify GAGs and collagen from various animal tissues and sources [260,401–403], however by-product to solvent ratios, protein removal methods and dialysis times were modified or added for GAG extraction from alligator waste carcasses, feet and backstraps. Moreover, a process for GAG extraction from alligator eyeball vitreous humor was developed. Of the by-products studied carcasses were the bulkiest (942.00 ± 109.12 g/ farmed alligator) and had a total GAG content of 0.60±0.00 mg/g wet carcass, however backstraps had the highest ($p \leq 0.05$) GAG yield (15.53±0.27 mg/g wet backstrap) and they were easier to extract. This was due to the much less complex nature of the backstrap compared to the structure and composition of carcasses, feet and eyeballs. The GAGs extracted from all four by-products studied add up to ~2.13 g GAGs per harvest-size (~24 cm belly-width) farmed alligator or an estimated GAG production of ~0.73 tons/year in Louisiana alone based on the 2014 farm-raised harvest data. This indicates that alligators are a potentially high yield source of GAGs, which compares favorably to marine sources that have been studied and that are generally perceived as "clean" [263]. All extracts contained 0.72-3.68% protein and eyeball extracts had the lowest protein content therefore posing the lowest risk of hypersensitivity in downstream applications. FTIR revealed spectra showing characteristic animal GAG features with which included -OH, -NH and -CH signals, as well as amide signals originated from the residual protein content of the samples. The GAGs in all samples were predominantly (>97%) ns-GAGs or HA with a poly-disperse MW ranging from ~30 to 1600 kDa after a final micro-dialysis unit operation. We encountered abundance of HMW and MMW GAGs in *Alligator*

mississippiensis by-products which offers a new potential to improve waste management practices and increase revenue in the Louisiana alligator industry through their marketing in the US$1 billion global HA market [33] for biomedical, cosmetic, human nutrition and animal nutrition applications.

The results of the *Scnn1b*-Tg MTEC *ex-vivo* gene expression analysis suggest that alligator eyeball GAGs (0.5 mg/ 12 mm insert) may be effective in recovering the protease/anti-protease balance through regulation of *Slpi* (+6.38-fold) and *Itga2* (-3.59-fold); reducing inflammation through regulation of *Kit* (-3.88-fold), *Ace* (-3.35-fold), *Nfkb1* (-2.96-fold), *Nr4a2* (-1.92-fold), and *Tlr4* (-1.85-fold); and regulating ASL osmotic homeostasis through regulation of *Slc9a3r2* (-3.25-fold), *Slc9a3r1* (-2.84-fold)*1*, *Ezr* (-3.23-fold), *Prkaa1* (-2.42-fold), and *Prkaa2* (-2.28-fold). The regulation of this triad of key factors in dehydrated airways may have supported an apparent lower stress condition as indicated by the downregulation of *Hsph1* (-3.61-fold), *Hsp90aa1* (-3.35-fold) and *Hspa8* (-1.94). In conclusion, although the *ex-vivo* responses to AEB GAGs in *Scnn1b*-Tg MTEC may not be fully predictive of the responses in humans or other animal models, our findings indicate the potential importance of AEB GAGs in ameliorating some of the negative responses of dehydrated airways in CF. These pilot study results also justify future studies to explore other cosmetic or biomedical applications of alligator GAGs which include but are not limited to: : wound repair, tumorigenesis, lung injury repair, skin humectation, healing of equine joint disease and canine arthritis care.

It would also be productive to focus future studies deriving from this research on the industrial up-scalability to pilot and commercial scale of the processes proposed in Figures 3.1 and

3.2, as well as their financial feasibility. It would also be relevant to evaluate the content and characteristics of the GAGs contained in the by-products of other Louisiana animals such as catfish, Asian carp, oysters, nutria, and others.

REFERENCES

[1] LDWF. Historical Data 2010. http://www.wlf.louisiana.gov/historical-data.

[2] Schanté CE, Zuber G, Herlin C, Vandamme TF. Chemical modifications of hyaluronic acid for the synthesis of derivatives for a broad range of biomedical applications. Carbohydr Polym 2011;85:469–89. doi:10.1016/j.carbpol.2011.03.019.

[3] Lennon FE, Singleton P a. Role of hyaluronan and hyaluronan-binding proteins in lung pathobiology Role of hyaluronan and hyaluronan-binding proteins in lung pathobiology 2012;60637. doi:10.1152/ajplung.00071.2010.

[4] Raia V, Sepe A, Tosco A, Gregorio F De, Amato F. Aerosolized hyaluronic acid and its applications 2014;85:22–5.

[5] Monslow J, Govindaraju P, PurÃ© E. Hyaluronan â€“ A Functional and Structural Sweet Spot in the Tissue Microenvironment. Front Immunol 2015;6:4–10. doi:10.3389/fimmu.2015.00231.

[6] Cyphert JM, Trempus CS, Garantziotis S. Size Matters : Molecular Weight Specificity of Hyaluronan Effects in Cell Biology 2015.

[7] Quero L, Klawitter M, Schmaus A, Rothley M, Sleeman J, Tiaden AN, et al. Hyaluronic acid fragments enhance the inflammatory and catabolic response in human intervertebral disc cells through modulation of toll-like receptor 2 signalling pathways. Arthritis Res Ther 2013;15:R94. doi:10.1186/ar4274.

[8] Dicker KT, Gurski L a., Pradhan-Bhatt S, Witt RL, Farach-Carson MC, Jia X. Hyaluronan: A simple polysaccharide with diverse biological functions. Acta Biomater 2014;10:1558–70. doi:10.1016/j.actbio.2013.12.019.

[9] Lauer ME, Dweik RA, Garantziotis S, Aronica MA. The Rise and Fall of Hyaluronan in Respiratory Diseases 2015.

[10] Gavina M, Luciani A, Villella VR, Esposito S, Ferrari E, Bressani I, et al. Nebulized Hyaluronan Ameliorates lung inflammation in cystic fibrosis mice. Pediatr Pulmonol 2013;48:761–71. doi:10.1002/ppul.22637.

[11] Scuri M, Abraham WM. Hyaluronan blocks human neutrophil elastase (HNE)-induced airway responses in sheep. Pulm Pharmacol Ther 2003;16:335–40. doi:10.1016/S1094-5539(03)00089-0.

[12] Cantor JO, Turino GM. Can Exogenously Administered Hyaluronan Improve Respiratory Function in Patients with Pulmonary Emphysema? Chest 2004;125:288–92. doi:10.1378/chest.125.1.288.

[13] Hunter GK, Wong KS, Kim JJ. Binding of Calcium to Glycosaminoglycans : An Equilibrium Dialysis Study ’ Binding of calcium to the glycosaminoglycans (GAGS) heparin , chondroitin sulfate (CS), keratan sulfate (KS), and hyaluronic acid (HA) has been studied by equilibrium dialy 1988;260:161–7.

[14] Lamontagne CA, Plante GE, Grandbois M. Characterization of hyaluronic acid interaction with calcium oxalate crystals: implication of crystals faces, pH and citrate. J Mol Recognit 2011;24:733–40. doi:10.1002/jmr.1110.

[15] Cutting GR. Cystic fibrosis genetics: from molecular understanding to clinical application. Nat Rev Genet 2014;16:45–56. doi:10.1038/nrg3849.

[16] De Rose V. Mechanisms and markers of airway inflammation in cystic fibrosis. Eur Respir J 2002;19:333–40. doi:10.1183/09031936.02.00229202.

[17] Aldallal N, McNaughton EE, Manzel LJ, Richards AM, Zabner J, Ferkol TW, et al. Inflammatory response in airway epithelial cells isolated from patients with cystic fibrosis. Am J Respir Crit Care Med 2002;166:1248–56. doi:10.1164/rccm.200206-627OC.

[18] Venkatakrishnan a, Stecenko a a, King G, Blackwell TR, Brigham KL, Christman JW, et al. Exaggerated activation of nuclear factor-kappaB and altered IkappaB-beta processing in cystic fibrosis bronchial epithelial cells. Am J Respir Cell Mol Biol 2000;23:396–403. doi:10.1165/ajrcmb.23.3.3949.

[19] Li J, Johnson XD, Iazvovskaia S, Tan A, Lin A, Hershenson MB. Signaling intermediates required for NF-kappa B activation and IL-8 expression in CF bronchial epithelial cells. Am J Physiol Lung Cell Mol Physiol 2003;284:L307–15. doi:10.1152/ajplung.00086.2002.

[20] Chmiel JF, Konstan MW, Saadane A, Krenicky JE, Lester Kirchner H, Berger M. Prolonged inflammatory response to acute pseudomonas challenge in interleukin-10 knockout mice. Am J Respir Crit Care Med 2002;165:1176–81. doi:10.1164/rccm.2107051.

[21] Cantin AM, Hartl D, Konstan MW, Chmiel JF. In fl ammation in cystic fi brosis lung disease : Pathogenesis and therapy ☆. J Cyst Fibros 2015;14:1–12. doi:10.1016/j.jcf.2015.03.003.

[22] Muhlebach MS, Stewart PW, Leigh MW, Noah TL. Quantitation of inflammatory responses to bacteria in young cystic fibrosis and control patients. Am J Respir Crit Care Med 1999;160:186–91. doi:10.1164/ajrccm.160.1.9808096.

[23] Downey DG, Bell SC, Elborn JS. Neutrophils in cystic fibrosis. Thorax 2009;64:81–8. doi:10.1136/thx.2007.082388.

[24] Ros M, Rosario C, Lucca F, Troiani P, Salonini E, Favilli F, et al. Hyaluronic Acid Improves the Tolerability of Hypertonic Saline in the Chronic Treatment of Cystic Fibrosis Patients: A Multicenter, Randomized, Controlled Clinical Trial. J Aerosol Med Pulm Drug Deliv 2014;27:133–7.

[25] Editorial. The challenges of developing effective anti-inflammatory agents in cystic fibrosis. J Cyst Fibros 2015;14:164–6. doi:10.1016/j.jcf.2014.12.004.

[26] Lai H-C, Stacey C. F, David B. A, Michael R. K, Beryl J. R, Preston W. C, et al. Risk of Persistent Growth Impairment after Alternate-Day Prednisone Treatment in Children with Cystic Fibrosis. N Engl J Med 2000;345:851–9.

[27] Malorni W, Farrace MG, Rodolfo C PM. Type 2 transglutaminase in neurodegenerative diseases: the mitochondrial connection. Curr Pharm Des 2008;14:278–88. doi:10.2174/138161208783413220.

[28] Aluko RE, Yada RY. Effect of a microbial calcium-independent transglutaminase on functional properties of a partially purified cowpea (Vigna unguiculata) globulin. J Sci Food Agric 1999;79:286–90.

[29] Luciani A, Villella VR, Vasaturo A, Giardino I, Raia V, Pettoello-Mantovani M, et al. SUMOylation of tissue transglutaminase as link between oxidative stress and inflammation. J Immunol 2009;183:2775–84. doi:10.4049/jimmunol.0900993.

[30] Maiuri L, Luciani a., Giardino I, Raia V, Villella VR, D'Apolito M, et al. Tissue Transglutaminase Activation Modulates Inflammation in Cystic Fibrosis via PPAR Down-Regulation. J Immunol 2008;180:7697–705. doi:10.4049/jimmunol.180.11.7697.

[31] Di Cicco M, Alicandro G, Claut L, Cariani L, Luca N, Defilippi G, et al. Efficacy and tolerability of a new nasal spray formulation containing hyaluronate and tobramycin in cystic fibrosis patients with bacterial rhinosinusitis. J Cyst Fibros 2014;13:455–60. doi:10.1016/j.jcf.2014.02.006.

[32] Buonpensiero P, De Gregorio F, Sepe A, Di Pasqua A, Ferri P, Siano M, et al. Hyaluronic acid improves "pleasantness" and tolerability of nebulized hypertonic saline in a cohort of patients with cystic fibrosis. Adv Ther 2010;27:870–8. doi:10.1007/s12325-010-0076-8.

[33] Liu L, Liu Y, Li J, Du G, Chen J. Microbial production of hyaluronic acid: current state, challenges, and perspectives. Microb Cell Fact 2011;10:99. doi:10.1186/1475-2859-10-99.

[34] Chong BF, Blank LM, Mclaughlin R, Nielsen LK. Microbial hyaluronic acid production. Appl Microbiol Biotechnol 2005;66:341–51. doi:10.1007/s00253-004-1774-4.

[35] LWFD. Best Management Practices for Louisiana Alligator Farming. 2011.

[36] LWFD. Louisiana's Alligator Management Program. 2014. doi:10.1017/CBO9781107415324.004.

[37] Brannen D, Roberts K, Keithly W. Louisiana alligator farming 1991 economic impact. 1991.

[38] Caldwell J. World Trade in Crocodilian Skins 2009-2011. 2013.

[39] AAC. Alligator Advisory Council 2015 Annual Report. 2015.

[40] Grenard S. Handbook of alligators and crocodiles. 1991.

[41] Nevarez J, Mitchell M. Lymphohistiocytic proliferative syndrome of alligators (Alligator mississippiensis): A cutaneous manifestation of West Nile Virus. 2007.

[42] Leak FW, Lane TJ, Johnson DD, Lamkey JW. Increasing the Profitability of Florida Alligator. Boards 2010:1–9.

[43] Padmanabhan P, Sujana KA. Animal products in traditional medicine from Attappady hills of Western Ghats. Indian J Tradit Knowl 2008;7:326–9.

[44] Soewu DA. Wild animals in ethnozoological practices among the Yorubas of southwestern Nigeria and the implications for biodiversity conservation. African J Agric Res 2008;3:421–7.

[45] Jacobo-Salcedo MDR, Alonso-Castro AJ, Zarate-Martinez A. Folk medicinal use of fauna in Mapimi, Durango, Mexico. J Ethnopharmacol 2011;133:902–6. doi:10.1016/j.jep.2010.10.005.

[46] Cupul-Magaña FG. Cocodrilo: medicina para el alma y el cuerpo. Rev Biomédica 2003;14:45–8.

[47] Buthelezi S, Southway C, Govinden U, Bodenstein J, Du Toit K. An investigation of the antimicrobial and anti-inflammatory activities of crocodile oil. J Ethnopharmacol 2012;143:325–30. doi:10.1016/j.jep.2012.06.040.

[48] Merchant ME, Pallansch M, Paulman RL, Wells JB, Nalca A, Ptak R. Antiviral activity of serum from the American alligator (Alligator mississippiensis). Antiviral Res 2005;66:35–8. doi:10.1016/j.antiviral.2004.12.007.

[49] Merchant, Mark Thibodeaux, Damon Loubser K, Elsey RM. Amoebicidal effects of serum from the American Alligator (Alligator mississippiensis). J Parasitol 2004;90:1480–3.

[50] Day JJ, Yanez Arancibia A, Misch W, Lara-Dominguez A, Day J, Ko J, et al. Using Ecotechnology to address water quality and wetland habitat loss problems in the Mississippi basin: a hierarchical approach. 2Biotechnology Adv 2003;22:135–9.

[51] Jackson CR, Vallaire SC. Effects of salinity and nutrients on microbial assemblages in Louisiana wetland sediments. Wetlands 2009;29:277–87.

[52] Ferguson MWJ. Reproductive biology and embryology of the crocodilians. Biol. Reptil., vol. 14, 1985, p. 329–491.

[53] Liu Z, Zhang F, Li L, Li G, He W, Linhardt RJ. Compositional analysis and structural elucidation of glycosaminoglycans in chicken eggs. Glycoconj J 2014;31:593–602. doi:10.1007/s10719-014-9557-3.

[54] Ziment I, Tashkin DP. Alternative medicine for allergy and asthma. J Allergy Clin Immunol 2000;106:603–14. doi:10.1067/mai.2000.109432.

[55] Davis S. Chinese keen to chomp on Aussie crocs. ABC Far North Queensl 2011. http://www.abc.net.au/local/audio/2011/05/30/3230778.htm.

[56] Gomez-Guillen MC, Gimenez B, Lopez-Caballero ME, Montero MP. Functional and bioactive properties of collagen and gelatin from alternative sources: A review. Food Hydrocoll 2011;25:1813–27. doi:10.1016/j.foodhyd.2011.02.007.

[57] Merchant ME, Roche CM, Thibodeaux D, Elsey RM. Identification of alternative pathway serum complement activity in the blood of the American alligator (Alligator mississippiensis). Comp Biochem Physiol B Biochem Mol Biol 2005;141:281–8. doi:10.1016/j.cbpc.2005.03.009.

[58] Merchant ME, Leger N, Jerkins E, Mills K, Pallansch MB, Paulman RL, et al. Broad spectrum antimicrobial activity of leukocyte extracts from the American alligator (Alligator mississippiensis). Vet Immunol Immunopathol 2006;110:221–8. doi:10.1016/j.vetimm.2005.10.001.

[59] Pata S, Yaraksa N, Daduang S, Temsiripong Y, Svasti J, Araki T, et al. Characterization of the novel antibacterial peptide Leucrocin from crocodile (Crocodylus siamensis) white blood cell extracts. Dev Comp Immunol 2011;35:545–53. doi:10.1016/j.dci.2010.12.011.

[60] Merchant ME, Mills K, Leger N, Jerkins E, Vliet KA, McDaniel N. Comparisons of innate immune activity of all known living crocodylian species. Comp Biochem Physiol - B Biochem Mol Biol 2006;143:133–7. doi:10.1016/j.cbpb.2005.10.005.

[61] Vigetti D, Karousou E, Viola M, Deleonibus S, De Luca G, Passi A. Hyaluronan: Biosynthesis and signaling. Biochim Biophys Acta - Gen Subj 2014;1840:2452–9. doi:10.1016/j.bbagen.2014.02.001.

[62] Karamanos NK, Tzanakakis GN. Glycosaminoglycans: from "cellular glue" to novel therapeutical agents. Curr Opin Pharmacol 2012;12:220–2. doi:10.1016/j.coph.2011.12.003.

[63] DeAngelis PL. Glycosaminoglycan polysaccharide biosynthesis and production: today and tomorrow. Appl Microbiol Biotechnol 2012;94:295–305. doi:10.1007/s00253-011-3801-6.

[64] Gandhi NS, Mancera RL. The structure of glycosaminoglycans and their interactions with proteins. Chem Biol Drug Des 2008;72:455–82. doi:10.1111/j.1747-0285.2008.00741.x.

[65] Palmer W, John KM. Polysaccharide of Vitreous Humor. Ophthalmology n.d.:629–34.

[66] Dreyfuss JL, Regatieri C V., Jarrouge TR, Cavalheiro RP, Sampaio LO, Nader HB. Heparan sulfate proteoglycans: structure, protein interactions and cell signaling. An Acad Bras Cienc 2009;81:409–29. doi:10.1590/S0001-37652009000300007.

[67] Girish KS, Kemparaju K, Nagaraju S, Vishwanath BS. Hyaluronidase inhibitors: a biological and therapeutic perspective. Curr Med Chem 2009;16:2261–88. doi:10.2174/092986709788453078.

[68] Itano N, Sawai T, Yoshida M, Lenas P, Yamada Y, Imagawa M, et al. Three isoforms of mammalian hyaluronan synthases have distinct enzymatic properties. J Biol Chem 1999;274:25085–92. doi:10.1074/jbc.274.35.25085.

[69] Tien JYL, Spicer AP. Three vertebrate hyaluronan synthases are expressed during mouse development in distinct spatial and temporal patterns. Dev Dyn 2005;233:130–41. doi:10.1002/dvdy.20328.

[70] Noble PW, Liang J, Jiang D. Hyaluronan as an Immune Regulator in Human Diseases. Physiol Rev 2011;91:221–64. doi:10.1152/physrev.00052.2009.Hyaluronan.

[71] STERN R, ASARI A, SUGAHARA K. Hyaluronan fragments: An information-rich system. Eur J Cell Biol 2006;85:699–715. doi:10.1016/j.ejcb.2006.05.009.

[72] Jordan AR, Racine RR, Hennig MJP, Lokeshwar VB. The Role of CD44 in Disease Pathophysiology and Targeted Treatment. Front Immunol 2015;6:1–14. doi:10.3389/fimmu.2015.00182.

[73] Teder P, Vandivier RW, Jiang D, Liang J, Cohn L, Puré E, et al. Resolution of lung inflammation by CD44. Science 2002;296:155–8. doi:10.1126/science.1069659.

[74] Liang J, Jiang D, Griffith J, Yu S, Fan J, Zhao X, et al. CD44 is a negative regulator of acute pulmonary inflammation and lipopolysaccharide-TLR signaling in mouse macrophages. J Immunol 2007;178:2469–75. doi:10.4049/jimmunol.178.4.2469.

[75] Jiang D, Liang J, Fan J, Yu S, Chen S, Luo Y, et al. Regulation of lung injury and repair by Toll-like receptors and hyaluronan. Nat Med 2005;11:1173–9. doi:10.1038/nm1315.

[76] Muto J, Yamasaki K, Taylor KR, Gallo RL. Engagement of CD44 by hyaluronan suppresses TLR4 signaling and the septic response to LPS. Mol Immunol 2009;47:449–56. doi:10.1016/j.molimm.2009.08.026.

[77] Kouvidi K, Berdiaki A, Nikitovic D, Katonis P, Afratis N, Hascall VC, et al. Role of receptor for hyaluronic acid-mediated motility (RHAMM) in low molecular weight hyaluronan (LMWHA)-mediated fibrosarcoma cell adhesion. J Biol Chem 2011;286:38509–20. doi:10.1074/jbc.M111.275875.

[78] Zaman A, Cui Z, Foley JP, Zhao H, Grimm PC, DeLisser HM, et al. Expression and role of the hyaluronan receptor RHAMM in inflammation after bleomycin injury. Am J Respir Cell Mol Biol 2005;33:447–54. doi:10.1165/rcmb.2004-0333OC.

[79] Forteza R, Lieb T, Aoki T, Savani RC, Conner GE, Salathe M. Hyaluronan serves a novel role in airway mucosal host defense. FASEB J 2001;15:2179–86. doi:10.1096/fj.01-0036com.

[80] Šoltés L, Mendichi R, Kogan G, Schiller J, Stankovská M, Arnhold J. Degradative action of reactive oxygen species on hyaluronan. Biomacromolecules 2006;7:659–68. doi:10.1021/bm050867v.

[81] del Fresno C, Otero K, Gómez-García L, González-León MC, Soler-Ranger L, Fuentes-Prior P, et al. Tumor cells deactivate human monocytes by up-regulating IL-1 receptor associated kinase-M expression via CD44 and TLR4. J Immunol 2005;174:3032–40. doi:174/5/3032 [pii].

[82] Pandey MS, Baggenstoss B a., Washburn J, Harris EN, Weigel PH. The hyaluronan receptor for endocytosis (HARE) activates NF-κB-mediated gene expression in response to 40-400-kDa, but not smaller or larger, hyaluronans. J Biol Chem 2013;288:14068–79. doi:10.1074/jbc.M112.442889.

[83] de la Motte C a, Hascall VC, Drazba J, Bandyopadhyay SK, Strong S a. Mononuclear leukocytes bind to specific hyaluronan structures on colon mucosal smooth muscle cells treated with polyinosinic acid:polycytidylic acid: inter-alpha-trypsin inhibitor is crucial to structure and function. Am J Pathol 2003;163:121–33. doi:10.1016/S0002-9440(10)63636-X.

[84] Lesley J, Gál I, Mahoney DJ, Cordell MR, Rugg MS, Hyman R, et al. TSG-6 modulates the interaction between hyaluronan and cell surface CD44. J Biol Chem 2004;279:25745–54. doi:10.1074/jbc.M313319200.

[85] Selbi W, de la Motte C a, Hascall VC, Day a J, Bowen T, Phillips a O. Characterization of hyaluronan cable structure and function in renal proximal tubular epithelial cells. Kidney Int 2006;70:1287–95. doi:10.1038/sj.ki.5001760.

[86] Cantor JO. Potential therapeutic applications of hyaluronan in the lung. Int J Chron Obstruct Pulmon Dis 2007;2:283–8.

[87] Lauer ME, Fulop C, Mukhopadhyay D, Comhair S, Erzurum SC, Hascall VC. Airway smooth muscle cells synthesize hyaluronan cable structures independent of inter-??-inhibitor heavy chain attachment. J Biol Chem 2009;284:5313–23. doi:10.1074/jbc.M807979200.

[88] Milner CM, Tongsoongnoen W, Rugg MS, Day a J. The molecular basis of inter-alpha-inhibitor heavy chain transfer on to hyaluronan. Biochem Soc Trans 2007;35:672–6. doi:10.1042/BST0350672.

[89] Yasuda T. Hyaluronan inhibits cytokine production by lipopolysaccharide-stimulated U937 macrophages through down-regulation of NF-κB via ICAM-1. Inflamm Res 2007;56:246–53. doi:10.1007/s00011-007-6168-5.

[90] Zhang H, Huang S, Yang X, Zhai G. Current research on hyaluronic acid-drug bioconjugates. Eur J Med Chem 2014;86:310–7. doi:10.1016/j.ejmech.2014.08.067.

[91] Iovu M, Dumais G, du Souich P. Anti-inflammatory activity of chondroitin sulfate. Osteoarthr Cartil 2008;16:14–8. doi:10.1016/j.joca.2008.06.008.

[92] Lambert C, Mathy-Hartert M, Dubuc J-E, Montell E, Vergés J, Munaut C, et al. Characterization of synovial angiogenesis in osteoarthritis patients and its modulation by chondroitin sulfate. Arthritis Res Ther 2012;14:R58. doi:10.1186/ar3771.

[93] Andrés RM, Payá M, Montesinos MC, Ubeda A, Navalón P, Herrero M, et al. Potential antipsoriatic effect of chondroitin sulfate through inhibition of NF-κB and STAT3 in human keratinocytes. Pharmacol Res 2013;70:20–6. doi:10.1016/j.phrs.2012.12.004.

[94] Laparra JM, López-Rubio A, Lagaron JM, Sanz Y. Dietary glycosaminoglycans interfere in bacterial adhesion and gliadin-induced pro-inflammatory response in intestinal epithelial (Caco-2) cells. Int J Biol Macromol 2010;47:458–64. doi:10.1016/j.ijbiomac.2010.06.015.

[95] Yamada S, Sugahara K. Potential therapeutic application of chondroitin sulfate/dermatan sulfate. Curr Drug Discov Technol 2008;5:289–301. doi:10.2174/157016308786733564.

[96] Bergefall K, Trybala E, Johansson M, Uyama T, Naito S, Yamada S, et al. Chondroitin Sulfate Characterized by the E-disaccharide Unit Is a Potent Inhibitor of Herpes Simplex Virus Infectivity and Provides the Virus Binding Sites on gro2C Cells. J Biol Chem %R 101074/jbcM503645200 2005;280:32193–9. doi:10.1074/jbc.M503645200.

[97] Rogerson S, Chaiyaroj S. Chondroitin sulfate A is a cell surface receptor for Plasmodium falciparum-infected erythrocytes. J Exp Med 1995;182:15–20.

[98] Rolls A, Avidan H, Cahalon L, Schori H, Bakalash S, Litvak V, et al. A disaccharide derived from chondroitin sulphate proteoglycan promotes central nervous system repair in rats and mice+. Eur J Neurosci 2004;20:1973–83. doi:10.1111/j.1460-9568.2004.03676.x.

[99] Lee CM, Tanaka T, Murai T, Kondo M, Kimura J, Su W, et al. Novel chondroitin sulfate-binding cationic liposomes loaded with cisplatin efficiently suppress the local growth and liver metastasis of tumor cells in vivo. Cancer Res 2002;62:4282–8.

[100] Barańska-Rybak W, Sonesson a., Nowicki R, Schmidtchen a. Glycosaminoglycans inhibit the antibacterial activity of LL-37 in biological fluids. J Antimicrob Chemother 2006;57:260–5. doi:10.1093/jac/dki460.

[101] Hori Y, Hoshino J, Yamazaki C, Sekiguchi T, Miyauchi S, Horie K. Effects of chondroitin sulfate on colitis induced by dextran sulfate sodium in rats. Jpn J Pharmacol 2001;85:155–60. doi:10.1254/jjp.85.155.

[102] Herrero-Beaumont G, Marcos ME, Sánchez-Pernaute O, Granados R, Ortega L, Montell E, et al. Effect of chondroitin sulphate in a rabbit model of atherosclerosis aggravated by chronic arthritis. Br J Pharmacol 2008;154:843–51. doi:10.1038/bjp.2008.113.

[103] Vallières M, du Souich P. Modulation of inflammation by chondroitin sulfate. Osteoarthr Cartil 2010;18:18–23. doi:10.1016/j.joca.2010.02.017.

[104] Saranraj P, Naidu MA. Hyaluronic Acid Production and its Applications - A Review 2013;4:853–9.

[105] Stern R, Jedrzejas MJ. The Hyaluronidases: Their Genomics, Structures, and Mechanisms of Action. Chem Rev 2006;106:818–39. doi:10.1021/cr050247k.The.

[106] Lokeshwar V, Cerwinka W, Lokeshwar B. HYAL1 hyaluroni- dase: A molecular determinant of bladder tumor growth and invasion. Cancer Res 2005;65:2243–50.

[107] Chao KL, Muthukumar L, Herzberg O. Structure of human hyaluronidase-1, a hyaluronan hydrolyzing enzyme involved in tumor growth and angiogenesis. Biochemistry 2007;46:6911–20. doi:10.1021/bi700382g.

[108] Li Y, Rahmanian M, Widström C, Lepperdinger G, Frost GI, Heldin P. Irradiation-induced expression of hyaluronan (HA) synthase 2 and hyaluronidase 2 genes in rat lung tissue accompanies active turnover of HA and induction of types I and III collagen gene expression. Am J Respir Cell Mol Biol 2000;23:411–8. doi:10.1165/ajrcmb.23.3.4102.

[109] Papakonstantinou E, Roth M, Klagas I, Karakiulakis G, Tamm M, Stolz D. COPD Exacerbations Are Associated With Proinflammatory Degradation of Hyaluronic Acid. CHEST J 2015;148.

[110] Rinaudo M, Lardy B, Grange L, Conrozier T. Effect of mannitol on hyaluronic acid stability in two In vitro models of oxidative stress. Polymers (Basel) 2014;6:1948–57. doi:10.3390/polym6071948.

[111] Bracke KR, Dentener M a, Papakonstantinou E, Vernooy JHJ, Demoor T, Pauwels NS, et al. Enhanced deposition of low-molecular-weight hyaluronan in lungs of cigarette smoke-exposed mice. Am J Respir Cell Mol Biol 2010;42:753–61. doi:10.1165/rcmb.2008-0424OC.

[112] Lurie Z, Offer T, Russo A, Samuni A, Nitzan D. Do stable nitroxide radicals catalyze or inhibit the degradation of hyaluronic acid? Free Radic Biol Med 2003;35:169–78. doi:10.1016/S0891-5849(03)00270-3.

[113] Hawkins CL, Davies MJ. Direct detection and identification of radicals generated during the hydroxyl radical-induced degradation of hyaluronic acid and related materials. Free Radic Biol Med 1996;21:275–90. doi:10.1016/0891-5849(96)00042-1.

[114] Greenwald RA, Moak SA. Degradation of hyaluronic acid by polymorphonuclear leukocytes. Inflammation 1986;10:15–30.

[115] Fuchs B, Schiller J. Glycosaminoglycan Degradation by Selected Reactive Oxygen Species. Antioxidants Redox Signal 2015;21:1044–62.

[116] Gao F, Koenitzer JR, Tobolewski JM, Jiang D, Liang J, Noble PW, et al. Extracellular Superoxide Dismutase Inhibits Inflammation by Preventing Oxidative Fragmentation of Hyaluronan. J Biol Chem 2008;283:6058–66. doi:10.1074/jbc.M709273200.

[117] Eberlein M, Scheibner K a, Black KE, Collins SL, Chan-Li Y, Powell JD, et al. Anti-oxidant inhibition of hyaluronan fragment-induced inflammatory gene expression. J Inflamm (Lond) 2008;5:20. doi:10.1186/1476-9255-5-20.

[118] Esser PR, Wölfle U, Dürr C, von Loewenich FD, Schempp CM, Freudenberg MA, et al. Contact sensitizers induce skin inflammation via ROS production and hyaluronic acid degradation. PLoS One 2012;7:e41340. doi:10.1371/journal.pone.0041340.

[119] Stern R, Kogan G, Jedrzejas MJ, Šoltés L. The many ways to cleave hyaluronan. Biotechnol Adv 2007;25:537–57. doi:10.1016/j.biotechadv.2007.07.001.

[120] Rosa CS Da, Tovar AF, Mourão P, Pereira R, Barreto P, Beirão LH. Purification and characterization of hyaluronic acid from chicken combs. Ciência Rural 2012;42:1682–7. doi:10.1590/S0103-84782012005000056.

[121] Nakano T, Nakano K, Sim JS. A Simple Rapid Method To Estimate Hyaluronic Acid Concentrations in Rooster Comb and Wattle Using Cellulose Acetate. J Agric Food Chem 1994;42:2766–8. doi:10.1021/jf00048a022.

[122] Nakano T, Sim JS. Glycosaminoglycans from the rooster comb and wattle. Poult Sci 1989;68:1303–6. doi:10.3382/ps.0681303.

[123] Kang DY, Kim WS, Heo IS, Park YH, Lee S. Extraction of hyaluronic acid (HA) from rooster comb and characterization using flow field-flow fractionation (FlFFF) coupled with multiangle light scattering (MALS). J Sep Sci 2010;33:3530–6. doi:10.1002/jssc.201000478.

[124] Murado M a., Montemayor MI, Cabo ML, Vázquez J a., González MP. Optimization of extraction and purification process of hyaluronic acid from fish eyeball. Food Bioprod Process 2012;90:491–8. doi:10.1016/j.fbp.2011.11.002.

[125] Luo XM, Fosmire GJ, Leach RM. Chicken keel cartilage as a source of chondroitin sulfate. Poult Sci 2002;81:1086–9.

[126] Vázquez J, Pastrana L, Piñeiro C, Teixeira J, Pérez-Martín R, Amado I. Production of Hyaluronic Acid by Streptococcus zooepidemicus on Protein Substrates Obtained from Scyliorhinus canicula Discards. Mar Drugs 2015;13:6537–49. doi:10.3390/md13106537.

[127] Patil KP, Patil DK, Chaudhari BL, Chincholkar SB. Production of hyaluronic acid from Streptococcus zooepidemicus MTCC 3523 and its wound healing activity. J Biosci Bioeng 2011;111:286–8. doi:10.1016/j.jbiosc.2010.10.012.

[128] Videbaek T. Hyaluronic Acid; Technology, Market & Timing 2011:1–20.

[129] Chien L-J, Lee C-K. Hyaluronic acid production by recombinant Lactococcus lactis. Appl Microbiol Biotechnol 2007;77:339–46. doi:10.1007/s00253-007-1153-z.

[130] Mao Z, Chen RR. Recombinant synthesis of hyaluronan by Agrobacterium sp. Biotechnol Prog 2007;23:1038–42. doi:10.1021/bp070113n.

[131] Mao Z, Shin HD, Chen R. A recombinant E. coli bioprocess for hyaluronan synthesis. Appl Microbiol Biotechnol 2009;84:63–9. doi:10.1007/s00253-009-1963-2.

[132] Ratjen F, Döring G. Cystic fibrosis. Lancet 2003;361:681–9. doi:10.1016/S0140-6736(03)12567-6.

[133] CFF. Patient Registry Annual Data Report. 2014.

[134] Kreindler JL. Cystic fibrosis: Exploiting its genetic basis in the hunt for new therapies. Pharmacol Ther 2010;125:219–29. doi:10.1016/j.pharmthera.2009.10.006.

[135] Schindler T, Michel S, Wilson a. WM. Nutrition Management of Cystic Fibrosis in the 21st Century. Nutr Clin Pract 2015;30:488–500. doi:10.1177/0884533615591604.

[136] CFF. Cystic Fibrosis Foundation Patient Registry. 2013 Annu Data Rep 2014:Bethesda, MD.

[137] Amaral MD. Novel personalized therapies for cystic fibrosis: treating the basic defect in all patients. J Intern Med 2015;277:155–66. doi:10.1111/joim.12314.

[138] Di Sant'Agnese PA, Darling RC, Perera GA, Shea E. Abnormal electrolyte composition of sweat in cystic fibrosis of the pancreas: clinical significance and relationship to the disease. Pediatrics 1953;12:549–63.

[139] Mishra A, Greaves R, Massie J. The relevance of sweat testing for the diagnosis of cystic fibrosis in the genomic era. Clin Biochem Rev 2005;26:135–53.

[140] Gibson LE, Cooke RE. A test for concentration of electrolytes in sweat in cystic fibrosis of the pancreas utilizing pilocarpine by iontophoresis. Pediatrics 1959;23:545–9.

[141] Welsh MJ, Liedtke CM. Chloride and potassium channels in cystic fibrosis. Nature 1986;322:467–70. doi:10.1038/322467a0.

[142] Quinton PM. Chloride impermeability in cystic fibrosis. Nature 1983;301:421–2.

[143] Li M, McCann JD, Liedtket CM, Nairn AC, Greengard P, Welsh MJ. Cyclic AMP-dependent protein kinase opens chloride channels in normal but not cystic fibrosis airway epithelium. , Publ Online 28 January 1988; | doi101038/331358a0 1988;331:358–60. doi:10.1038/331358a0.

[144] Kerem B, Rommens JM, Buchanan JA, Markiewicz D, Cox TK, Chakravarti A, et al. Identification of the Cystic Fibrosis Gene: Genetic Analysis. Science (80-) 1989;245:1073–80.

[145] Riordan JR, Rommens JM, Kerem B, Alon N, Rozmahel R, Grzelczak Z, et al. Identification of the cystic fibrosis gene: cloning and characterization of complementary DNA. Science 1989;245:1066–73. doi:10.1126/science.2475911.

[146] Cohen-Cymberknoh M, Shoseyov D, Kerem E. Managing Cystic Fibrosis. Am J Respir Crit Care Med 2011;183:1463–71. doi:10.1164/rccm.201009-1478CI.

[147] Sheppard DN, Welsh MJ. Structure and Function of the CFTR Chloride Channel. Physiol Rev 1999;79:23–45.

[148] Cheng SH, Gregory RJ, Marshall J, Paul S, Souza DW, White G a, et al. Defective intracellular transport and processing of CFTR is the molecular basis of most cystic fibrosis. Cell 1990;63:827–34. doi:10.1016/0092-8674(90)90148-8.

[149] CFMDB Statistics. Cystic Fibrosis Mutation Database 2011:http://www.genet.sickkids.on.ca/StatisticsPage.htm.

[150] Bergougnoux A, Taulan-cadars M, Claustres M, Raynal C. New Molecular Diagnosis Approaches — From the Identification of Mutations to their Characterization. Cyst. Fibros. Light New Res., 2015, p. 201–31.

[151] Smith JJ, Travis SM, Greenberg EP, Welsh MJ. Cystic fibrosis airway epithelia fail to kill bacteria because of abnormal airway surface fluid. Cell 1996;85:229–36. doi:10.1016/S0092-8674(00)81099-5.

[152] O'Sullivan BP, Baker D, Leung KG, Reed G, Baker SS, Borowitz D. Evolution of pancreatic function during the first year in infants with cystic fibrosis. J Pediatr 2013;162:808–12.e1. doi:10.1016/j.jpeds.2012.10.008.

[153] Elia J, Mazzilli R, Delfino M. Impact of Cystic Fibrosis Transmembrane Regulator (CFTR) gene mutations on male infertility. Arch Ital Di … 2014;86:171–4.

[154] Briel M, Greger R, Kunzelmann K. Cl- transport by cystic fibrosis transmembrane conductance regulator (CFTR) contributes to the inhibition of epithelial Na+ channels (ENaCs) in Xenopus oocytes co-expressing CFTR and ENaC. J Physiol 1998;508 (Pt 3:825–36. doi:10.1111/j.1469-7793.1998.825bp.x.

[155] König J, Schreiber R, Voelcker T, Mall M, Kunzelmann K. The cystic fibrosis transmembrane conductance regulator (CFTR) inhibits ENaC through an increase in the intracellular Cl- concentration. EMBO Rep 2001;2:1047–51. doi:10.1093/embo-reports/kve232.

[156] Matsui H, Grubb BR, Tarran R, Randell SH, Gatzy JT, Davis CW, et al. Evidence for periciliary liquid layer depletion, not abnormal ion composition, in the pathogenesis of cystic fibrosis airways disease. Cell 1998;95:1005–15. doi:10.1016/S0092-8674(00)81724-9.

[157] Berdiev BK, Qadri YJ, Benos DJ. Assessment of the CFTR and ENaC association. Mol Biosyst 2009;5:123–7. doi:10.1039/b810471a.

[158] Hull J. Cystic fibrosis transmembrane conductance regulator dysfunction and its treatment. J R Soc Med 2012;105 Suppl :S2–8. doi:10.1258/jrsm.2012.12s001.

[159] Rosenstein BJ, Cutting GR. The diagnosis of cystic fibrosis: A consensus statement. J Pediatr 1998;132:589–95. doi:10.1016/S0022-3476(98)70344-0.

[160] Voter KZ, Ren CL. Diagnosis of Cystic Fibrosis 2008:100–6. doi:10.1007/s12016-008-8078-x.

[161] Tomashefski JJ, Konstan M, Bruce M, Abramowsky C. The pathologic characteristics of interstitial pneumonia cystic fibrosis. A retrospective autopsy study. Am J Clin Pathol 1989;91:522–30.

[162] Engelhardt JF, Yankaskas JR, Ernst S a, Yang Y, Marino CR, Boucher RC, et al. Submucosal glands are the predominant site of CFTR expression in the human bronchus. Nat Genet 1992;2:240–8. doi:10.1038/ng1192-240.

[163] Moss RB. Infection, inflammation, and the downward spiral of cystic fibrosis lung disease. J Pediatr 2009;154:162–3. doi:10.1016/j.jpeds.2008.09.042.

[164] Luciani A, Villella VR, Esposito S, Brunetti-Pierri N, Medina D, Settembre C, et al. Defective CFTR induces aggresome formation and lung inflammation in cystic fibrosis through ROS-mediated autophagy inhibition. Nat Cell Biol 2010;12:863–75. doi:10.1038/ncb2090.

[165] Galli F, Battistoni A, Gambari R, Pompella A, Bragonzi A, Pilolli F, et al. Oxidative stress and antioxidant therapy in cystic fibrosis. Biochim Biophys Acta 2012;1822:690–713. doi:10.1016/j.bbadis.2011.12.012.

[166] Kawaguchi Y, Kovacs JJ, McLaurin A, Vance JM, Ito A, Yao T-P. The Deacetylase HDAC6 Regulates Aggresome Formation and Cell Viability in Response to Misfolded Protein Stress. Cell 2003;115:727–38. doi:10.1016/S0092-8674(03)00939-5.

[167] Gifford AM, Chalmers JD. The role of neutrophils in cystic fibrosis. Curr Opin Hematol 2014;21:16–22.

[168] Venaille TJ, Ryan G, Robinson BWS. Epithelial cell damage is induced by neutrophil-derived, not pseudomonas-derived, proteases in cystic fibrosis sputum. Respir Med 1998;92:233–40. doi:10.1016/S0954-6111(98)90101-9.

[169] Janoff A, White R, Carp H, Harel S, Dearing R, Lee D. Lung injury induced by leukocytic proteases. Am J Pathol 1979;97:111–36.

[170] Amitani R, Wilson R, Rutman a, Read R, Ward C, Burnett D, et al. Effects of human neutrophil elastase and Pseudomonas aeruginosa proteinases on human respiratory epithelium. Am J Respir Cell Mol Biol 1991;4:26–32. doi:10.1165/ajrcmb/4.1.26.

[171] Garratt LW, Sutanto EN, Ling K-M, Looi K, Iosifidis T, Martinovich KM, et al. Matrix metalloproteinase activation by free neutrophil elastase contributes to bronchiectasis progression in early cystic fibrosis. Eur Respir J 2015;46.

[172] Witko-sarsat V, Allen RC, Padais M, Nguyen AT, Bessou G, Lenoir G, et al. Disturbed myeloperoxidase dependent activity of neutrophils in cystic fibrosis homozygotes and heterozygotes and its correction by ameloride. J Immunol 1996;157:2728–35.

[173] Erdeve O, Uras N, Atasay B, Arsan S. Efficacy and safety of nebulized recombinant human DNase as rescue treatment for persistent atelectasis in newborns: case-series. Croat Med J 2007;48:234–9.

[174] Matsui H, Randell SH, Peretti SW, Davis CW, Boucher RC. Coordinated clearance of periciliary liquid and mucus from airway surfaces. J Clin Invest 1998;102:1125–31. doi:10.1172/JCI2687.

[175] Boucher RC. Evidence for airway surface dehydration as the initiating event in CF airway disease. J Intern Med 2007;261:5–16. doi:10.1111/j.1365-2796.2006.01744.x.

[176] Donaldson SH, Corcoran TE, Laube BL, Bennett WD. Mucociliary Clearance as an Outcome Measure for Cystic Fibrosis Clinical Research. Proc Am Thorac Soc 2007;4:399–405. doi:10.1513/pats.200703-042BR.

[177] Robinson M, Bye PTB. Mucociliary clearance in cystic fibrosis. Pediatr Pulmonol 2002;33:293–306. doi:10.1002/ppul.10079.

[178] Tarran R, Grubb B., Parsons D, Picher M, Hirsh A., Davis C., et al. The CF Salt Controversy: In Vivo Observations and Therapeutic Approaches. Mol Cell 2001;8:149–58. doi:10.1016/S1097-2765(01)00286-6.

[179] Mall M, Grubb BR, Harkema JR, O'Neal WK, Boucher RC. Increased airway epithelial Na+ absorption produces cystic fibrosis-like lung disease in mice. Nat Med 2004;10:487–93. doi:10.1038/nm1028.

[180] CFF. Cystic Fibrosis Foundation Annual Report 2013 2013.

[181] Elkins MR, Robinson M, Rose BR, Harbour C, Moriarty CP, Marks GB, et al. A Controlled Trial of Long-Term Inhaled Hypertonic Saline in Patients with Cystic Fibrosis. N Engl J Med 2006;354:229–40. doi:10.1056/NEJMoa1109071.

[182] di Sant'Agnese P, Davis P. Cystic fibrosis in adults: 75 cases and a review of 232 cases in the literature. Am J Med 1979;66:121–32.

[183] Milla CE. Risk of Death in Cystic Fibrosis Patients With Severely Compromised Lung Function. CHEST J 1998;113:1230. doi:10.1378/chest.113.5.1230.

[184] Belkin R a., Henig NR, Singer LG, Chaparro C, Rubenstein RC, Xie SX, et al. Risk factors for death of patients with cystic fibrosis awaiting lung transplantation. Am J Respir Crit Care Med 2006;173:659–66. doi:10.1164/rccm.200410-1369OC.

[185] Pezzulo AA, Tang XX, Hoegger MJ, Alaiwa MHA, Ramachandran S, Moninger TO, et al. Reduced airway surface pH impairs bacterial killing in the porcine cystic fibrosis lung. Nature 2012;487:109–13. doi:10.1038/nature11130.

[186] Smith JJ, Welsh MJ. cAMP stimulates bicarbonate secretion across normal, but not cystic fibrosis airway epithelia. J Clin Invest 1992;89:1148–53. doi:10.1172/JCI115696.

[187] Nordin SL, Jovic S, Kurut A, Andersson C, Gela A, Bjartell A, et al. High expression of midkine in the airways of patients with cystic fibrosis. Am J Respir Cell Mol Biol 2013;49:935–42. doi:10.1165/rcmb.2013-0106OC.

[188] Gibson RL, Burns JL, Ramsey BW. Pathophysiology and management of pulmonary infections in cystic fibrosis. Am J Respir Crit Care Med 2003;168:918–51. doi:10.1164/rccm.200304-505SO.

[189] Emerson J, Rosenfeld M, McNamara S, Ramsey B, Gibson RL. Pseudomonas aeruginosa and other predictors of mortality and morbidity in young children with cystic fibrosis. Pediatr Pulmonol 2002;34:91–100. doi:10.1002/ppul.10127.

[190] Kosorok MR, Zeng L, West SE, Rock MJ, Splaingard ML, Laxova a, et al. Acceleration of lung disease in children with cystic fibrosis after Pseudomonas aeruginosa acquisition. Pediatr Pulmonol 2001;32:277–87. doi:10.1002/ppul.1120.

[191] Aaron SD, Stephenson AL, Cameron DW, Whitmore G a. A statistical model to predict one-year risk of death in patients with cystic fibrosis. J Clin Epidemiol 2014;68:1336–45. doi:10.1016/j.jclinepi.2014.12.010.

[192] Maselli JH, Sontag MK, Norris JM, MacKenzie T, Wagener JS, Accurso FJ. Risk factors for initial acquisition of Pseudomonas aeruginosa in children with cystic fibrosis identified by newborn screening. Pediatr Pulmonol 2003;35:257–62. doi:10.1002/ppul.10230.

[193] Oliver A, Canton R, Campo P, Baquero F, Blázquez J. High frequency of hypermutable Pseudomonas aeruginosa in cystic fibrosis lung infection. Science (80-) 2000;288:1251–3. doi:10.1126/science.288.5469.1251.

[194] Lutz L, Leão RS, Ferreira AG, Pereira DC, Raupp C, Pitt T, et al. Hypermutable Pseudomonas aeruginosa in Cystic fibrosis patients from two Brazilian cities. J Clin Microbiol 2013;51:927–30. doi:10.1128/JCM.02638-12.

[195] Zlosnik JE a., Zhou G, Brant R, Henry D a., Hird TJ, Mahenthiralingam E, et al. Burkholderia Species Infections in Patients with Cystic Fibrosis in British Columbia, Canada. 30 Years' Experience. Ann Am Thorac Soc 2015;12:70–8. doi:10.1513/AnnalsATS.201408-395OC.

[196] Ratjen A, Yau Y, Wettlaufer J, Matukas L, Zlosnik JE a, Speert DP, et al. In Vitro Efficacy of High-Dose Tobramycin against Burkholderia cepacia Complex and Stenotrophomonas maltophilia Isolates from Cystic Fibrosis Patients. Antimicrob Agents Chemother 2015;59:711–3. doi:10.1128/AAC.04123-14.

[197] Stanojevic S, Ratjen F, Stephens D, Lu A, Yau Y, Tullis E, et al. Factors influencing the acquisition of Stenotrophomonas maltophilia infection in cystic fibrosis patients. J Cyst Fibros 2013;12:575–83. doi:10.1016/j.jcf.2013.05.009.

[198] Llorca Otero L, Girón Moreno, Rosa Buendía Moreno B, Valenzuela C, Guiu Martínez, Alba Alarcón Cavero T. Achromobacter xylosoxidans infection in an adult cystic fibrosis unit in Madrid. Enferm Infecc Microbiol Clin 2015;E-pub ahea.

[199] Baxter CG, Dunn G, Jones AM, Webb K, Gore R, Richardson MD, et al. Novel immunologic classification of aspergillosis in adult cystic fibrosis. J Allergy Clin Immunol 2013;132:560–6.e10. doi:10.1016/j.jaci.2013.04.007.

[200] Seddon P, Fidler K, Raman S, Wyatt H, Ruiz G, Elston C, et al. Prevalence of nontuberculous mycobacteria in cystic fibrosis clinics, United Kingdom, 2009. Emerg Infect Dis 2013;19:1128–30. doi:10.3201/eid/1907.120615.

[201] van Gool K, Norman R, Delatycki MB, Hall J, Massie J. Understanding the Costs of Care for Cystic Fibrosis: An Analysis by Age and Health State. Value Heal 2013;16:345–55. doi:10.1016/j.jval.2012.12.003.

[202] Smyth AR, Bell SC, Bojcin S, Bryon M, Duff A, Flume P, et al. European Cystic Fibrosis Society Standards of Care: Best Practice guidelines. J Cyst Fibros 2014;13:S23–42. doi:10.1016/j.jcf.2014.03.010.

[203] DeWitt EM, Grussemeyer CA, Friedman JY, Dinan MA, Lin L, Schulman KA, et al. Resource Use, Costs, and Utility Estimates for Patients with Cystic Fibrosis with Mild Impairment in Lung Function: Analysis of Data Collected Alongside a 48-Week Multicenter Clinical Trial. Value Heal 2012;15:277–83. doi:http://dx.doi.org/10.1016/j.jval.2011.11.027.

[204] Angelis A, Kanavos P, López-Bastida J, Linertová R, Nicod E, Serrano-Aguilar P. Social and economic costs and health-related quality of life in non-institutionalised patients with cystic fibrosis in the United Kingdom. BMC Health Serv Res 2015;15:428. doi:10.1186/s12913-015-1061-3.

[205] Fitzgerald DA. A Crossover, Randomized, Controlled Trial of Dornase Alfa Before Versus After Physiotherapy in Cystic Fibrosis. Pediatrics 2005;116:e549–54. doi:10.1542/peds.2005-0308.

[206] Fuchs H, Borowitz D, Christiansen DH, Morris EM, Nash M, Ramsey B, et al. Effect of aerosolized recombinant human DNase on exacerbations of respiratory symptoms and on pulmonary function in patients with cystic fibrosis. N Engl J Med 1994;331:637–42.

[207] Ratjen F, Paul K, van Koningsbruggen S, Breitenstein S, Rietschel E, Nikolaizik W. DNA concentrations in BAL fluid of cystic fibrosis patients with early lung disease: influence of treatment with dornase alpha. Pediatr Pulmonol 2005;39:1–4. doi:10.1002/ppul.20134.

[208] Paul K, Rietschel E, Ballmann M, Griese M, Worlitzsch D, Shute J, et al. Effect of treatment with dornase alpha on airway inflammation in patients with cystic fibrosis. Am J Respir Crit Care Med 2004;169:719–25. doi:10.1164/rccm.200307-959OC.

[209] Yildiz C, Palaniyar N, Otulakowski G, Khan MA, Post M, Kuebler WM, et al. Mechanical ventilation induces neutrophil extracellular trap formation. Anesthesiology 2015;122:864–75. doi:10.1097/ALN.0000000000000605.

[210] Reeves EP, Molloy K, Pohl K, McElvaney NG. Hypertonic Saline in Treatment of Pulmonary Disease in Cystic Fibrosis. Sci World J 2012;2012:1–11. doi:10.1100/2012/465230.

[211] Gould NS, Gauthier S, Kariya CT, Min E, Huang J, Brian DJ. Hypertonic saline increases lung epithelial lining fluid glutathione and thiocyanate: two protective CFTR-dependent thiols against oxidative injury. Respir Res 2010;11:119. doi:10.1186/1465-9921-11-119.

[212] Reeves EP, McCarthy C, McElvaney OJ, Vijayan MSN, White MM, Dunlea DM, et al. Inhaled hypertonic saline for cystic fibrosis: Reviewing the potential evidence for modulation of neutrophil signalling and function. World J Crit Care Med 2015;4:179–91. doi:10.5492/wjccm.v4.i3.179.

[213] Hebestreit A, Kersting U, Hebestreit H. Hypertonic saline inhibits luminal sodium channels in respiratory epithelium. Eur J Appl Physiol 2007;100:177–83. doi:10.1007/s00421-007-0420-0.

[214] Anderson GG, O'Toole G a. Innate and induced resistance mechanisms of bacterial biofilms. Curr Top Microbiol Immunol 2008;322:85–105. doi:10.1007/978-3-540-75418-3_5.

[215] Michon A-L, Jumas-Bilak E, Chiron R, Lamy B, Marchandin H. Advances toward the elucidation of hypertonic saline effects on Pseudomonas aeruginosa from cystic fibrosis patients. PLoS One 2014;9:e90164. doi:10.1371/journal.pone.0090164.

[216] Chmiel JF, Konstan MW, Accurso FJ, Lymp J, Mayer-Hamblett N, VanDevanter DR, et al. Use of ibuprofen to assess inflammatory biomarkers in induced sputum: Implications for clinical trials in cystic fibrosis. J Cyst Fibros 2015;14:720–6. doi:10.1016/j.jcf.2015.03.007.

[217] Konstan MW, Byard PJ, Hoppel CL, Davis PB. Effect of high-dose ibuprofen in patients with cystic fibrosis. N Engl J Med 1995;332:848–54. doi:10.1056/NEJM199503303321303.

[218] Konstan MW, Schluchter MD, Xue W, Davis PB. Clinical use of ibuprofen is associated with slower FEV1 decline in children with cystic fibrosis. Am J Respir Crit Care Med 2007;176:1084–9. doi:10.1164/rccm.200702-181OC.

[219] Konstan MW, Wagener JS, Pasta DJ, Millar SJ, Morgan WJ. Clinical use of tobramycin inhalation solution (TOBI®) shows sustained improvement in FEV1 in cystic fibrosis. Pediatr Pulmonol 2014;49:529–36. doi:10.1002/ppul.22874.

[220] Ramsey B, Pepe M, Quan J, Otto K, Montgomery B, Williams-Warren J, et al. Intermitent Administration of Inhaled Tobramycin in Patients with Cystic Fibrosis. New 1999;340:23–30.

[221] Shteinberg M, Elborn JS. Use of Inhaled Tobramycin in Cystic Fibrosis. Adv Ther 2015;32:1–9. doi:10.1007/s12325-015-0179-3.

[222] Principi N, Blasi F, Esposito S. Azithromycin use in patients with cystic fibrosis. Eur J Clin Microbiol Infect Dis 2015:1071–9. doi:10.1007/s10096-015-2347-4.

[223] Assael BM, Pressler T, Bilton D, Fayon M, Fischer R, Chiron R, et al. Inhaled aztreonam lysine vs. inhaled tobramycin in cystic fibrosis: A comparative efficacy trial. J Cyst Fibros 2013;12:130–40. doi:10.1016/j.jcf.2012.07.006.

[224] Lieb T, Forteza R, Salathe M. Hyaluronic Acid in Cultured Ovine Tracheal Cells and Its Effect on Ciliary Beat Frequency In Vitro. J Aerosol Med 2000;13:231–7.

[225] Gelardi M, Guglielmi AVN, De Candia N, Maffezzoni E, Berardi P, Quaranta N. Effect of sodium hyaluronate on mucociliary clearance after functional endoscopic sinus surgery. Eur Ann Allergy Clin Immunol 2013;45:1–6.

[226] Serisier DJ, Shute JK, Hockey PM, Higgins B, Conway J, Carroll MP. Inhaled heparin in cystic fibrosis. Eur Respir J Off J Eur Soc Clin Respir Physiol 2006;27:354–8. doi:10.1183/09031936.06.00069005.

[227] Solic N, Wilson J, Wilson SJ, Shute JK. Endothelial activation and increased heparan sulfate expression in cystic fibrosis. Am J Respir Crit Care Med 2005;172:892–8. doi:10.1164/rccm.200409-1207OC.

[228] Frevert CW, Kinsella MG, Vathanaprida C, Goodman RB, Baskin DG, Proudfoot A, et al. Binding of interleukin-8 to heparan sulfate and chondroitin sulfate in lung tissue. Am J Respir Cell Mol Biol 2003;28:464–72. doi:10.1165/rcmb.2002-0084OC.

[229] Nori SL, Aquino RP, Nicolin V, Santoro A. Flavonoids and flavonoid-rich natural extracts inhibit cytokine release in cystic fibrosis bronchial epithelial cells by regulating NF-kB pathway. Ital J Anat Embryol 2015;120:2015.

[230] Taggart C, Coakley RJ, Greally P, Canny G, O'Neill SJ, McElvaney NG. Increased elastase release by CF neutrophils is mediated by tumor necrosis factor-alpha and interleukin-8. Am J Physiol Lung Cell Mol Physiol 2000;278:L33–41.

[231] Bergin DA, Hurley K, Mehta A, Cox S, Ryan D, O'Neill SJ, et al. Airway inflammatory markers in individuals with cystic fibrosis and non-cystic fibrosis bronchiectasis. J Inflamm Res 2013;6:1–11. doi:10.2147/JIR.S40081.

[232] McGarvey LP a, Dunbar K, Martin SL, Brown V, MacMahon J, Ennis M, et al. Cytokine concentrations and neutrophil elastase activity in bronchoalveolar lavage and induced sputum from patients with cystic fibrosis, mild asthma and healthy volunteers. J Cyst Fibros 2002;1:269–75. doi:10.1016/S1569-1993(02)00098-X.

[233] Dean T, Dai Y, Shute J, Church M, Warner J. Interleukin-8 Concentrations Are Elevated in Bronchoalveolar Lavage , Sputum , and Sera of Children with Cystic Fibrosis Interleukin3 Concentrations Are Elevated in Bronchoalveolar Lavage , Sputum , and Sera of Children with Cystic Fibrosis. Pediatr Res 1993;34:159–61. doi:10.1203/00006450-199308000-00010.

[234] Kube D, Sontich UTE, Fletcher D, Davis PB, Sontich U, Physiol AJ, et al. Proinflammatory cytokine responses to P. aeruginosa infection in human airway epithelial cell lines. Am J Physiol Lung Cell Mol Physiol 2001;280:493–502.

[235] Hoffmann E, Dittrich-Breiholz O, Holtmann H, Kracht M. Multiple control of interleukin-8 gene expression. J Leukoc Biol 2002;72:847–55.

[236] Bonfield TL, Konstan MW, Berger M. Altered respiratory epithelial cell cytokine production in cystic fibrosis. J Allergy Clin Immunol 1999;104:72–8.

[237] Liou TG, Adler FR, Keogh RH, Li Y, Jensen JL, Walsh W, et al. Sputum biomarkers and the prediction of clinical outcomes in patients with cystic fibrosis. PLoS One 2012;7. doi:10.1371/journal.pone.0042748.

[238] Mitola S, Sorbello V, Ponte E, Copreni E, Mascia C, Bardessono M, et al. Tumor necrosis factor-alpha in airway secretions from cystic fibrosis patients upregulate endothelial adhesion molecules and induce airway epithelial cell apoptosis: implications for cystic fibrosis lung disease. Int J Immunopthology Pharmacol 2008;21:851–65.

[239] Fischer BM, Wong JK, Degan S, Kummarapurugu AB, Zheng S, Haridass P, et al. Increased Expression of Senescence Markers in Cystic Fibrosis Airways. Am J Physiol Lung Cell Mol Physiol 2013;0258:L394–400. doi:10.1152/ajplung.00091.2012.

[240] Nichols DP, Chmiel JF. Inflammation and its genesis in cystic fibrosis. Pediatr Pulmonol 2015;50:S39–56. doi:10.1002/ppul.23242.

[241] Sheller JR, Polosukhin V V, Mitchell D, Cheng D-S, Peebles RS, Blackwell TS. Nuclear factor kappa B induction in airway epithelium increases lung inflammation in allergen-challenged mice. Exp Lung Res 2009;35:883–95. doi:10.3109/01902140903019710.

[242] Ogawa M, Moody MW, Portier RJ, Bell J, Schexnayder M a., Losso JN. Biochemical Properties of Black Drum and Sheepshead Seabream Skin Collagen. J Agric Food Chem 2003;51:8088–92. doi:10.1021/jf034350r.

[243] Losso JN, Ogawa M, Portier R, Schexnayder MA. Extraction of collagen from calcified tissues, 2006.

[244] Kittiphattanabawon P, Benjakul S, Visessanguan W, Nagai T, Tanaka M. Characterisation of acid-soluble collagen from skin and bone of bigeye snapper (Priacanthus tayenus). Food Chem 2005;89:363–72. doi:10.1016/j.foodchem.2004.02.042.

[245] Garnjanagoonchorn W, Wongekalak L, Engkagul a. Determination of chondroitin sulfate from different sources of cartilage. Chem Eng Process Process Intensif 2007;46:465–71. doi:10.1016/j.cep.2006.05.019.

[246] Khanmohammadi M, Khoshfetrat AB, Eskandarnezhad S, Sani NF, Ebrahimi S. Sequential optimization strategy for hyaluronic acid extraction from eggshell and its partial characterization. J Ind Eng Chem 2014;20:4371–6. doi:10.1016/j.jiec.2014.02.001.

[247] Panagos CG, Thomson D, Moss C, Bavington CD, Ólafsson HG, Uhrín D. Characterisation of hyaluronic acid and chondroitin/dermatan sulfate from the lumpsucker fish, C. lumpus. Carbohydr Polym 2014;106:25–33. doi:10.1016/j.carbpol.2014.01.090.

[248] Cesaretti M, Luppi E, Maccari F, Volpi N. A 96-well assay for uronic acid carbazole reaction. Carbohydr Polym 2003;54:59–61. doi:10.1016/S0144-8617(03)00144-9.

[249] Cowman MK, Chen CC, Pandya M, Yuan H, Ramkishun D, LoBello J, et al. Improved agarose gel electrophoresis method and molecular mass calculation for high molecular mass hyaluronan. Anal Biochem 2011;417:50–6. doi:10.1016/j.ab.2011.05.023.

[250] Livraghi-butrico A, Duncan E a, Wells SM, Weigel J, Xiao F. Mechanisms of Host Defense during Airway Mucus Obstruction in Scnn1b Transgenic Mice : A Mouse Model Of Chronic Obstructive Pulmonary Disease Cigarette Smoke Suppresses PPAR- g Expression and Activation In Murine Pulmonary Epithelial Cells Promoter Hyperm 2012;9:82–3.

[251] Zhou Z, Duerr J, Johannesson B, Schubert SC, Treis D, Harm M, et al. The ENaC-overexpressing mouse as a model of cystic fibrosis lung disease. J Cyst Fibros 2011;10:S172–82. doi:10.1016/S1569-1993(11)60021-0.

[252] Legssyer R, Huaux F, Lebacq J, Delos M, Marbaix E, Lebecque P, et al. Azithromycin reduces spontaneous and induced inflammation in DeltaF508 cystic fibrosis mice. Respir Res 2006;7:134. doi:10.1186/1465-9921-7-134.

[253] Saini Y, Dang H, Livraghi-Butrico A, Kelly EJ, Jones LC, O'Neal WK, et al. Gene expression in whole lung and pulmonary macrophages reflects the dynamic pathology associated with airway surface dehydration. BMC Genomics 2014;15:726. doi:10.1186/1471-2164-15-726.

[254] Lam HC, Choi AMK, Ryter SW. Isolation of mouse respiratory epithelial cells and exposure to experimental cigarette smoke at air liquid interface. J Vis Exp 2011:2–5. doi:10.3791/2513.

[255] Kwak YG, Song CH, Yi HK, Hwang PH, Kim JS, Lee KS, et al. Involvement of PTEN in airway hyperresponsiveness and inflammation in bronchial asthma. J Clin Invest 2003;111:1083–92. doi:10.1172/JCI200316440.

[256] Lee KS, Park SJ, Kim SR, Min KH, Lee KY, Choe YH, et al. Inhibition of VEGF blocks TGF-?? 1 production through a PI3K/Akt signalling pathway. Eur Respir J 2008;31:523–31. doi:10.1183/09031936.00125007.

[257] Davidson DJ, Gray MA, Kilanowski FM, Tarran R, Randell SH, Sheppard DN, et al. Murine epithelial cells: Isolation and culture. J Cyst Fibros 2004;3:59–62. doi:10.1016/j.jcf.2004.05.013.

[258] Mehta DP, Shodhan K, Modi RI, Ghosh PK. Sodium hyaluronate of defined molecular size for treating osteoarthritis. Curr Sci 2007;92:209–13.

[259] Shimojo AAM, De Souza Brissac IC, Pina LM, Lambert CS, Santana MHA. Sterilization of auto-crosslinked hyaluronic acid scaffolds structured in microparticles and sponges. Biomed Mater Eng 2015;26:183–91. doi:10.3233/BME-151558.

[260] Volpi N, Maccari F. Purification and characterization of hyaluronic acid from the mollusc bivalve Mytilus galloprovincialis. Biochimie 2003;85:619–25. doi:10.1016/S0300-9084(03)00083-X.

[261] Frazier SB, Roodhouse K a., Hourcade DE, Zhang L. The Quantification of Glycosaminoglycans: A Comparison of HPLC, Carbazole, and Alcian Blue Methods. Open Glycosci 2008;1:31–9. doi:10.2174/1875398100801010031.

[262] Cassaro C, Dietrich P. Distribution of Sulfated Mucopolysaccharides in Invertebrates *. J Biol Chem 1977;252:2254–61.

[263] Arima K, Fujita H, Toita R, Imazu-Okada A, Tsutsumishita-Nakai N, Takeda N, et al. Amounts and compositional analysis of glycosaminoglycans in the tissue of fish. Carbohydr Res 2013;366:25–32. doi:10.1016/j.carres.2012.11.010.

[264] Vázquez JA, Rodríguez-Amado I, Montemayor MI, Fraguas J, Del González MP, Murado MA. Chondroitin sulfate, hyaluronic acid and chitin/chitosan production using marine waste sources: Characteristics, applications and eco-friendly processes: A review. Mar Drugs 2013;11:747–74. doi:10.3390/md11030747.

[265] Kono H, Takai M. Salmon-Origin Chondroitin Sulphate, 2003.

[266] Gargiulo V, Lanzetta R, Parrilli M, De Castro C. Structural analysis of chondroitin sulfate from Scyliorhinus canicula: A useful source of this polysaccharide. Glycobiology 2009;19:1485–91. doi:10.1093/glycob/cwp123.

[267] Kariya Y, Watabe S, Ochiai Y, Hashimoto K, Murata K. Glycosaminoglycan from the body wall of the sea cucumber Stichopus japonicus 1990;95:387–92.

[268] Gherezghiher T, Koss M, Nordquist R, Wilkinson C. Analysis of vitreous and aqueous levels of hyaluronic acid: application of high-performance liquid chromatography. Exp Eye Res 1987;45:347–9.

[269] Clinic C. Hyaluronan Size Analysis by Agarose Gel - NHLBI AWARD NUMBER PO1HL107147. 2015.

[270] Long F, Adams R, DeVore D. Preparation of hyaluronic acid from eggshell membrane - United States patent US 6946551, 2005.

[271] Prescott A. Method for purifying high molecular weight hyaluronic acid - US Patent 6660853, 2003.

[272] Sigma-Aldrich. Product Information: Hyaluronidase from bovine testes. vol. 4. 2008.

[273] Takagaki K, Nakamura T, Izumi J, Saitoh H, Endo M, Kojima K, et al. Characterization of Hydrolysis and Transglycosilation by Testicular Hyaluronidase Using Ion-Spray Mass Spectrometry. Biochemistry 1994;33:6503–7.

[274] Saitoh H, Takagaki K, Majima M, Nakamura T, Matsuki A, Kasai M, et al. Enzymatic Reconstruction of Glycosaminoglycan Oligosaccharide Chains Using the Transglycosylation Reaction of Bovine Testicular Hyaluronidase. J Biol Chem 1995;270:3741–7.

[275] Yamagata T, Saito H, Habuchi O, Suzuki S. Purification and Properties and Chondrosulfatases ” of Bacterial Chondroitinases. J Biol Chem 1967;243:1523–35.

[276] Sigma-Aldrich. Product Information: Chondroitinase ABC from Proteus vulgaris. vol. 1543. 2007.

[277] Volpi N. Chondroitin Sulfate: Structure, Role and Pharmacological Activity. 2006.

[278] Vijayabaskar P, Vaseela N. In vitro antioxidant properties of sulfated polysaccharide from brown marine algae Sargassum swartzii. Asian Pacific J Trop Dis 2012:S890–6. doi:10.1016/S1875-5364(12)60082-X.

[279] Becker LC, Bergfeld WF, Belsito D V, Klaassen CD, Marks JG, Shank RC, et al. Final report of the safety assessment of hyaluronic acid, potassium hyaluronate, and sodium hyaluronate. Int J Toxicol 2009;28:5–67. doi:10.1177/1091581809337738.

[280] Pharmacopoeia E. Sodium Hyaluronate. 2005.

[281] Shiedlin A, Bigelow R, Christopher W, Arbabi S, Yang L, Maier R V., et al. Evaluation of hyaluronan from different sources: Streptococcus zooepidemicus, rooster comb, bovine vitreous, and human umbilical cord. Biomacromolecules 2004;5:2122–7. doi:10.1021/bm0498427.

[282] Bucci LR, Ph D, Turpin A a, Sc M. Will the Real Hyaluronan Please Stand Up ? J Appl Nutr 2004;54.

[283] Alkrad JA, Mrestani Y, Stroehl D, Wartewig S, Neubert R. Characterization of enzymatically digested hyaluronic acid using NMR, Raman, IR, and UV-Vis spectroscopies. J Pharm Biomed Anal 2003;31:545–50. doi:10.1016/S0731-7085(02)00682-9.

[284] Lokwani R, Singh R, Kukreti G. Extraction and quantification of sulfated glycosaminoglycan content in five aquatic species of Malaysia. J Coast Life Med 2015;3:677–81. doi:10.12980/JCLM.3.201514B336.

[285] Matmaroh K, Benjakul S, Prodpran T, Encarnacion AB, Kishimura H. Characteristics of acid soluble collagen and pepsin soluble collagen from scale of spotted golden goatfish (Parupeneus heptacanthus). Food Chem 2011;129:1179–86. doi:10.1016/j.foodchem.2011.05.099.

[286] Kumar CG, Joo H-S, Choi J-W, Koo Y-M, Chang C-S. Purification and characterization of an extracellular polysaccharide from haloalkalophilic Bacillus sp. I-450. Enzyme Microb Technol 2004;34:673–81. doi:10.1016/j.enzmictec.2004.03.001.

[287] Su C, Xu X, Liu D, Wu M, Zeng F, Zeng M, et al. Isolation and characterization of exopolysaccharide with immunomodulatory activity from fermentation broth of Morchella conica. DARU J Pharm Sci 2013;21:5. doi:10.1186/2008-2231-21-5.

[288] Horani A, Dickinson JD, Brody SL. Applications of Mouse Airway Epithelial Cell Culture for Asthma Research. Mouse Model. Allerg. Dis. Methods Protoc. Methods Mol. Biol., vol. 1032, 2013, p. 91–107. doi:10.1007/978-1-62703-496-8.

[289] Qiagen. RT2 Profiler PCR Array Data Analysis v3.5 Handbook. 2015.

[290] Schroeder A, Mueller O, Stocker S, Salowsky R, Leiber M, Gassmann M, et al. The RIN: an RNA integrity number for assigning integrity values to RNA measurements. BMC Mol Biol 2006;7:3. doi:10.1186/1471-2199-7-3.

[291] O'Neill LAJ. TLRs play good cop, bad cop in the lung. Nat Med 2005;11:1161–2. doi:nm1105-1161 [pii]\n10.1038/nm1105-1161.

[292] Kennel SJ, Lankford TK, Foote LJ, Shinpock SG, Stringer C. CD44 expression on murine tissues. J Cell Sci 1993;104 (Pt 2:373–82.

[293] Dusio GF, Cardani D, Zanobbio L, Mantovani M, Luchini P, Battini L, et al. Stimulation of TLRs by LMW-HA induces self-defense mechanisms in vaginal epithelium. Immunol Cell Biol 2011;89:630–9. doi:10.1038/icb.2010.140.

[294] Korkmaz B, Moreau T, Gauthier F. Neutrophil elastase, proteinase 3 and cathepsin G: Physicochemical properties, activity and physiopathological functions. Biochimie 2008;90:227–42. doi:10.1016/j.biochi.2007.10.009.

[295] Eisenberg SP, Hale KK, Heimdal P, Thompson RC. Location of the protease-inhibitory region of secretory leukocyte protease inhibitor. J Biol Chem 1990;265:7976–81.

[296] Twigg MS, Brockbank S, Lowry P, FitzGerald SP, Taggart C, Weldon S. The Role of Serine Proteases and Antiproteases in the Cystic Fibrosis Lung. Mediators Inflamm 2015:1–10. doi:10.1155/2015/293053.

[297] Reeves EP, Bergin D a, Murray M a, McElvaney NG. The involvement of glycosaminoglycans in airway disease associated with cystic fibrosis. ScientificWorldJournal 2011;11:959–71. doi:10.1100/tsw.2011.81.

[298] Sagel SD, Chmiel JF, Konstan MW. Sputum biomarkers of inflammation in cystic fibrosis lung disease. Proc Am Thorac Soc 2007;4:406–17. doi:10.1513/pats.200703-044BR.

[299] Iba T, Kidokoro A, Fukunaga M, Takuhiro K, Yoshikawa S, Sugimotoa K. Pretreatment of Sivelestat Sodium Hydrate Improves the Lung Microcirculation and Alveolar Damage in Lipopolysaccharide-Induced Acute Lung Inflammation in Hamsters. Shock 2006;26:95–8. doi:10.1097/01.shk.0000223126.34017.d9.

[300] Cantor JO, Shteyngart B, Cerreta JM, Liu M, Armand G, Turino GM. The effect of hyaluronan on elastic fiber injury in vitro and elastase-induced airspace enlargement in vivo. Proc Soc Exp Biol Med 2000;225:65–71. doi:10.1046/j.1525-1373.2000.22508.x.

[301] Fonslow BR, Stein BD, Webb KJ, Xu T, Choi J, Kyu S, et al. Acute Lung Injury Regulation by Hyaluronan. J Allergy Ther 2013;10:54–6. doi:10.1038/nmeth.2250.Digestion.

[302] Riikonen T, Westermarck J, Koivisto L, Broberg A, Kahari V-M, Heino J. Integrin a2B1 is a positive regulator of collagenase (MMP-1) and collagen a1(I) gene expression. J Biol Chem 1995;270:13548–52.

[303] Greenlee KJ, Werb Z, Kheradmand F. Matrix Metalloproteinases in Lung: Multiple, Multifarious, and Multifaceted. Medicine (Baltimore) 2009;87:69–98. doi:10.1152/physrev.00022.2006.Matrix.

[304] Balloy V, Varet H, Dillies M-A, Proux C, Jagla B, Coppée J-Y, et al. Normal and Cystic Fibrosis Human Bronchial Epithelial Cells Infected with Pseudomonas aeruginosa Exhibit Distinct Gene Activation Patterns. PLoS One 2015;10:e0140979. doi:10.1371/journal.pone.0140979.

[305] Okamoto T, Akuta T, Tamura F, van der Vliet A, Akaike T. Molecular mechanism for activation and regulation of matrix metalloproteinases during bacterial infections and respiratory inflammation. Biol Chem 2004;385:997–1006. doi:10.1515/BC.2004.130.

[306] Gaggar a, Hector a, Bratcher PE, Mall M a, Griese M, Hartl D. The role of matrix metalloproteinases in cystic fibrosis lung disease. Eur Respir J 2011;38:721–7. doi:10.1183/09031936.00173210.

[307] Sanjabi S, Zenewicz LA, Kamanaka M, Flavell RA. Anti- and Pro-inflammatory Roles of TGF-β, IL-10, and IL-22 In Immunity and Autoimmunity. Curr Opin Pharmacol 2009;9:447–53. doi:10.1016/j.coph.2009.04.008.Anti-.

[308] Arkwright P, Laurie S, Super M, Pravica V, Schwarz M, Webb A, et al. TGF-β1 genotype and accelerated decline in lung function of patients with cystic fibrosis. Thorax 2000;55:459–62. doi:10.1136/thorax.55.6.459.

[309] Wesselkamper SC, Case LM, Henning LN, Borchers MT, Tichelaar JW, Mason JM, et al. Gene expression changes during the development of acute lung injury: Role of transforming growth factor ?? Am J Respir Crit Care Med 2005;172:1399–411. doi:10.1164/rccm.200502-286OC.

[310] Zeki AA, Yeganeh B, Kenyon NJ, Post M, Ghavami S, Medicine E, et al. Autophagy in airway diseases: a new frontier in human asthma? Allergy 2016;71:5–14. doi:10.1111/all.12761.Autophagy.

[311] Honeyman L, Bazett M, Tomko TG HC. MicroRNA profiling implicates the insulin-like growth factor pathway in bleomycin-induced pulmonary fibrosis in mice. Fibrogenes Tissue Repair 2013;6:16. doi:10.1186/1755-1536-6-16.

[312] Pilewski JM, Liu L, Henry AC, Knauer A V, Feghali-Bostwick CA. Insulin-like growth factor binding proteins 3 and 5 are overexpressed in idiopathic pulmonary fibrosis and contribute to extracellular matrix deposition. Am J Pathol 2005;166:399–407. doi:10.1016/S0002-9440(10)62263-8.

[313] Spira A, Beane J, Pinto-Plata V, Kadar A, Liu G, Shah V, et al. Gene expression profiling of human lung tissue from smokers with severe emphysema. Am J Respir Cell Mol Biol 2004;31:601–10. doi:10.1165/rcmb.2004-0273OC.

[314] Petrigni G, Allegra L. Aerosolised hyaluronic acid prevents exercise-induced bronchoconstriction, suggesting novel hypotheses on the correction of matrix defects in asthma. Pulm Pharmacol Ther 2006;19:166–71. doi:10.1016/j.pupt.2005.03.002.

[315] Han G, Li F, Singh TP, Wolf P, Wang XJ. The pro-inflammatory role of TGFB1: A paradox? Int J Biol Sci 2012;8:28–235. doi:10.7150/ijbs.8.228.

[316] Ashcroft GS, Lei K, Jin W, Longenecker G, Kulkarni AB, Greenwell-Wild T, et al. Secretory leukocyte protease inhibitor mediates non-redundant functions necessary for normal wound healing. Nat Med 2000;6:1147–53.

[317] Schultz GS, Wysocki A. Interactions between extracellular matrix and growth factors in wound healing. Wound Repair Regen 2009;17:153–62. doi:10.1111/j.1524-475X.2009.00466.x.

[318] Reeves EP, Banville N, Ryan DM, O'Reilly N, Bergin DA, Pohl K, et al. Intracellular secretory leukoprotease inhibitor modulates inositol 1,4,5-triphosphate generation and exerts an anti-inflammatory effect on neutrophils of individuals with cystic fibrosis and chronic obstructive pulmonary disease. Biomed Res Int 2013;2013. doi:10.1155/2013/560141.

[319] Dagenais NJ, Jamali F. Protective effects of angiotensin II interruption: Evidence for antiinflammatory actions. Pharmacotherapy 2005;25:1213–29. doi:http://dx.doi.org/10.1592/phco.2005.25.9.1213.

[320] Richardson M a, Gupta A, O'Brien L a, Berg DT, Gerlitz B, Syed S, et al. Treatment of sepsis-induced acquired protein C deficiency reverses Angiotensin-converting enzyme-2 inhibition and decreases pulmonary inflammatory response. J Pharmacol Exp Ther 2008;325:17–26. doi:10.1124/jpet.107.130609.

[321] Ayada C, Toru U, Genc O, Sahin S, Bulut I, Arik O, et al. Evaluation of Serum Levels of Renin Angiotensin System Components in Asthmatic Patients. Erciyes Tıp Dergisi/Erciyes Med J 2015;37:87–90. doi:10.5152/etd.2015.0027.

[322] Sahli C, Fredj SH, Siala H, Bibi A, Messaoud T. First study of angiotensin converting enzyme in cystic fibrosis Tunisian patients. Clin Chem Lab Med 2014;52:211–5. doi:10.1515/cclm-2013-1001.

[323] Tham D, Martin-McNulty B, Wang Y, Wilson D, Vergona R, Sullivan M, et al. Angiotensin II is associated with activation of NF-kB-mediated genes and downregulation of PPARs. Physiol Genomics 2002;2:21–30.

[324] Celec P. Nuclear factor kappa B - Molecular biomedicine: The next generation. Biomed Pharmacother 2004;58:365–71. doi:10.1016/j.biopha.2003.12.015.

[325] Bodas M, Vij N. The NF-kappaB signaling in cystic fibrosis lung disease: pathophysiology and therapeutic potential. Discov Med 2010;9:346–56.

[326] Venkatakrishnan A, Stecenko A, King G, Blackwell T, Bringham K, Christman J, et al. Exaggerated Activation of Nuclear Factor-kB and Altered IkB-B Processin in Cystic Fibrosis Bronchial Epithelial Cells. Am J Respir Cell Mol Biol 2000;23:396–403.

[327] Kazi JU. The mechanism of protein kinase C regulation 2011;6:328–36. doi:10.1007/s11515-011-1070-5.

[328] Gray RD, Lucas CD, Mackellar A, Li F, Hiersemenzel K, Haslett C, et al. Activation of conventional protein kinase C (PKC) is critical in the generation of human neutrophil extracellular traps. J Inflamm (Lond) 2013;10:12. doi:10.1186/1476-9255-10-12.

[329] Alcantara C, Korehisa Maza P, Silva BC, Barros C, Suzuki E. Role of protein kinase C in cytokine secretion by lung epithelial cells during infection with Paracoccidioides brasiliensis. Pathog Dis 2015;Epub ahead.

[330] Zhang H, Xu Y, ZX Z, Ni W, Chen S. Expression of protein kinase C and nuclear factor kappa B in lung tissue of patients with chronic obstructive pulmonary disease. Zhonghua Nei Ke Za Zhi 2004;43:756–9.

[331] Papayannopoulos V, Staab D, Zychlinsky A. Neutrophil elastase enhances sputum solubilization in cystic fibrosis patients receiving dnase therapy. PLoS One 2011;6:1–7. doi:10.1371/journal.pone.0028526.

[332] Marcos V, Zhou Z, Yildirim AO, Bohla A, Hector A, Vitkov L, et al. CXCR2 mediates NADPH oxidase-independent neutrophil extracellular trap formation in cystic fibrosis airway inflammation. Nat Med 2010;16:1018–23. doi:10.1038/nm0711-899a.

[333] McEvoy AN, Murphy EA, Ponnio T, Conneely OM, Bresnihan B, FitzGerald O, et al. Activation of Nuclear Orphan Receptor NURR1 Transcription by NF- B and Cyclic Adenosine 5'-Monophosphate Response Element-Binding Protein in Rheumatoid Arthritis Synovial Tissue. J Immunol 2002;168:2979–87. doi:10.4049/jimmunol.168.6.2979.

[334] Holla VR, Mann JR, Shi Q, DuBois RN. Prostaglandin E2 regulates the nuclear receptor NR4A2 in colorectal cancer. J Biol Chem 2006;281:2676–82. doi:10.1074/jbc.M507752200.

[335] Davies MR, Harding CJ, Raines S, Tolley K, Parker AE, Downey-Jones M, et al. Nurr1 dependent regulation of pro-inflammatory mediators in immortalised synovial fibroblasts. J Inflamm (Lond) 2005;2:15. doi:10.1186/1476-9255-2-15.

[336] Ryan SM, McMorrow J, Umerska A, Patel HB, Kornerup KN, Tajber L, et al. An intra-articular salmon calcitonin-based nanocomplex reduces experimental inflammatory arthritis. J Control Release 2013;167:120–9. doi:10.1016/j.jconrel.2013.01.027.

[337] Liew FY, Xu D, Brint EK, O'Neill LA. Negative regulation of Toll-like receptor-mediated immune responses. Nat Rev Immunol 2005;5:446–58.

[338] Anas A, van der Poll T, de Vos AF. Role of CD14 in lung inflammation and infection. Crit Care 2010;14:209. doi:10.1186/cc8850.

[339] Ito M, Hanaoka M, Droma Y, Kobayashi N, Yasuo M, Kitaguchi Y, et al. The association of Toll-like receptor 4 gene polymorphisms with the development of emphysema in Japanese subjects: a case control study. BMC Res Notes 2012;5:36. doi:10.1186/1756-0500-5-36.

[340] Devaney JM, Greene CM, Taggart CC, Carroll TP, O'Neill SJ, McElvaney NG. Neutrophil elastase up-regulates interleukin-8 via toll-like receptor 4. FEBS Lett 2003;544:129–32. doi:10.1016/S0014-5793(03)00482-4.

[341] Gough KC, Maddison BC, Shikotra A, Moiseeva EP, Yang W, Jarvis S, et al. Evidence for a novel Kit adhesion domain mediating human mast cell adhesion to structural airway cells. Respir Res 2015;16:86. doi:10.1186/s12931-015-0245-z.

[342] Bradding P, Walls AF, Holgate ST. The role of the mast cell in the pathophysiology of asthma. J Allergy Clin Immunol 2006;117:1277–84. doi:10.1016/j.jaci.2006.02.039.

[343] Carter R, Bradding P. The Role of Mast Cells in the Structural Alterations of the Airways as a Potential Mechanism in the Pathogenesis of Severe Asthma. Curr Pharm Des 2011;17:685–98.

[344] Andersson CK, Andersson-Sjöland A, Mori M, Hallgren O, Pardo A, Eriksson L, et al. Activated MCTC mast cells infiltrate diseased lung areas in cystic fibrosis and idiopathic pulmonary fibrosis. Respir Res 2011;12:139. doi:10.1186/1465-9921-12-139.

[345] Saunders WB, Bayless KJ, Davis GE. MMP-1 activation by serine proteases and MMP-10 induces human capillary tubular network collapse and regression in 3D collagen matrices. J Cell Sci 2005;118:2325–40. doi:10.1242/jcs.02360.

[346] Lenon GB, Xue CCL, Story DF, Thien FCK, McPhee S, Li CG. Inhibition of release of inflammatory mediators in primary and cultured cells by a Chinese herbal medicine formula for allergic rhinitis. Chin Med 2007;2:2. doi:10.1186/1749-8546-2-2.

[347] Roca-Ferrer J, Pujols L, Gartner S, Moreno A, Pumarola F, Mullol J, et al. Upregulation of COX-1 and COX-2 in nasal polyps in cystic fibrosis. Thorax 2006;61:592–6. doi:10.1136/thx.2004.039842.

[348] Saito Y, Yamagishi N, Hatayama T. Different localization of Hsp105 family proteins in mammalian cells. Exp Cell Res 2007;313:3707–17. doi:10.1016/j.yexcr.2007.06.009.

[349] Vignola A, Chanez P, Polla B, Vic P, Godard P, Bousquet J. Increased expression of heat shock protein 70 on airway cells in asthma and chronic bronchitis. Am J Respir Cell Mol Biol 1995;13:683–91.

[350] Qian X, Zhu Y, Xu W, Lin Y. Glucocorticoid receptor and heat shock protein 90 in peripheral blood mononuclear cells from asthmatics. Chin MedJ(Engl) 2001;114:1051–4.

[351] Hacker S, Lambers C, Hoetzenecker K, Pollreisz A, Aigner C, Lichtenauer M, et al. Elevated HSP27, HSP70 and HSP90a in chronic obstructive pulmonary disease: Markers for immune activation and tissue destruction. Clin Lab 2009;55:31–40.

[352] Dong J, Guo L, Liao Z, Zhang M, Zhang M, Wang T, et al. Increased expression of heat shock protein 70 in chronic obstructive pulmonary disease. Int Immunopharmacol 2013;17:885–93. doi:10.1016/j.intimp.2013.09.003.

[353] Roudkenar MH, Kuwahara Y, Baba T, Roushandeh AM, Ebishima S, Abe S, et al. Oxidative stress induced lipocalin 2 gene expression: addressing its expression under the harmful conditions. J Radiat Res 2007;48:39–44. doi:10.1269/jrr.06057.

[354] Roudkenar MH, Halabian R, Ghasemipour Z, Roushandeh AM, Rouhbakhsh M, Nekogoftar M, et al. Neutrophil Gelatinase-associated Lipocalin Acts as a Protective Factor against H2O2 Toxicity. Arch Med Res 2008;39:560–6. doi:10.1016/j.arcmed.2008.05.003.

[355] Ebrahimi M, Roudkenar MH, Imani Fooladi AA, Halabian R, Ghanei M, Kondo H, et al. Discrepancy between mRNA and Protein Expression of Neutrophil Gelatinase-Associated Lipocalin in Bronchial Epithelium Induced by Sulfur Mustard. J Biomed Biotechnol 2010;2010:823131. doi:10.1155/2010/823131.

[356] Li W, Cui T, Hu L, Wang Z, Li Z, He Z-G. Cyclic diguanylate monophosphate directly binds to human siderocalin and inhibits its antibacterial activity. Nat Commun 2015;6:8330. doi:10.1038/ncomms9330.

[357] Eichler I, Nilsson M, Rath R, Enander I, Venge P, Koller DY. Human neutrophil lipocalin, a highly specific marker for acute exacerbation in cystic fibrosis. Eur Respir J 1999;14:1145–9.

[358] Livraghi A, Grubb BR, Hudson EJ, Wilkinson KJ, Sheehan K, Mall MA, et al. Airway and lung pathology due to mucosal surface dehydration in β-Epithelial Na+ Channel-overexpressing mice: role of TNFα and IL-4Rα signaling, influence of neonatal development, and limited efficacy of glucocorticoid treatment 2010;182:4357–67. doi:10.4049/jimmunol.0802557.Airway.

[359] Alkhouri J, Moir L, Armour C, Hughes J. CXCL1 is a negative regulator of mast cell chemotaxis to airway smooth muscle cell products in vitro. Clin Exp Allergy 2014;44:381–92.

[360] Marcos V, Zhou-Suckow Z, ??nder Yildirim A, Bohla A, Hector A, Vitkov L, et al. Free DNA in cystic fibrosis airway fluids correlates with airflow obstruction. Mediators Inflamm 2015;2015. doi:10.1155/2015/408935.

[361] Jin L, Batra S, Douda DN, Palaniyar N, Jeyaseelan S. CXCL1 contributes to host defense in polymicrobial sepsis via modulating T cell and neutrophil functions. J Immunol 2014;193:3549–58. doi:10.4049/jimmunol.1401138.

[362] de Oliveira Magalhães P, Lopes AM, Mazzola PG, Rangel-Yagui C, Penna TC V, Pessoa A. Methods of endotoxin removal from biological preparations: A review. J Pharm Pharm Sci 2007;10:388–404.

[363] Bagorda A, Guerra L, Sole F Di, Hemle-kolb C, Cardone RA, Fanelli T, et al. Reciprocal Protein Kinase A Regulatory Interactions between Cystic Fibrosis Transmembrane Conductance Regulator and Na □ / H □ Exchanger Isoform 3 in a Renal Polarized Epithelial Cell Model *. J Biol Chem 2002;277:21480–8. doi:10.1074/jbc.M112245200.

[364] Castello A, Girardi C, Carraro-lacroix LR. Regulation of Na + / H + Exchanger Isoform 3 by Protein Kinase A in the Renal Proximal Tubule. Protein Kinases, 2012, p. 321–36.

[365] Reddy M, Jackson Stutts M. Status of Fluid and Electrolyte Absorption. Cold Spring Harb Perspect Med 2013;3:1–16. doi:10.1101/cshperspect.a009555.

[366] Soave D, Corvol H, Panjwani N, Gong J, Li W, Boëlle PY, et al. A Joint Location-Scale Test Improves Power to Detect Associated SNPs, Gene Sets, and Pathways. Am J Hum Genet 2015;97:125–38. doi:10.1016/j.ajhg.2015.05.015.

[367] Li Q, Li N, Liu CY, Xu R, Kolosov VP, Perelman JM, et al. Ezrin/exocyst complex regulates mucin 5AC secretion induced by neutrophil elastase in human airway epithelial cells. Cell Physiol Biochem 2015;35:326–38. doi:10.1159/000369699.

[368] Shirwany NA, Zou MH. AMPK: a cellular metabolic and redox sensor. A minireview. vol. 19. 2014. doi:10.2741/4218.

[369] Fryer LGD, Parbu-Patel A, Carling D. The anti-diabetic drugs rosiglitazone and metformin stimulate AMP-activated protein kinase through distinct signaling pathways. J Biol Chem 2002;277:25226–32. doi:10.1074/jbc.M202489200.

[370] Kahn BB, Alquier T, Carling D, Hardie DG. AMP-activated protein kinase: Ancient energy gauge provides clues to modern understanding of metabolism. Cell Metab 2005;1:15–25. doi:10.1016/j.cmet.2004.12.003.

[371] Kukavica-Ibrulj I, Levesque RC. Animal models of chronic lung infection with Pseudomonas aeruginosa: useful tools for cystic fibrosis studies. Lab Anim 2008;42:389–412. doi:10.1258/la.2007.06014e.

[372] Bevivino A, Pirone L, Pilkington R, Cifani N, Dalmastri C, Callaghan M, et al. Interaction of environmental Burkholderia cenocepacia strains with cystic fibrosis and noncystic fibrosis bronchial epithelial cells in vitro. Microbiology 2012;158:1325–33. doi:10.1099/mic.0.056986-0.

[373] Shin K, Fogg VC, Margolis B. Tight Junctions and Cell Polarity. Annu Rev Cell Dev Biol 2006;22:207–35. doi:10.1146/.

[374] Baldursson O. Regulating the barrier function of airway epithelia. A novel role for CFTR - does it make a difference this time? J Physiol 2010;588:1385. doi:10.1113/jphysiol.2010.189894.

[375] Rajasekaran SA, Beyenbach KW, Rajasekaran AK. Interactions of tight junctions with membrane channels and transporters. Biochim Biophys Acta - Biomembr 2008;1778:757–69. doi:10.1016/j.bbamem.2007.11.007.

[376] Högman M, Mörk AC, Roomans GM. Hypertonic saline increases tight junction permeability in airway epithelium. Eur Respir J 2002;20:1444–8. doi:10.1183/09031936.02.00017202.

[377] Nilsson H, Dragomir A, Ahlander A, Johannesson M, Roomans G. Effects of hyperosmotic stress on cultured airway epithelial cells. Cell Tissue Res 2007;330:257–69.

[378] Nilsson HE, Dragomir A, Lazorova L, Johannesson M, Roomans GM. CFTR and tight junctions in cultured bronchial epithelial cells. Exp Mol Pathol 2010;88:118–27. doi:10.1016/j.yexmp.2009.09.018.

[379] Zahm JM, Milliot M, Bresin A, Coraux C, Birembaut P. The effect of hyaluronan on airway mucus transport and airway epithelial barrier integrity: Potential application to the cytoprotection of airway tissue. Matrix Biol 2011;30:389–95. doi:10.1016/j.matbio.2011.07.003.

[380] Forteza RM, Casalino-Matsuda SM, Falcon NS, Gattas MV, Monzon ME. Hyaluronan and layilin mediate loss of airway epithelial barrier function induced by cigarette smoke by decreasing. J Biol Chem 2012;287:42288–98. doi:10.1074/jbc.M112.387795.

[381] Tilg H, Moschen AR. Adipocytokines: mediators linking adipose tissue, inflammation and immunity. Nat Rev Immunol 2006;6:772–83. doi:10.1038/nri1937.

[382] Oraby SS, Ahmed ES, Farag TS, Zayed AE, Ali NK. Adiponectin as inflammatory biomarker of chronic obstructive pulmonary disease. Egypt J Chest Dis Tuberc 2014;63:583–7. doi:10.1016/j.ejcdt.2014.02.006.

[383] Bianco A, Mazzarella G, Turchiarelli V, Nigro E, Corbi G, Scudiero O, et al. Adiponectin: An attractive marker for metabolic disorders in chronic obstructive pulmonary disease (COPD). Nutrients 2013;5:4115–25. doi:10.3390/nu5104115.

[384] Cheng J, Cebotaru V, Cebotaru L, Guggino WB. Syntaxin 6 and CAL Mediate the Degradation of the Cystic Fibrosis Transmembrane Conductance Regulator. Mol Biol Cell 2010;21:4042–56. doi:10.1091/mbc.E09.

[385] Li C, Naren AP. CFTR chloride channel in the apical compartments: spatiotemporal coupling to its interacting partners. Integr Biol (Camb) 2010;2:161–77. doi:10.1039/b924455g.

[386] Beineke P, Fitch K, Tao H, Elashoff MR, Rosenberg S, Kraus WE, et al. A whole blood gene expression-based signature for smoking status. BMC Med Genomics 2012;5:58. doi:10.1186/1755-8794-5-58.

[387] Gisler FM, von Kanel T, Kraemer R, Schaller A, Gallati S. Identification of SNPs in the cystic fibrosis interactome influencing pulmonary progression in cystic fibrosis. Eur J Hum Genet 2013;21:397–403. doi:10.1038/ejhg.2012.181.

[388] Geraghty P, Hardigan AA, Wallace AM, Mirochnitchenko O, Thankachen J, Arellanos L, et al. The glutathione peroxidase 1-protein tyrosine phosphatase 1B-protein phosphatase 2A axis: A key determinant of airway inflammation and alveolar destruction. Am J Respir Cell Mol Biol 2013;49:721–30. doi:10.1165/rcmb.2013-0026OC.

[389] Yang J, Wang B, Zhou H-X, Liang B-M, Chen H, Ma C-L, et al. Association of surfactant protein B gene with chronic obstructive pulmonary disease susceptibility. Int J Tuberc Lung Dis 2014;18:1378–84.

[390] Seifart C, Plagens A, Br”dje D, M• ller B, vonWichert P, Floros J. Surfactant protein B gene variation in patients with COPD and acute respiratory failure. Submitted 2001;18:129–36.

[391] Woodworth BA, Wood R, Bhargave G, Cohen NA, Baatz JE, Schlosser RJ. Surfactant protein B detection and gene expression in chronic rhinosinusitis. Laryngoscope 2007;117:1296–301. doi:10.1097/MLG.0b013e31805c9a28.

[392] Griese M, Essl R, Schmidt R, Ballmann M, Paul K, Rietschel E, et al. Sequential analysis of surfactant, lung function and inflammation in cystic fibrosis patients. Respir Res 2005;6:133. doi:10.1186/1465-9921-6-133.

[393] Jiang Y, Dey S, Matsunami H. Calreticulin: Roles in cell-surface protein expression. Membranes (Basel) 2014;4:630–41. doi:10.3390/membranes4030630.

[394] Ribeiro CMP, O’Neal WK. Endoplasmic reticulum stress in chronic obstructive lung diseases. Curr Mol Med 2012;12:872–82. doi:10.2174/156652412801318791.

[395] Martino MEB, Olsen JC, Fulcher NB, Wolfgang MC, O’Neal WK, Ribeiro CMP. Airway epithelial inflammation-induced endoplasmic reticulum Ca2+ store expansion is mediated by X-box binding protein-1. J Biol Chem 2009;284:14904–13. doi:10.1074/jbc.M809180200.

[396] Ribeiro CMP, Paradiso AM, Schwab U, Perez-Vilar J, Jones L, O'neal W, et al. Chronic airway infection/inflammation induces a Ca2+i-dependent hyperinflammatory response in human cystic fibrosis airway epithelia. J Biol Chem 2005;280:17798–806. doi:10.1074/jbc.M410618200.

[397] Blackman SM, Commander CW, Watson C, Arcara KM, Strug LJ, Stonebraker JR, et al. Genetic modifiers of cystic fibrosis-related diabetes. Diabetes 2013;62:3627–35. doi:10.2337/db13-0510.

[398] Wegner L, Hussain MS, Pilgaard K, Hansen T, Pedersen O, Vaag A, et al. Impact of TCF7L2 rs7903146 on insulin secretion and action in young and elderly danish twins. J Clin Endocrinol Metab 2008;93:4013–9. doi:10.1210/jc.2008-0855.

[399] Yang H, Li Q, Lee JH, Shu Y. Reduction in Tcf7l2 expression decreases diabetic susceptibility in mice. Int J Biol Sci 2012;8:791–801. doi:10.7150/ijbs.4568.

[400] Garantziotis S, Li Z, Potts EN, Kimata K, Zhuo L, Morgan DL, et al. Hyaluronan mediates ozone-induced airway hyperresponsiveness in mice. J Biol Chem 2009;284:11309–17. doi:10.1074/jbc.M802400200.

[401] Vieira RP, Mourão PA. Occurrence of a unique fucose-branched chondroitin sulfate in the body wall of a sea cucumber. J Biol Chem 1988;263:18176–83.

[402] Albano RM, Mourao PAS. Isolation, fractionation, and preliminary characterization of a novel class of sulfated glycans from the tunic of Styela plicata (Chordata tunicata). J Biol Chem 1986;261:758–65.

[403] Wood A, Ogawa M, Portier RJ, Schexnayder M, Shirley M, Losso JN. Biochemical properties of alligator (Alligator mississippiensis) bone collagen. Comp Biochem Physiol B Biochem Mol Biol 2008;151:246–9. doi:10.1016/j.cbpb.2008.05.015.

VITA

Jose Daniel Estrada Andino was born and raised in Tegucigalpa, Honduras. During high school he attended International School where he graduated in 2003. Jose Daniel graduated from Zamorano University (Honduras) with a B.S. in Food Agroindustry in 2007. There he completed a research thesis titled "Effect of Probiotics *L. acidophilus* and *B. bifidum* on the physical, chemical and sensory characteristics of Zamorano strawberry yogurt", under the guidance of Dr. Luis Osorio. After being granted a 3-month research scholar position at the LSU AgCenter in the summer of 2009, he joined the LSU graduate program in Food Science under the mentorship of Dr. Subramaniam Sathivel. In August 2011 he completed his research titled "Production And Processing of a Functional Yogurt Fortified With Microencapsulated Omega-3 and Vitamin E" and received his Master's Degree in Food Science. Jose Daniel has 3 years of experience in the food industry as Instructor of the Zamorano Dairy Processing Plant (2007-2008) and United Kingdom and Middle East Commercial Representative at Grupo Agrolibano, a fresh fruit grower and exporter (2011-2013). In the fall of 2013, Jose Daniel returned to LSU with an Economic Development Assistantship from the Graduate School to conduct research on the valorization of by-products from the alligator industry. In the summer of 2016, he is enrolled to receive a Doctor of Philosophy degree from the School of Nutrition and Food Sciences. He is married to Monika Estrada who will complete her Master's Degree in Hispanic Studies at LSU in August 2016.